Article:

Gulliford, AR, Flint, SS and Hodgson, DM orcid.org/0000-0003-3711-635X (2017) Crevasse splay processes and deposits in an ancient distributive fluvial system: The lower Beaufort Group, South Africa. Sedimentary Geology, 358. pp. 1-18. ISSN 0037-0738

https://doi.org/10.1016/j.sedgeo.2017.06.005

Crevasse splay processes and deposits in an ancient distributive fluvial system: the lower Beaufort Group, South Africa

Alice R. Gulliford[1†*], Stephen S. Flint[1], David M. Hodgson[2]

[1]Stratigraphy Group, School of Earth and Environmental Sciences, University of Manchester, Oxford Road, Manchester M13 9PL, U.K.

[2]Stratigraphy Group, School of Earth and Environment, University of Leeds, Leeds LS2 9JT, U.K.

[†]Shell International Ltd., 40 Bank Street, Canary Wharf, London. E14 5NR, U.K.

e-mail: alice.gulliford@shell.com

*Corresponding author.

Abstract

Up to 12% of the mud-prone, ephemeral distributive fluvial system stratigraphy in the Permo-Triassic lower Beaufort Group, South Africa, comprises tabular fine-grained sandstone to coarse-grained siltstone bodies, which are interpreted as proximal to distal crevasse splay deposits. Crevasse splay sandstones predominantly exhibit ripple to climbing ripple cross-lamination, with some structureless and planar laminated beds. A hierarchical architectural scheme is adopted, in which each ~1 m thick crevasse splay elements extend for tens to several hundreds of meters laterally, and stack with other splay elements to form crevasse splay sets up to 4 m thick and several kilometers in width and length. Paleosols and nodular horizons developed during periods, or in areas of reduced overbank flooding and are used to subdivide the stratigraphy, separating crevasse splay sets. Deposits from crevasse splays differ from frontal splays as their proximal deposits are much thinner and narrower, with paleocurrents oblique to the main paleochannel. In order for crevasse splay sets to develop, the parent channel belt and the location where crevasse splays form must stay relatively fixed during a period of multiple flood events. Beaufort Group splays have similar geometries to those of perennial rivers but exhibit more lateral variability in facies, which is interpreted to be the result of more extreme fluctuations in discharge regime. Sharp-based crevasse splay packages are associated with channel avulsion, but most are characterized by a gradual coarsening upward, interpreted to represent progradation. The dominance of progradational splays beneath channel belt deposits may be more characteristic of progradational stratigraphy in a distributive fluvial system rather than dominated by avulsion processes in a trunk river system. This stratigraphic motif may

therefore be an additional criterion for recognition of distributive fluvial systems in the ancient record.

Keywords: crevasse splay; overbank; avulsion; distributive fluvial system; Karoo Basin

1. Introduction

Fluvial sedimentological and stratigraphic research tends to focus on the internal architecture, geometry and stacking patterns of channel sandstone bodies, rather than their adjacent overbank successions (e.g., Allen, 1983; Blakey and Gubitosa, 1984; Bridge and Tye, 2000; Gouw and Berendsen, 2007; Pranter et al., 2009; Jenson and Pedersen, 2010). This is because channel-fills are coarser grained and better exposed, and channel elements are of greater importance as hydrocarbon reservoirs than their finer grained, usually less permeable, overbank counterparts. However, in aggradation-dominated systems, floodplain and crevasse splay deposits form a key constituent of the overall stratigraphic succession (Bristow et al., 1999). Local floodplain accommodation is controlled by the elevation of the bank-full channel relative to its surrounding floodbasin (Wright and Marriott, 1993). River avulsion processes, floodplain morphology, and controls on floodplain evolution have been a focus for previous research on crevasse splay deposits (e.g., Tyler and Ethridge, 1983; Nanson and Croke, 1992; Kraus and Aslan, 1993; Singh et al., 1993; Walling and He, 1998; Kraus and Wells, 1999; Slingerland and Smith, 2004; Jones and Hajek, 2007; Abels et al., 2013; Hajek and Edmonds, 2014; Burns et al., 2017). Crevasse splay successions provide evidence for the mechanisms of channel avulsion. For example, several authors have identified distinct types of splay stratigraphy (Kraus and Wells, 1999; Mohrig et al., 2000; Slingerland and Smith, 2004; Jones and Hajek, 2007) interpreted to represent either abrupt or gradual to failed avulsion.

The majority of depositional models for crevasse splays are derived from ancient and modern temperate to boreal climates where organic-rich strata dominate (e.g., Horne et al., 1978; Ethridge et al., 1981; Flores, 1983; Smith et al., 1989; Jørgensen and Fielding, 1996;

Bristow et al., 1999; Jerrett et al., 2011; Burns et al., 2017). Natural variability in river avulsion processes, and the architecture and dimensions of crevasse splay deposits, are not adequately constrained by these case studies (Nanson and Croke, 1992). Studies that focus on overbank successions within other climatic regimes include O'Brien and Wells (1986) on ephemeral stream crevasse splay deposits from the subtropical Clarence River of Australia, and ephemeral terminal splay deposits from Lake Eyre, Australia (Payenberg et al., 2004; Fisher et al., 2008).

In addition, the role of crevasse splay deposits in the distributive fluvial system (DFS) paradigm (i.e., Nichols and Fisher, 2007; Hartley et al., 2010a, 2010b; Sambrook Smith et al., 2010; Weissmann et al., 2010; Fielding et al., 2012; Gulliford et al., 2014) has not been examined specifically. From an applied perspective, research into the role of overbank successions in hydrocarbon reservoir development has been limited (e.g., Mjøs et al., 1993; Ambrose et al., 2008; Stuart et al., 2014; van Toorenenburg et al., 2016). However, recent interest in fine-grained overbank successions has increased due to a growth in coal bed methane extraction and the hydraulic fracturing of fluvial tight gas reservoirs (e.g., Pashin, 1998; Ayers, 2002; Shanley et al., 2004; Iwere et al., 2006).

The aim of this paper is to address the need for a more detailed analysis of sedimentary facies, geometries, stacking patterns and evolutionary development of ancient crevasse splay deposits from non-coal bearing strata. The large-scale outcrops from the Permo-Triassic lower Beaufort Group of the SW Karoo Basin, South Africa are used to address the following objectives: i) to propose a hierarchical architectural classification scheme enabling the characterization of different overbank elements over a range of spatial scales; ii) to test models that characterize splays in terms of either random overbank flooding or attempted channel avulsion; iii) to draw comparisons between modern and ancient crevasse splay datasets; and iv) to address the role of crevasse splay deposits in distributive fluvial system models.

2. Geological setting

The Permo-Triassic Karoo Basin fill of South Africa (

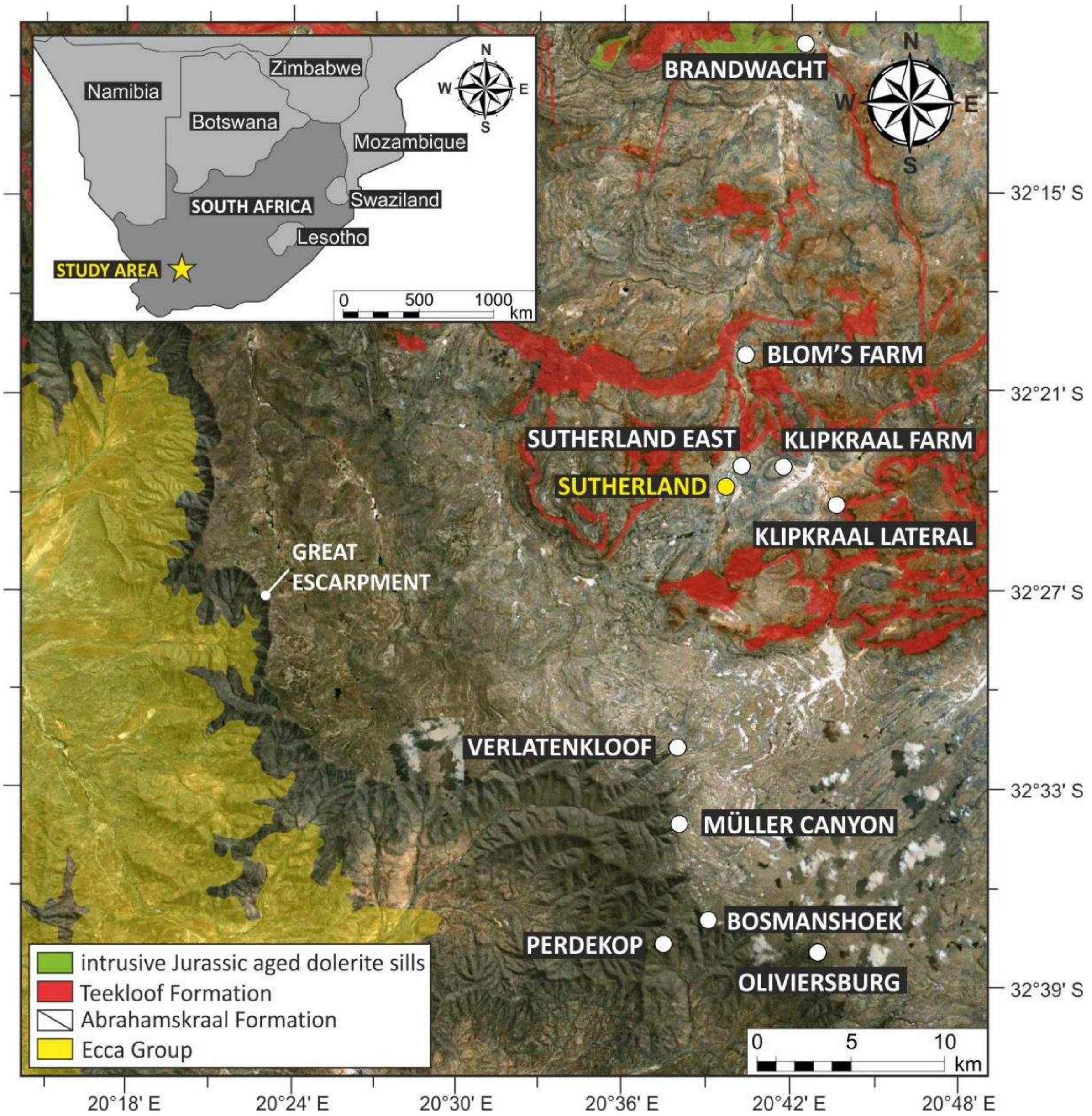

Fig. 1) contains deep-water submarine fans though submarine slope and shelf edge delta deposits of the 2 km thick Ecca Group (Flint et al., 2011), overlain by the 5 km+ thick fluvial

Beaufort Group (Johnson et al., 1997) (

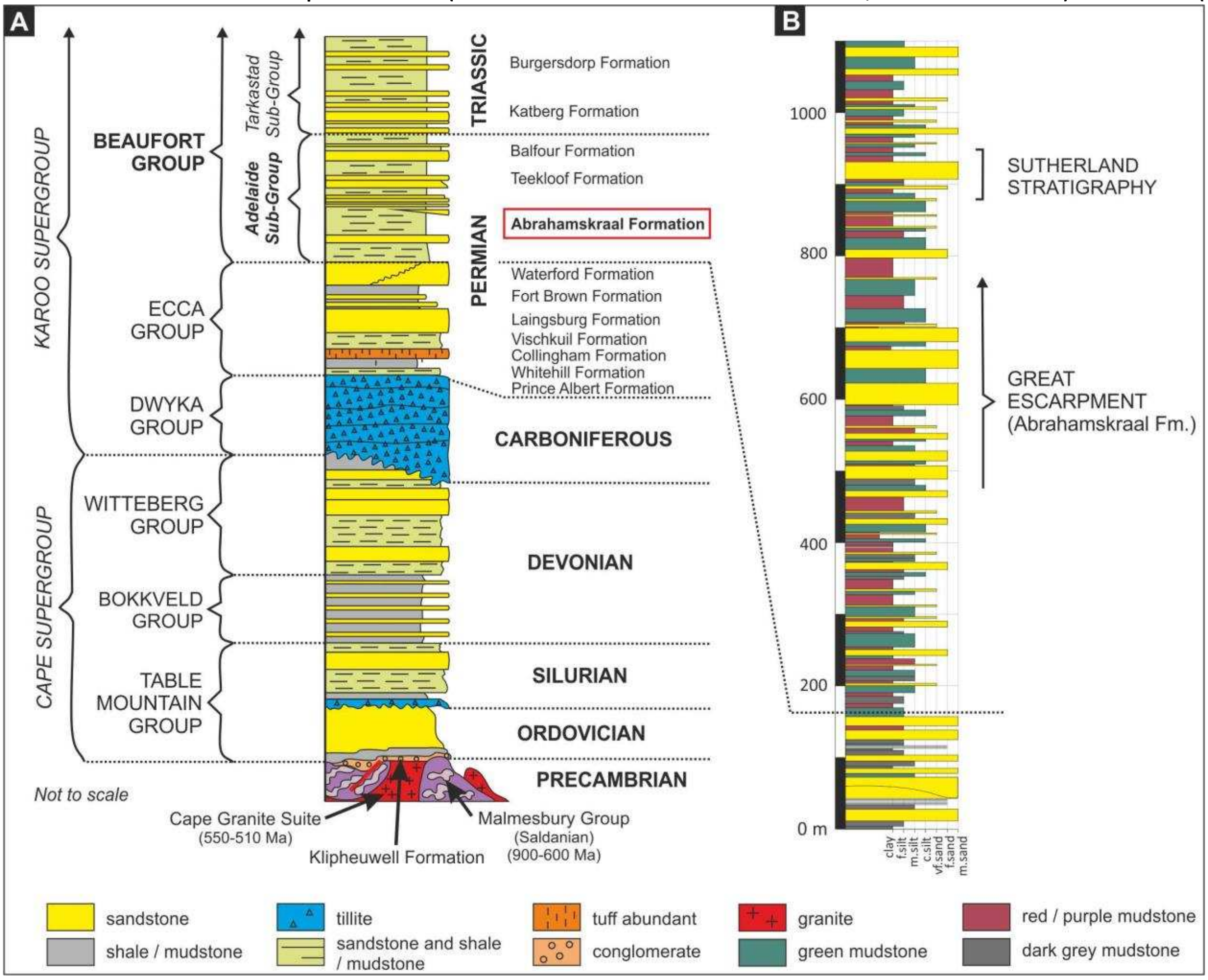

Fig. 2). Subsidence at this time was generated by dynamic topography associated with mantle flow processes (Pysklywec and Mitrovica, 1999; Tankard et al., 2009).

The lower 900 m of the Beaufort Group (Abrahamskraal Formation) forms the focus of this study, and is exposed over an area of 900 km^2 (

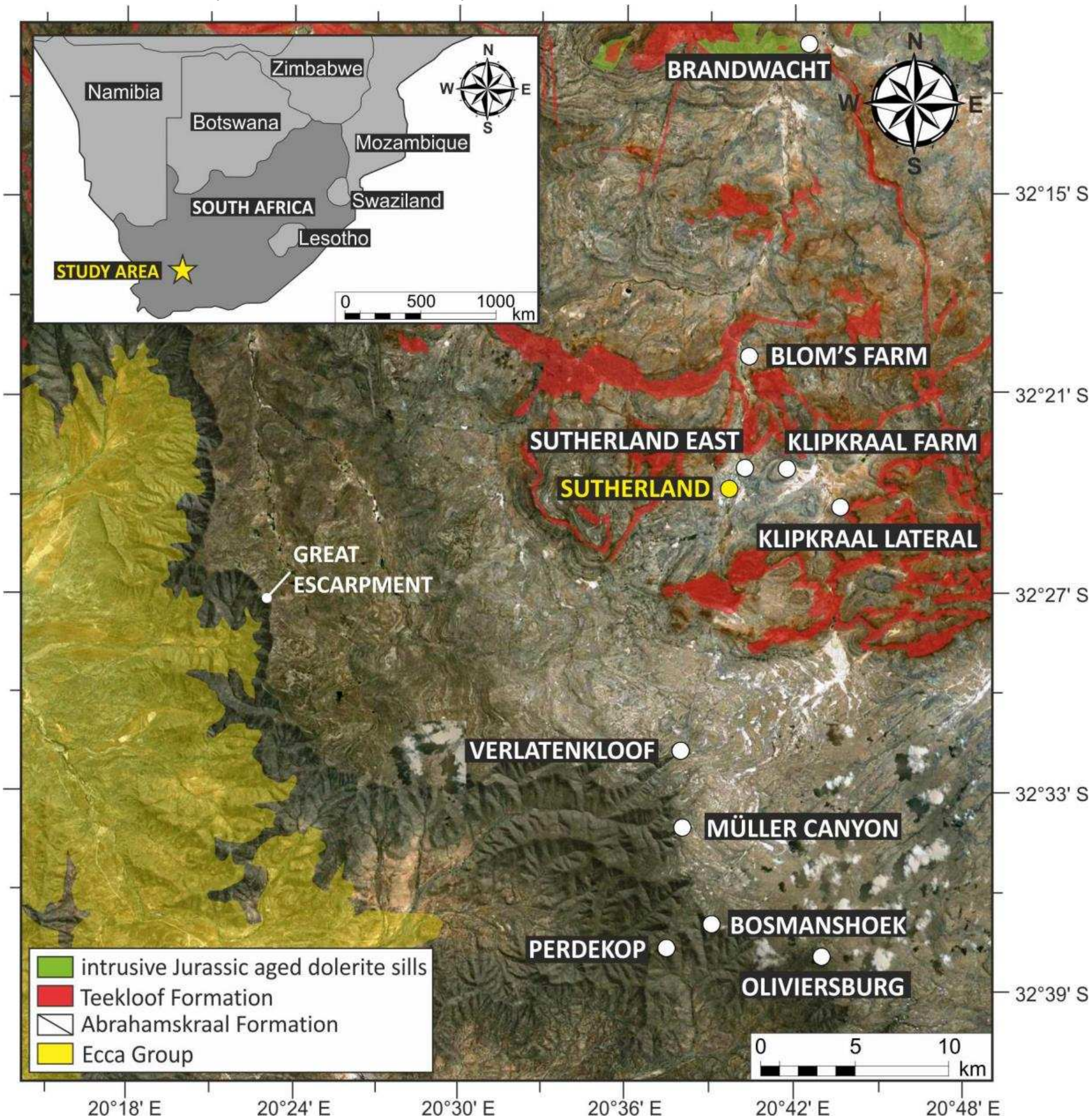

Fig. 1). Fluvial channel belt and overbank deposits are best observed around the edge of the Great Escarpment and in river cliffs, road cuts and hill sides. Tectonic dip is 1-2° to the east.

The stratigraphy is floodplain dominated, with crevasse splay deposits forming 12% (

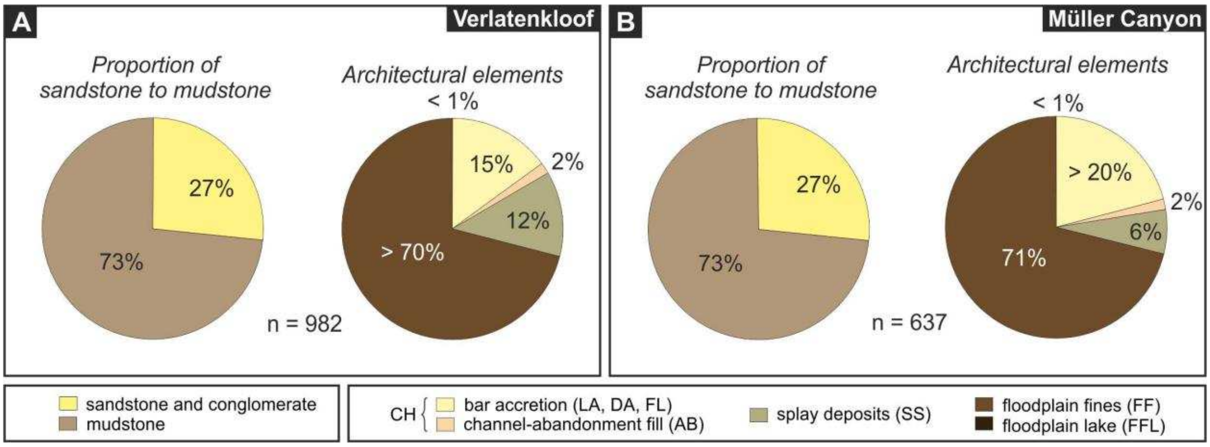

Fig. 3). Previous studies have interpreted the lower Beaufort Group as an ephemeral fluvial system (Smith, 1990a, 1990b, 1993a, 1993b). The abundance of planar and low angle laminated lower fine- to medium-grained sandstone with parting lineation in the channel belt deposits of the lower Beaufort Group has been interpreted to indicate upper flow regime conditions in grain size-limited rivers (Turner, 1981; Fielding et al., 2009; Gulliford et al., 2014; Wilson et al., 2014). The characteristics of splay deposits have been reported by Stear (1980, 1983), Jordaan (1990) and Smith (1993a), and recent studies have interpreted the lower Beaufort Group as a distributive fluvial system (Wilson et al., 2014; Gulliford et al., 2014).

3. Dataset and methods

The outcrop dataset comprises 33 sedimentary logs measured at centimeter-scale, high resolution photo panel interpretations and maps of key surfaces supported by paleocurrent measurements, from five main study sites (Supplementary Table 1). Apparent widths were corrected to true widths using paleotransport directions relative to the outcrop orientation. At the escarpment edge, sedimentary log sections through a ~330 m thick stratigraphic interval from Verlatenkloof and Müller Canyon (

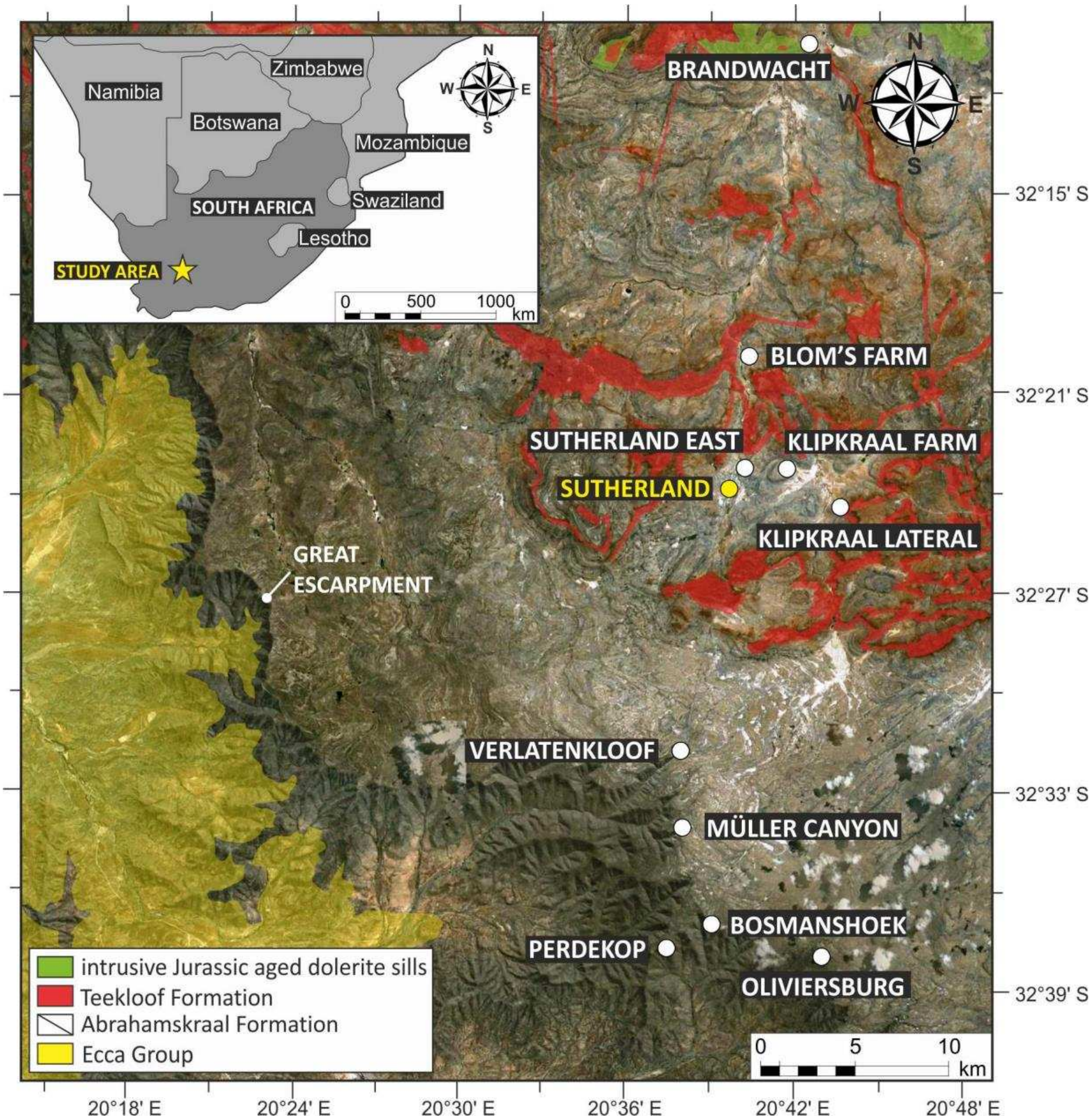

Fig. 1; Supplementary Figs. 1, 2) at a scale of 1:50 capture sedimentary facies and architectural elements (

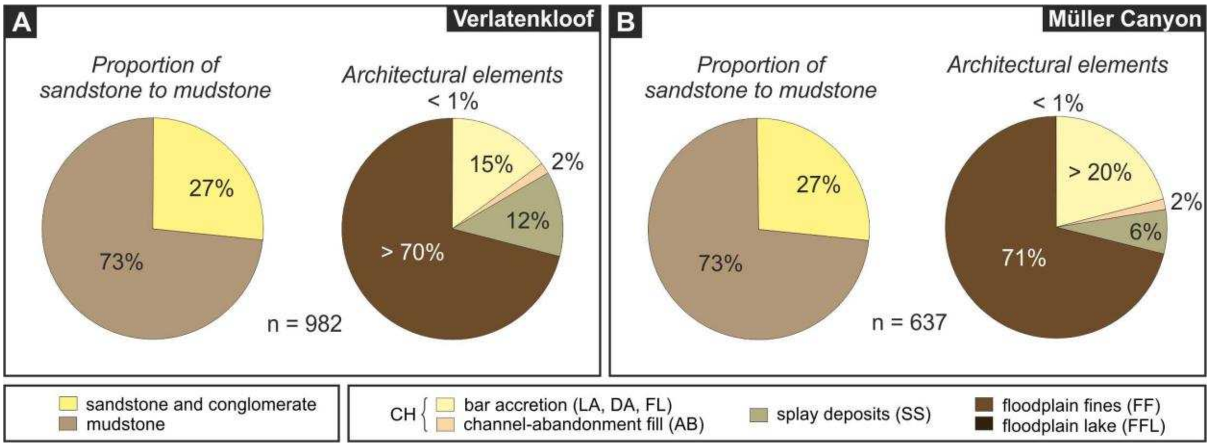

Fig. 3; Supplementary Spreadsheet 1). Grainsize was quantified in the field using a grainsize chart, with siltstones determined according to competency, degree of fissile character and weathering style, and claystones feeling smooth when rubbed against the teeth.

Adjacent to the town of Sutherland, three studies have been carried out to document overbank facies relationships, geometries, and stacking patterns. The main detailed study area at Sutherland East includes 14 sedimentary logs that were measured at a scale of 1:25. Individual beds (labeled A to Z, up to ZD) were walked out between logged sections and correlated on a photo panel. Sedimentary log thicknesses and paleocurrent readings were geo-referenced in GoogleEarth^{TM} to constrain spatial changes in architecture and splay thickness. Additional data were collected from study sites at Klipkraal Farm and

Blom's Farm (

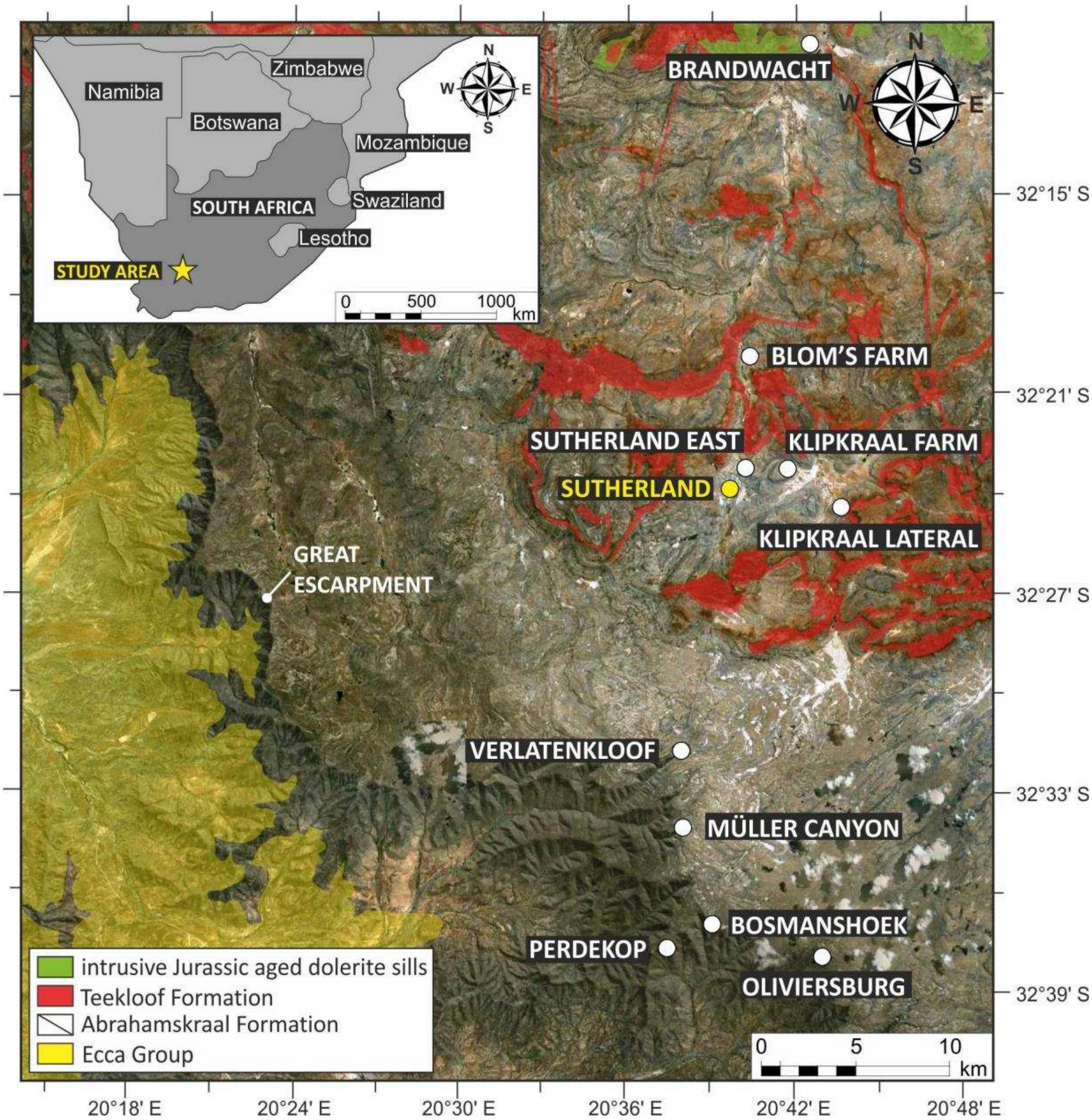

Fig. 1).

4. Facies

Within the Lower Abrahamskraal Formation, 11 overbank facies have been observed, including six mudstone facies and five sandstone facies. The mudstone facies comprise fissile purple mudstone, poorly-sorted purple siltstone, bright green massive mudstone, poorly-sorted green-gray-blue siltstone, laminated organic-rich dark gray mudstone and thinly-bedded coarse-grained siltstone and very fine-grained sandstone (

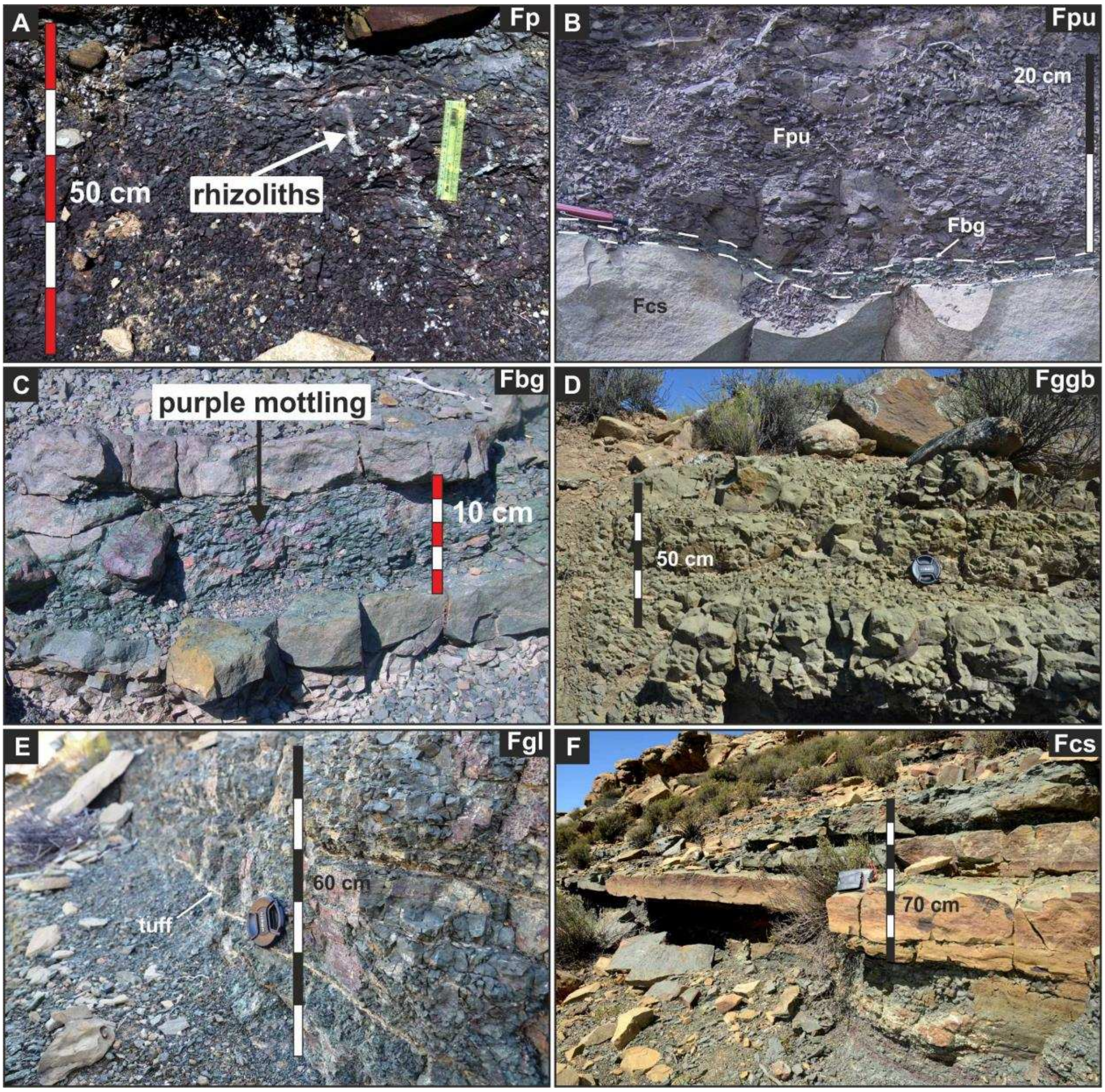

Fig. 4A-F) (Gulliford et al., 2014, Table 2). The sandstone facies comprise ripple cross-laminated very fine- to fine-grained sandstone, structureless and normally graded very fine- to fine-grained sandstone, planar laminated very fine- to fine-grained sandstone, low angle (< 10°) cross-stratified very fine- to fine-grained sandstone and trough cross-stratified fine-grained sandstone. Relative proportions of each overbank-related mudstone and sandstone facies averaged across all the study areas are provided in Table 1, and Figure 4 shows key features.

5. Architectural Elements

The facies have been grouped into eight architectural elements based on schemes by Allen (1983), Friend (1983), Miall (1985, 1988, 1996) and Colombera et al. (2012, 2013). These schemes combine sedimentary facies associations with grain size and geometries. Overbank architectural elements comprise crevasse splay deposits, floodplain fines and floodplain lake

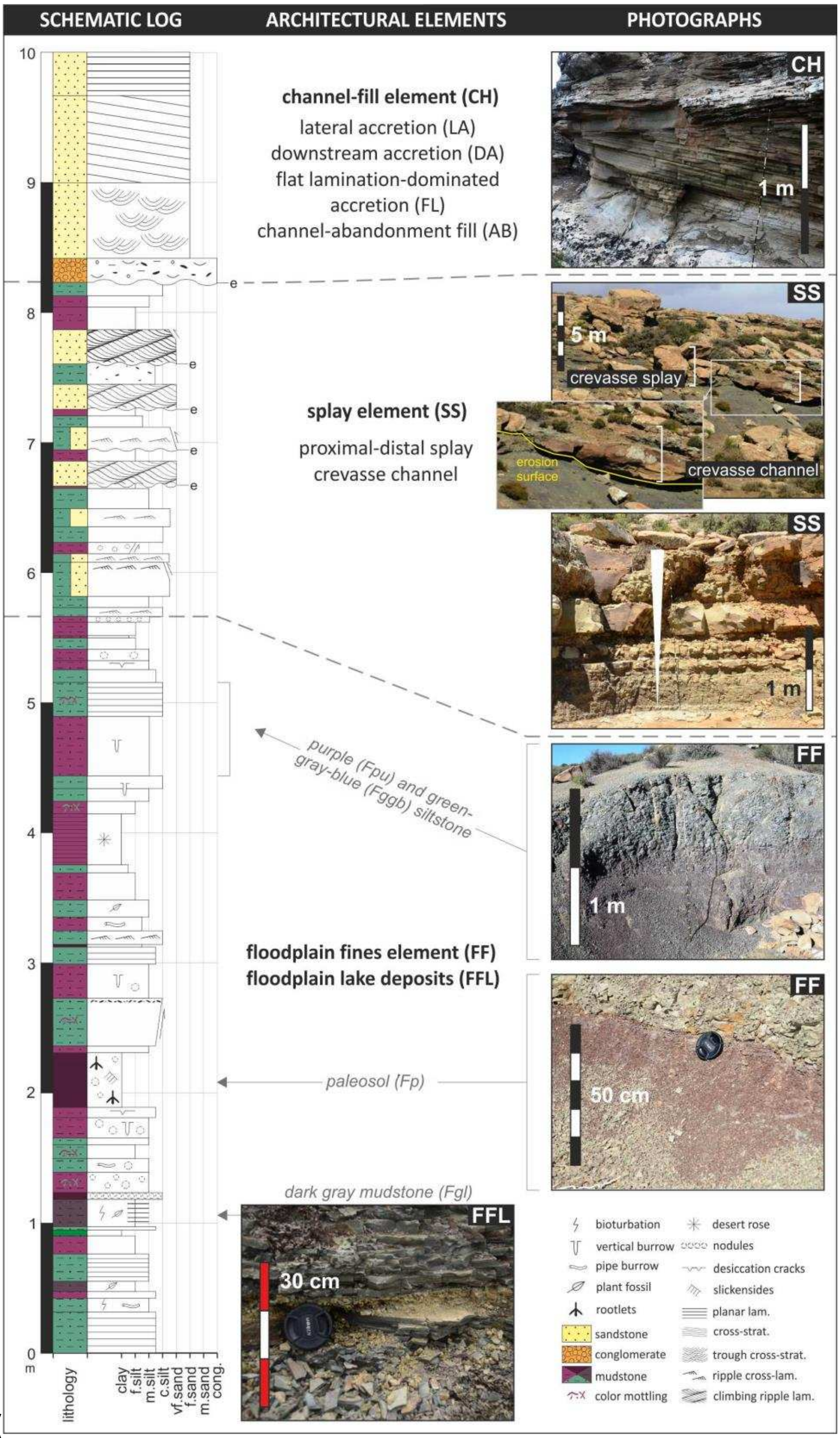

deposits (

Fig. 5). The proportion of fluvial-overbank architectural elements measured from sedimentary logs at the Great Escarpment is presented in Figure 3, and each element is described below.

5.1 Floodplain fines architectural element

Description: The floodplain fines architectural element includes fissile purple mudstone, poorly sorted purple siltstone, bright green massive mudstone and poorly sorted green-gray-blue siltstone facies (

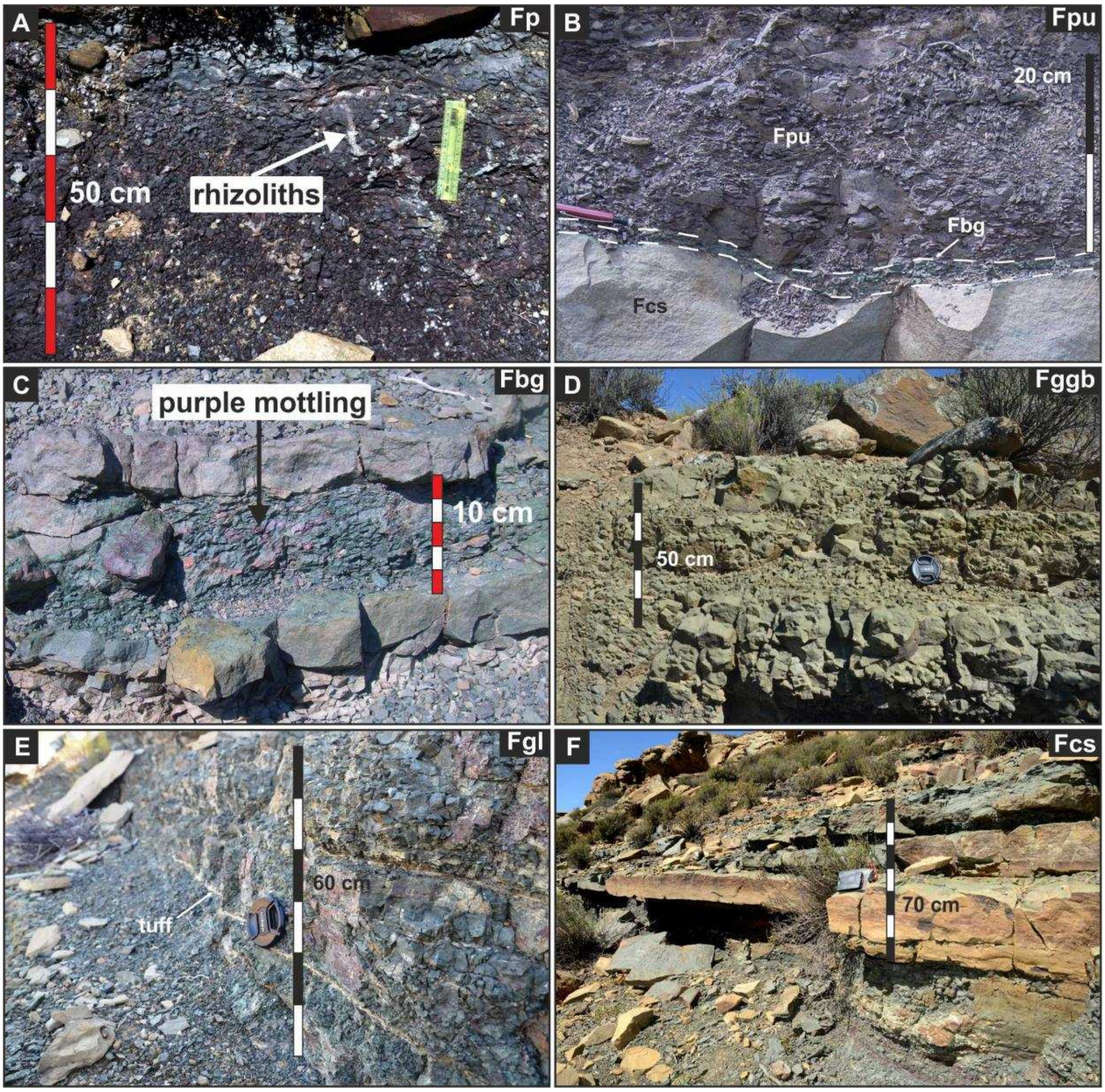

Fig. 4A-D), as described in Table 2 of Gulliford et al. (2014). Typically, the facies are moderately to highly bioturbated by roots and burrows (*Bioturbation Index* BI 3 to 4; Taylor and Goldring, 1993), thus destroying internal laminae. Polygonal features (1 cm across) are infilled by siltstone. Successions are up to 40 m thick with sharp bases and are overlain by sandstones with either gradational or sharp contact. The green siltstone deposits (minor Fbg

[

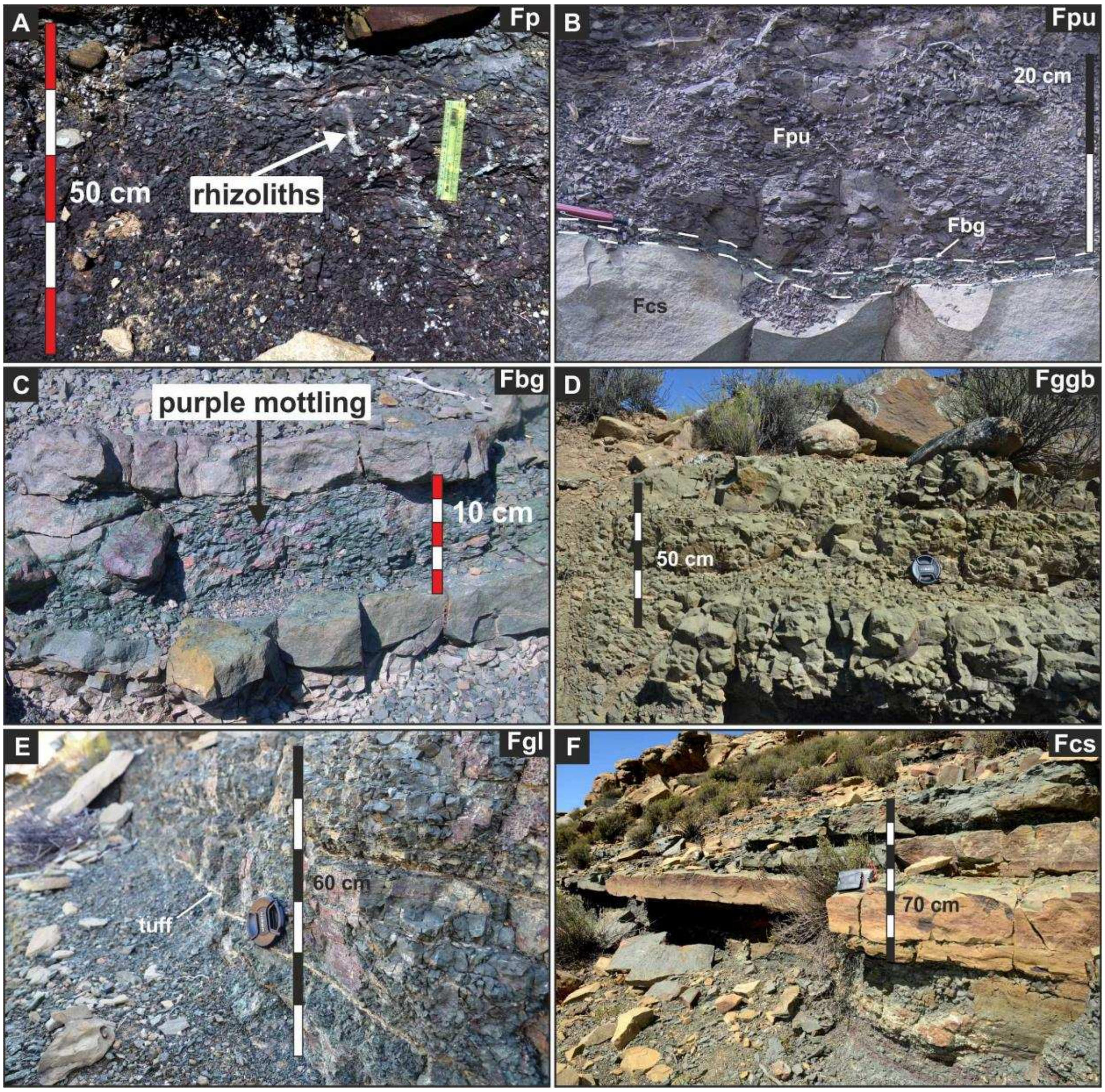

Fig. 4C]: Munsell distinction 5G3/6; Fggb [

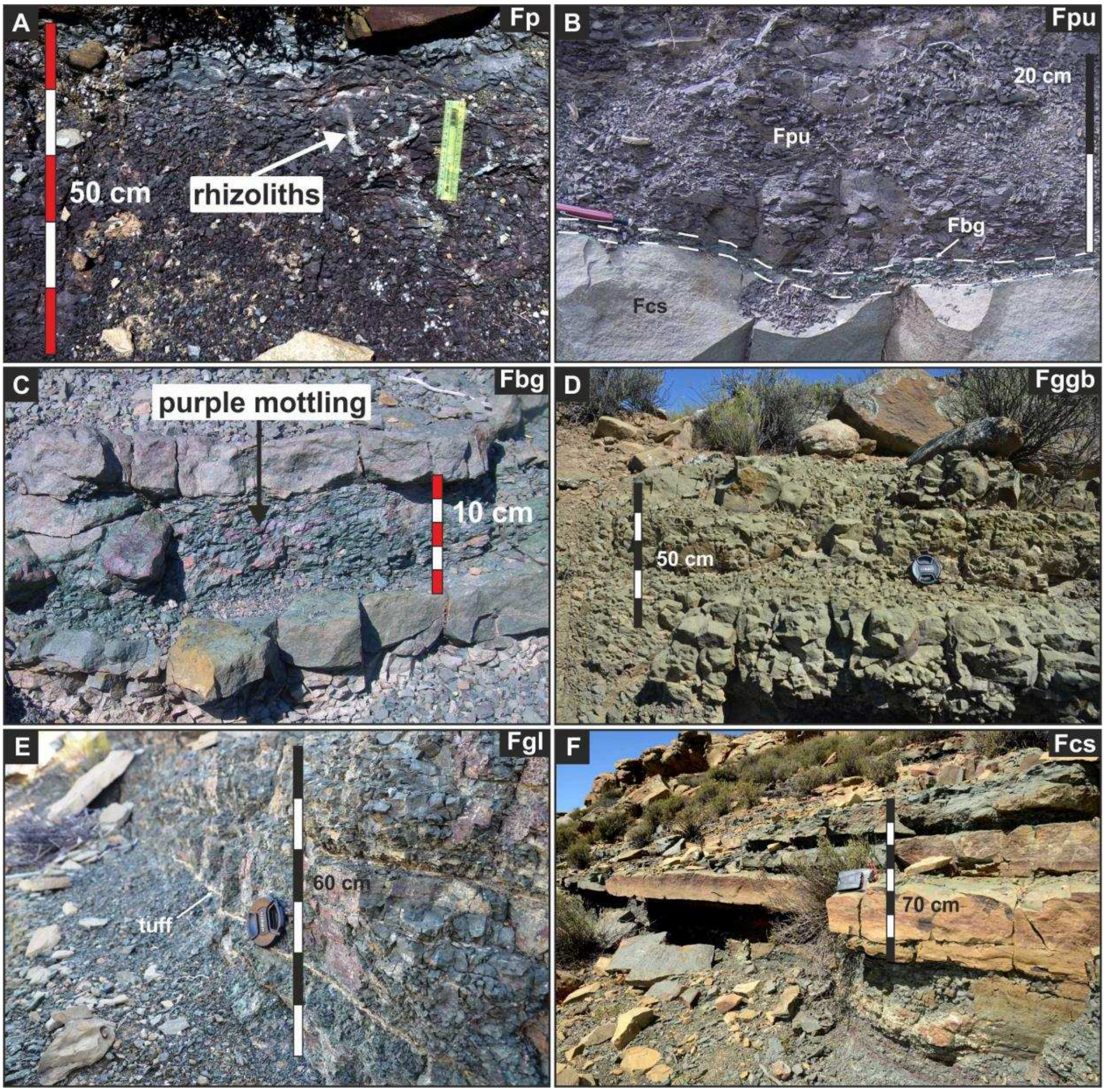

Fig. 4D]: Munsell distinction 10G5/2 to 5B5/2) are coarser grained than the purple siltstone (Fp; [

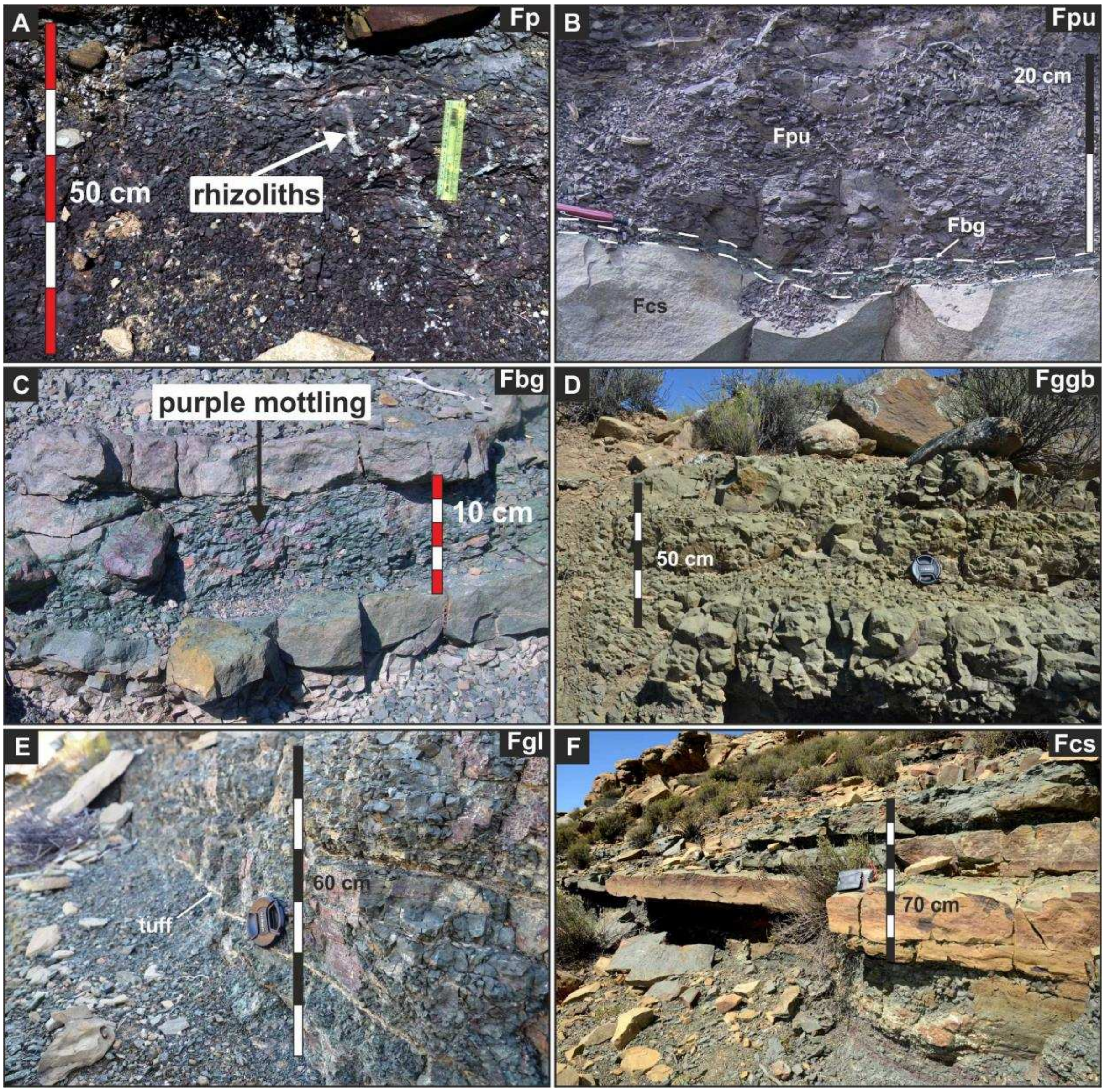

Fig. 4A]: Munsell distinction 5P1/6 to 10P1/6; Fpu [

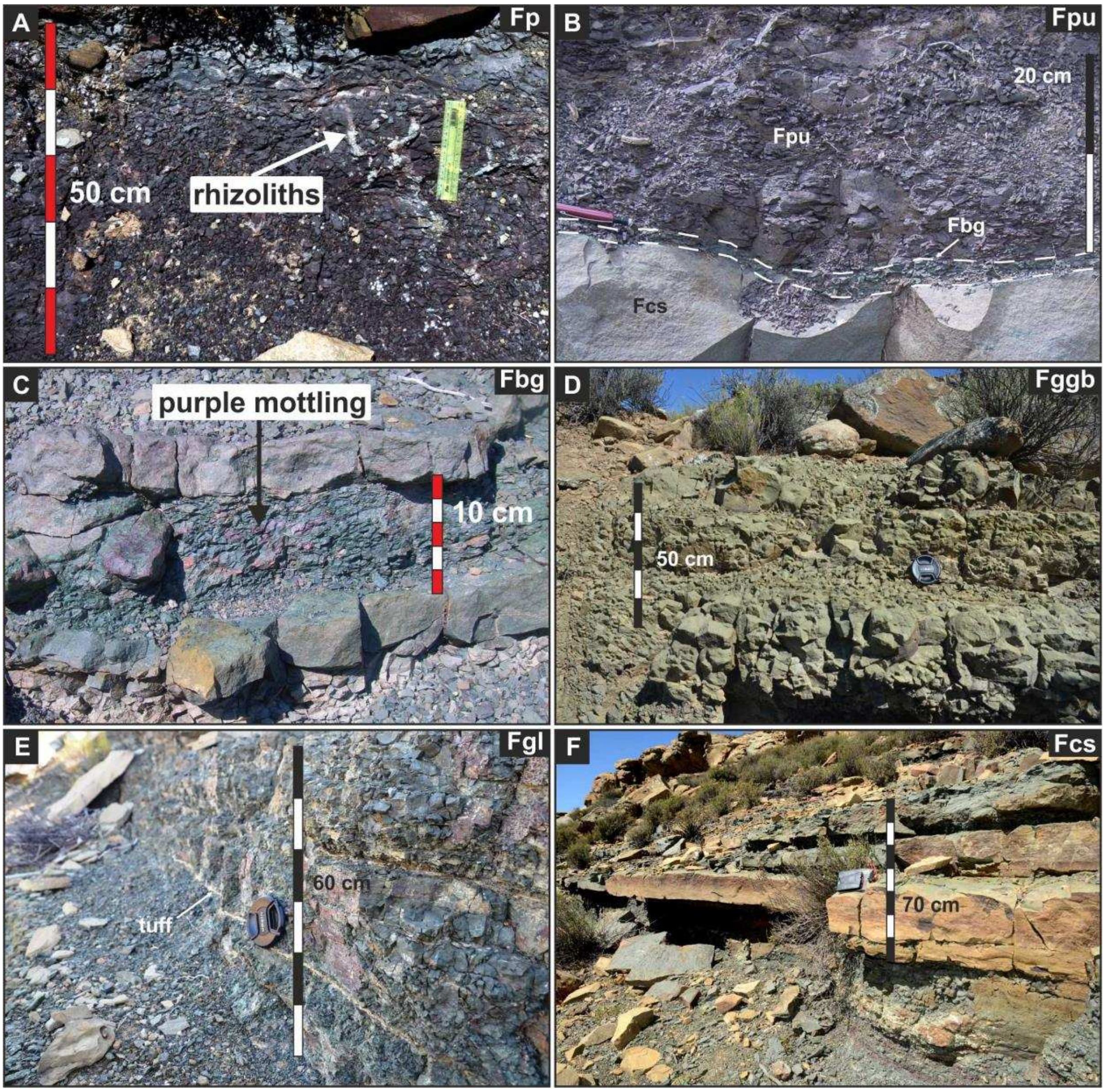

Fig. 4B]: Munsell distinction 5P2/2 to 10P2/2).

Interpretation: The root traces with reduction haloes and slickensides suggest prolonged subaerial exposure following suspension settling on subaqueous floodplains (Gulliford et al., 2014). The infilled polygonal features are interpreted as desiccation cracks, consistent with subaerial exposure.

The localized preservation of carbonate nodules and absence of a thick calcrete layer supports an interpretation of moderate maturity paleosols (*sensu* Leeder, 1975; Nichols, 2009), and a periodic and localized net moisture deficit (Wright et al., 2000). The purple coloration is indicative of hematite (Kraus and Hasiotis, 2006). Purple to green color changes and mottling have been previously associated with alternating oxidizing and reducing environments, signifying fluctuations in the height of the water table and variable fluvial discharge (Stear, 1980; Dubiel, 1987; Wilson et al., 2014). The grain size decrease associated with the color change from green to purple siltstone may indicate alternating overbank and distal crevasse deposits (Kraus and Aslan, 1993; Kraus and Wells, 1999; Abels et al., 2013).

The wide range of floodplain facies is thought to reflect the complicated discharge pattern of ephemeral rivers with standing water present for long periods in lakes and shorter periods on the draining floodplain.

5.2 Floodplain lake architectural element

Description: The floodplain lake architectural element comprises only laminated organic-rich dark gray facies of claystone and sometimes normally graded siltstone (Figs. 4E, 5; Table 1). Bedsets are 0.5 m to several meters thick (typically < 1 m thick) and stack into successions that extend over hundreds of meters, with a sharp basal contact and a gradational to sharp top surface. Bioturbation is moderate to intense (BI 3 to 5; Taylor and Goldring, 1993), including horizontal and vertical burrows.

Interpretation: Floodplain lake elements are interpreted to form through the settling from suspension of fines on waterlogged floodplains in topographic lows or in lakes, associated with poor drainage and high groundwater table.

5.3 Crevasse splay architectural element

Description: The crevasse splay architectural element includes sharp-based thinly-bedded coarse-grained siltstone and very fine-grained sandstone deposits < 2 m thick, comprising < 5 individual normally graded beds (Figs. 4F, 5). Packages are tabular and extend laterally over hundreds of meters to approximately three kilometers with sharp tops and low-relief (cm-scale) erosional basal contacts (Jordaan, 1990), which are overlain by rare sub-angular mudstone clasts (< 5 mm in diameter). Overall, packages typically coarsen-upward (

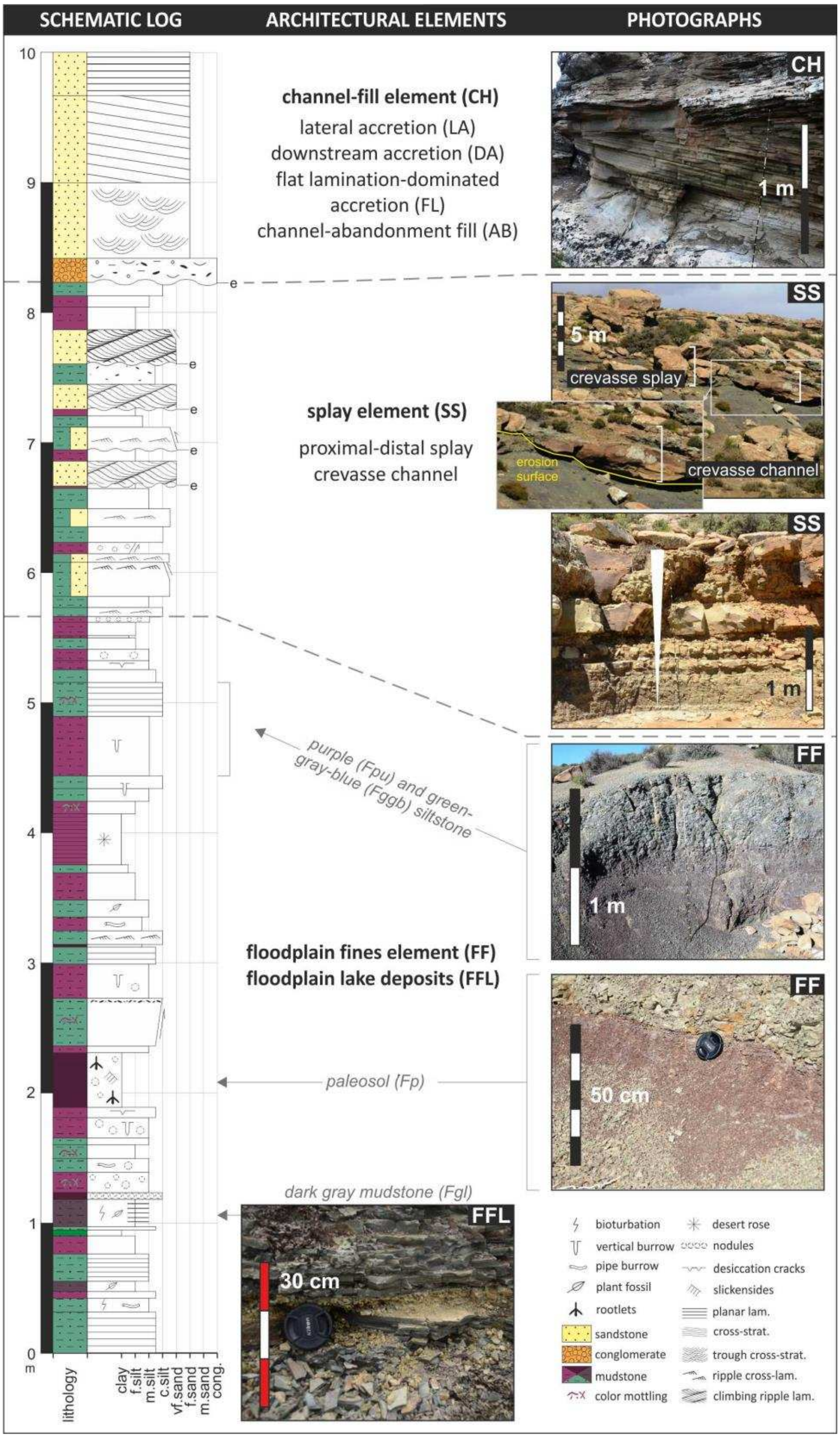

Fig. 5). The main sedimentary structures include ripple to climbing-ripple cross-lamination, with some planar lamination and structureless deposits. Bioturbation is sparse to intense (BI

1 to 5; Taylor and Goldring, 1993), with burrows, trackways (vertebrate and invertebrate) and trails common (Smith, 1990b, 1993a; Gulliford, 2014; Wilson et al., 2014). Burrow traces are widespread, consisting of both vertical and horizontal pipe burrows. Horizontal burrows are commonly straight, sinuous or branched, and may be seen cross-cutting one another. Vertical burrows are complex and variable, with either U-shaped, sub-vertical, bulbous, or chambered morphologies (Gulliford, 2014). *Scoyenia* traces are common and typically found intersecting one another, on the desiccated tops of splay deposits.

Lenticular sand bodies are 1 m to < 3 m thick (

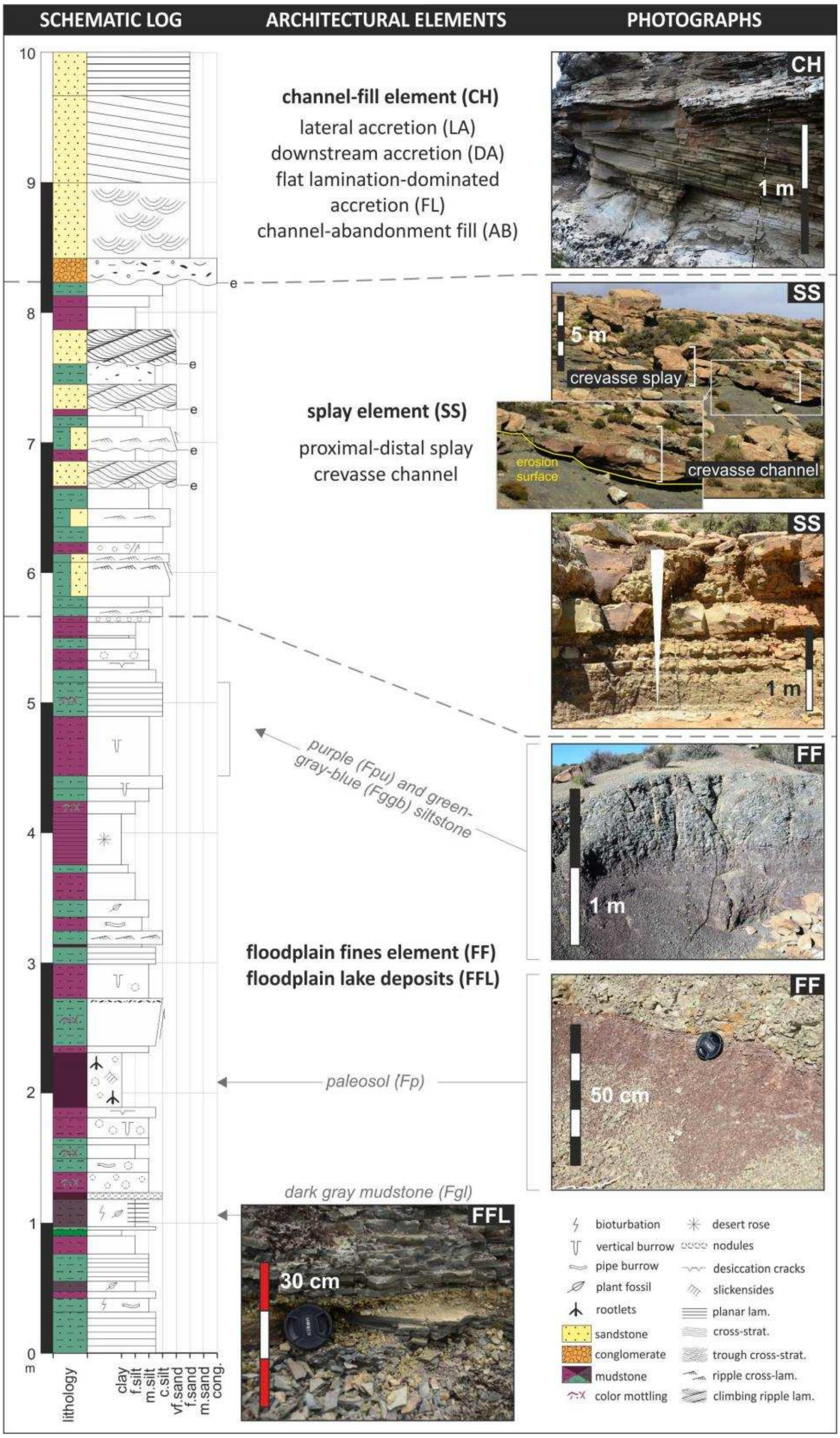

Fig. 5), single-storey and ~5-20 m wide with concave-up, scoured bases and sharp tops, and wings in cross-section, as previously noted by Stear (1983). The lenticular bodies comprise ripple cross-laminated sandstone (Sr), planar-laminated sandstone (Sh), structureless sandstone (Sm), and low angle cross-stratified sandstone (Sl), with rare trough cross-stratified sandstone (St).

Interpretation: The laterally extensive packages dominated by tractional sedimentary structures are interpreted as the products of rapid deposition from unconfined flow, and therefore as crevasse splays. The presence of structureless sandstone and/or climbing ripple cross-lamination is interpreted to indicate high rates of sediment fallout and tractional deposition that is attributed to rapid expansion and deposition from moderate to low concentration unconfined flows (Allen, 1973). The type of climbing ripple cross-lamination produced depends on the sediment fallout rate from suspension (Jopling and Walker, 1968; Allen, 1973).

The lenticular bodies are interpreted as crevasse channels. Crevasse splays and crevasse channel-fills are located adjacent to larger channel belt sandstones (3-12 m thick). These channel belts are coarser grained (i.e., upper fine-grained sandstone compared with lower fine-grained sandstone) and they typically exhibit a complex internal architecture with upper-flow-regime structures throughout. These characteristics are indicative of deposition under highly variable flow conditions (Turner, 1981; Fielding, 2006; Fielding et al., 2009; Gulliford et al., 2014; Wilson et al., 2014). Paleocurrent measurements obtained from ripple and climbing ripple cross-lamination in crevasse splay sandstones (Table 2) are typically oblique to orientations of channel belts, as reported by Gulliford et al. (2014).

5.4 Crevasse splay architecture

High-resolution 2-D analysis of two splay successions, from Klipkraal Farm (Figs. 6, 7) and Blom's Farm (Figs. 8, 9), combine sedimentary facies observations (

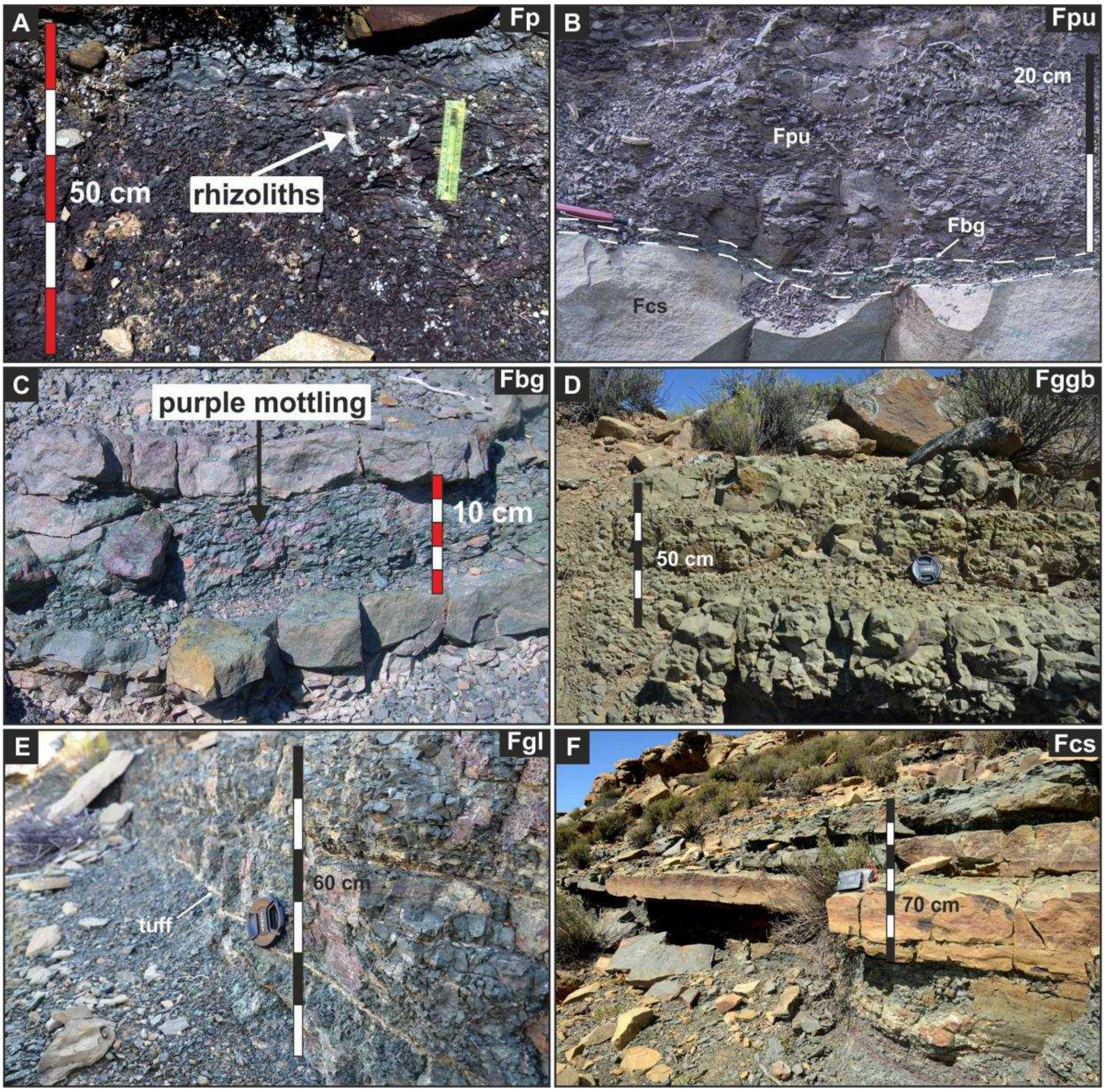

Fig. 4) with thickness and paleocurrent data (Table 2). The Klipkraal crevasse splay sand-body was analyzed in a section sub-parallel to paleoflow while the Blom's example is exposed perpendicular to paleoflow. Cross-sections illustrate horizontal and vertical changes in sedimentary facies and thickness. In both cases, the deposits are dominated by fine-grained sandstone with subordinate amounts of coarse-grained siltstone.

At Klipkraal Farm (

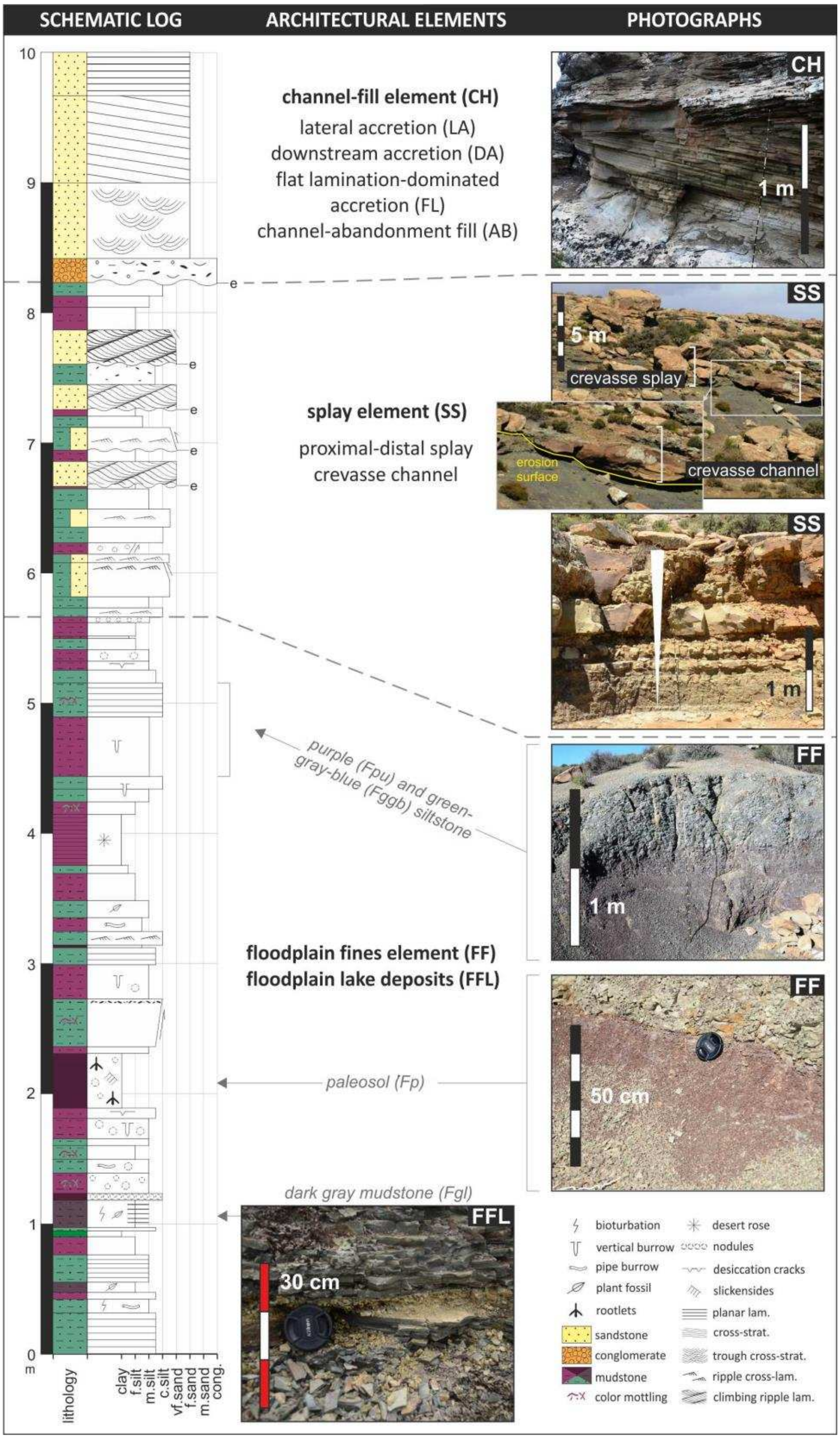

Fig. 5), the crevasse splay sand body has a measured outcrop width of 100 m, but the paleocurrent-corrected true width is 78 m (Table 2). A laterally extensive paleosol, characterized by calcrete nodules, lies < 1 m above the top of the sandstone unit and was

used as a marker bed (

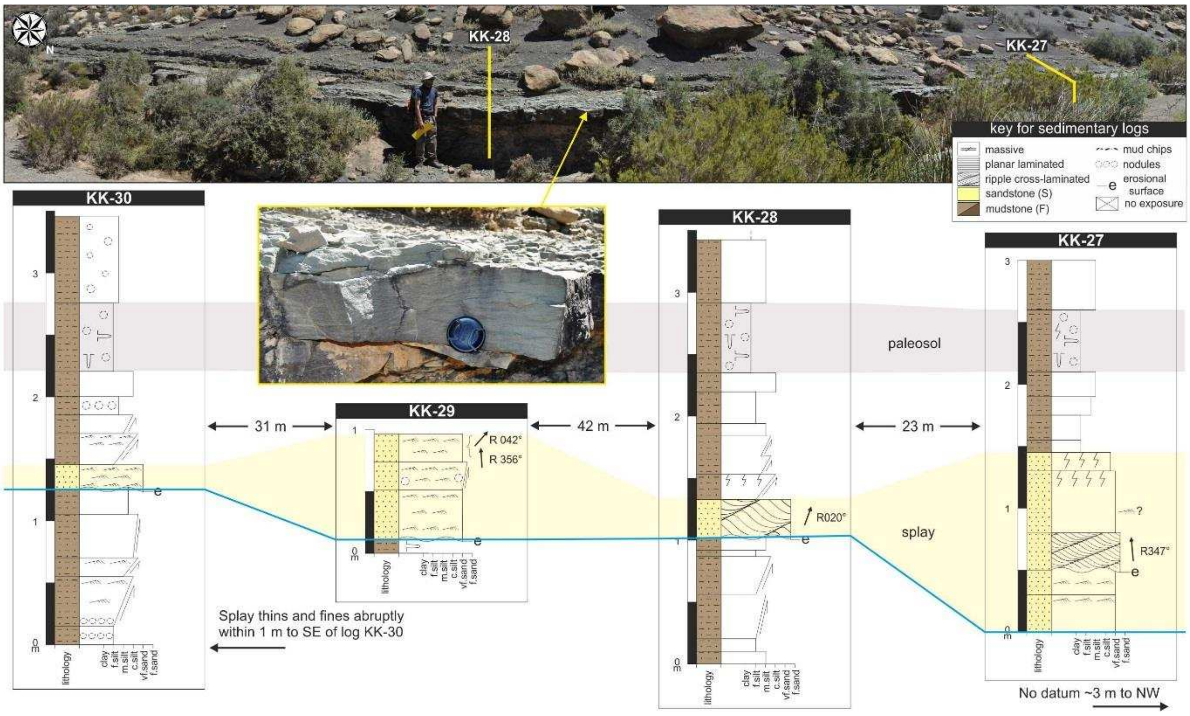

Fig. 7). The sand body varies in thickness between 0.2 m and ~1.5 m, and has a weakly erosional base into floodplain mudstone. The constituent very fine-grained sandstone beds are structureless to normally graded, or show ripple and climbing-ripple cross-lamination, with observed paleoflow ranging between 347-042° (n = 11) (

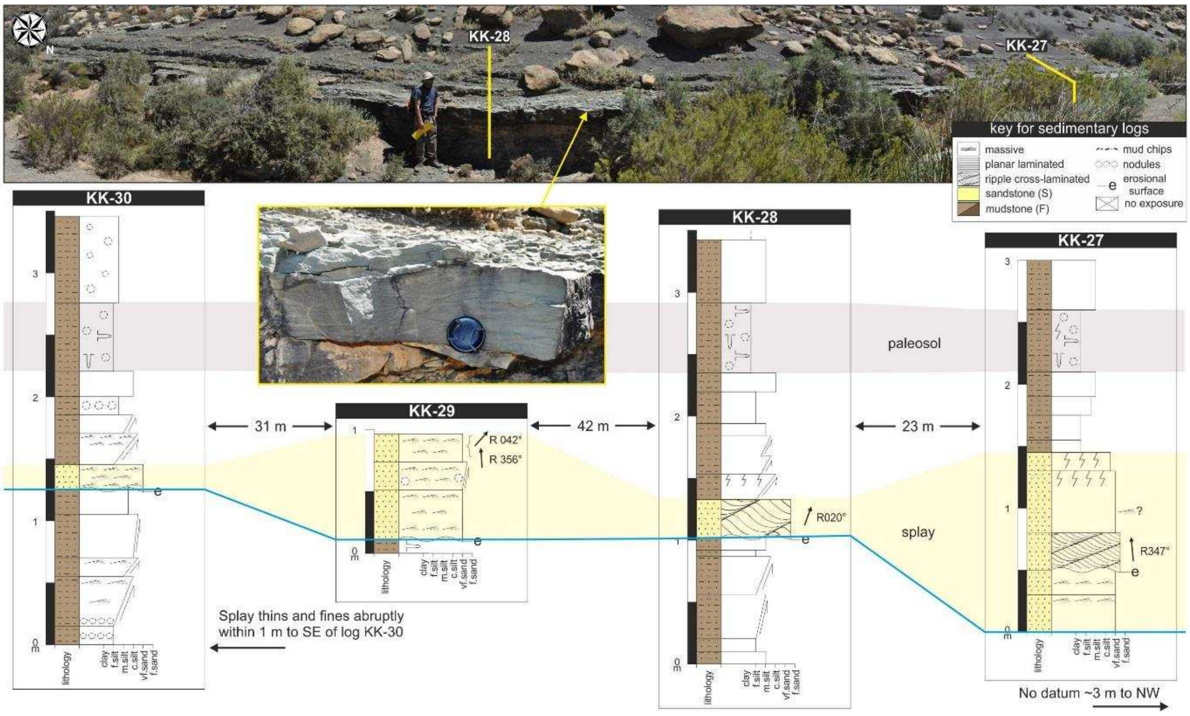

Fig. 7). The NW margin of the splay is not exposed, but the body thins and fines laterally SE of log KK-30 (

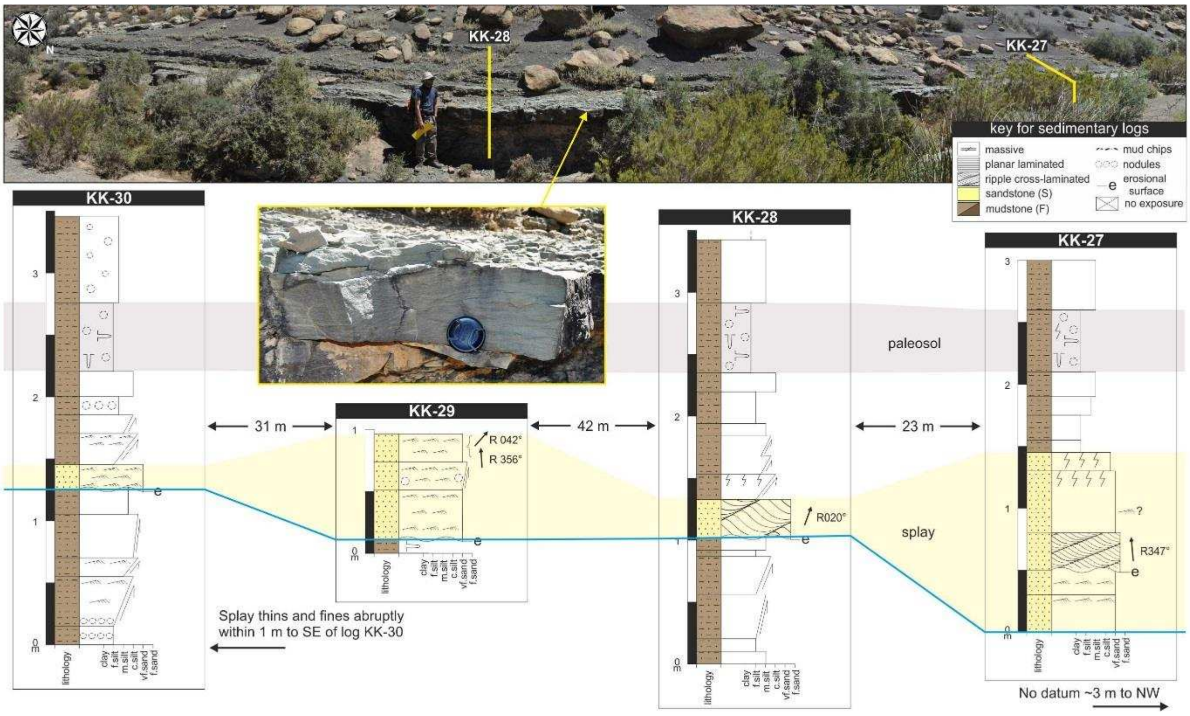

Fig. 7). In the thicker, axial section, there is a coarsening- then fining-upward profile (KK-27 and KK-29). Thin (millimeter-scale) claystone-siltstone laminae cap the splay and are characterized by horizontal and vertical burrows.

At Blom's Farm, a splay sandstone is characterized by climbing ripple cross-lamination overlain by current ripple cross-lamination (Figs. 8, 9). Measured paleocurrents range between 356-066° (n = 14), which indicates that the 190 m wide outcrop is perpendicular to paleoflow. The body thins laterally from 2 m to 1 m (

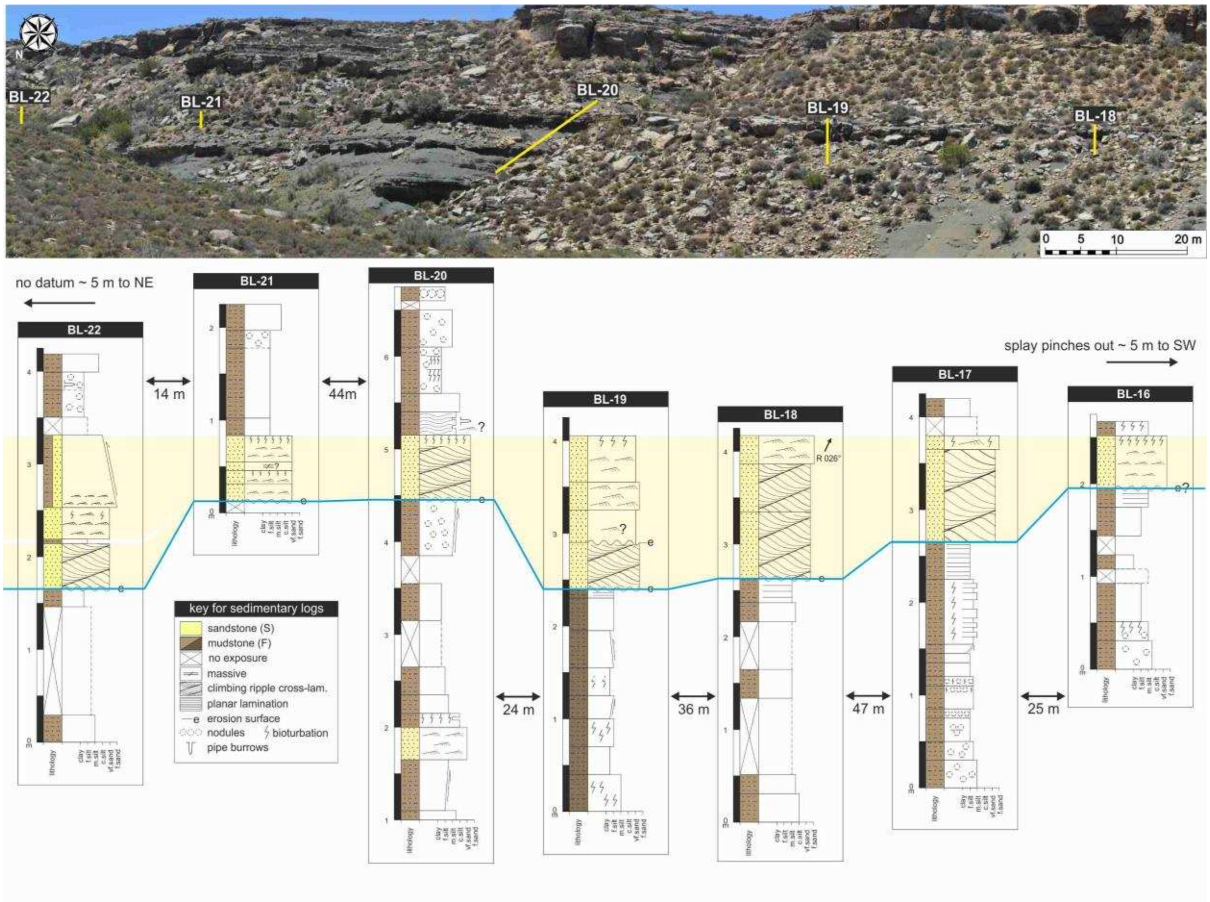

Fig. 9) and has a corrected width of 62 m (Table 2). Upper surfaces of the constituent sandstone beds are rippled or flat, with intense bioturbation destroying internal sedimentary structures. No apparent coarsening or fining trends are observed in the floodplain mudstone beneath the splay.

The geometry, sedimentology and paleoenvironmental context of these two sandstone units (Figs. 6-9) support an interpretation of crevasse splay deposits. They are finer grained than the fills of surrounding channel belts, which range from very fine- to lower medium-grained sandstone (Gulliford et al., 2014). The upward coarsening to fining trend in the splay axis is interpreted to reflect the waxing to waning of flood energy during deposition. The lateral decrease in grain size, both across strike and down dip, is attributed to reducing energy of the floodwater as the flow expanded abruptly away from the crevasse channel. The fine-grained drapes on top of crevasse splay deposits are interpreted as paleo-surfaces indicating periods of non-deposition (Stear, 1983; Smith, 1993a).

On a north-south oriented hillside at Sutherland East, sedimentary logs were measured through a continuously exposed 4 m thick package of crevasse splay deposits (Figs. 10, 11). A widespread nodular paleosol horizon forms a basal marker and logs were measured up through the package to the erosional base of an overlying channel belt sandstone. Six crevasse splay deposits with paleocurrent measurements from ripple and climbing-ripple cross-laminated very fine-grained sandstone that range between 010-079° (n = 12), are interpreted as genetically-related crevasse splays that extend for more than 700 m laterally (

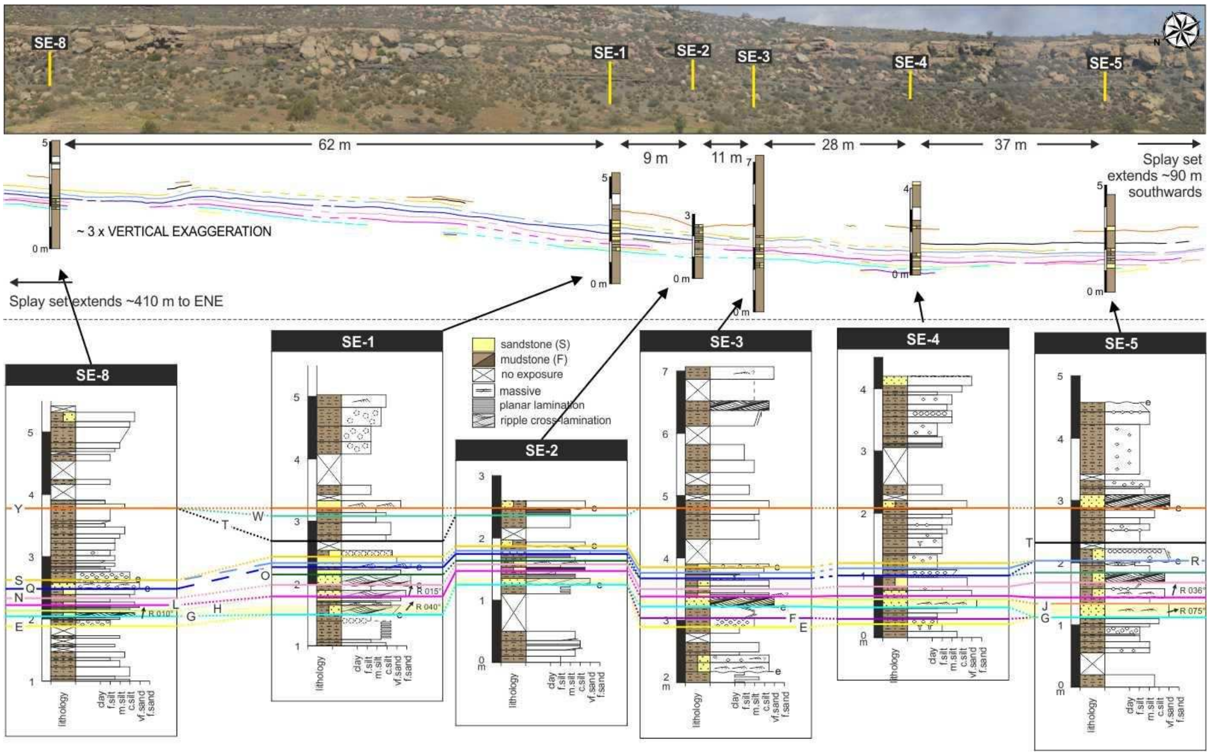

Fig. 11). The true extent of the package of crevasse splay deposits cannot be determined due to exposure limitations. Individual splay deposits comprise numerous lenticular sheets (< 0.2 m thick) of structureless or ripple cross-laminated siltstone and sandstone, and are separated by 10 cm thick but laterally extensive floodplain mudstone beds. The thin beds and abundance of coarse siltstone relative to (rare) fine-grained sandstone are interpreted to represent a distal crevasse splay setting.

6. Discussion

6.1 Crevasse splay hierarchical scheme

A hierarchical classification of fluvial channel elements is widely employed (Miall, 1985, 1996; Payenberg et al., 2011; Ford and Pyles, 2014; Gulliford et al., 2014). The same approach is more challenging to implement for overbank deposits because elements are laterally extensive and fine-grained, there is an absence of prominent erosional bounding surfaces, and their stratal relationship to parent channels is rarely preserved at outcrop. However, a crevasse splay deposit hierarchical scheme is proposed here, from bed-scale through crevasse splay element to crevasse splay set (

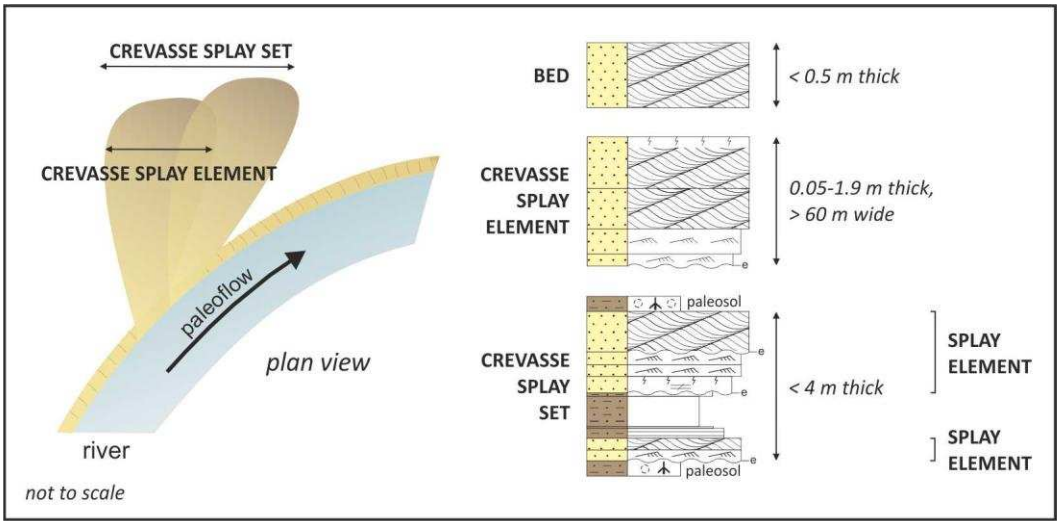

Fig. 12) that uses the presence of paleosols to subdivide the stratigraphy. In aggrading systems, deposits associated with crevasse and avulsion processes are commonly preserved (Slingerland and Smith, 2004). The floodplain aggrades due to the growth and subsequent abandonment of splay deposits (Smith et al., 1989), during periods when flow is diverted from the main fluvial channel to the floodplain, or through a full channel avulsion. Channel belt abandonment or avulsion to a position far away is represented by a paleosol or nodular horizon in the overbank deposits (Willis and Behrensmeyer, 1994) where sediment-laden

flood waters rarely encroach. Therefore, the succession between two paleosols can be considered to represent the increment of floodplain aggradation associated with a single channel belt that is close enough to actively supply sediment to the floodplain. Assuming that the rate of tectonic or compactional subsidence does not vary locally, then the thickness of the floodplain succession between paleosols will decrease with distance from the parent channel belt.

A single sandbody bounded by paleosols in a floodplain succession is a *crevasse splay element*, and is deposited during an overbank flooding event whereby a levee is breached or overtopped and material from within the channel builds up on the floodplain. The examples of well-defined sand-bodies from Klipkraal (Figs. 6, 7) and Blom's Farm (Figs. 8, 9) are interpreted as individual proximal crevasse splay elements bounded by paleosols. Stacked crevasse splay elements with similar paleocurrents and scale, and with no significant intercalated paleosols are defined as a genetically-related *crevasse splay set* that comprise two or more crevasse splay elements (

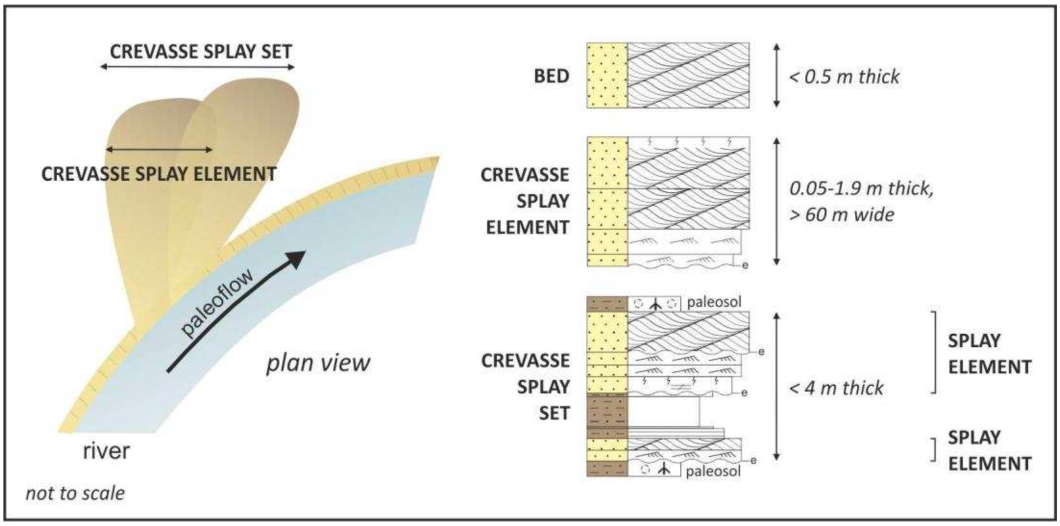

Fig. 12). Laterally, a crevasse splay set may thin and be expressed as a single crevasse splay element bounded by paleosols. The Sutherland East dataset (Figs. 10, 11) provides an example of a crevasse splay set that has significant vertical facies variability (Fig. 10B-G),

marked by repeated fining- and coarsening-upward profiles. These suggest either abrupt initiation/termination of splays or complicated, probably compensational, stacking of splay elements. Upward-coarsening above a slightly erosional base is interpreted as signifying preliminary floodplain incision and splay growth, followed by fining-upwards as flood conditions wane (Bridge, 1984).

The crevasse splay set at Sutherland East (Figs. 10, 11) is defined by a nodular horizon below and paleosol above. Each crevasse splay element within the crevasse splay set is much thinner (< 0.2 m thick) than crevasse splay elements observed at Klipkraal (Figs. 6, 7) and Blom's Farm (Figs. 8, 9) with average grain size between coarse siltstone and very fine sandstone. These characteristics together with abrupt vertical facies changes, associated with stacked, heterolithic deposits, are interpreted as a distal crevasse splay set (

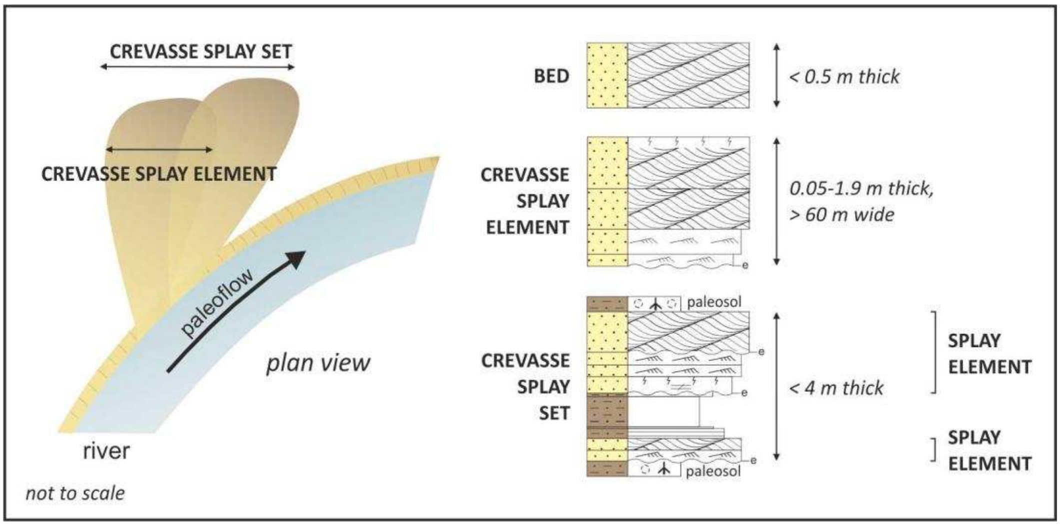

Fig. 12).

Lower in the Klipkraal Farm and Great Escarpment stratigraphy (

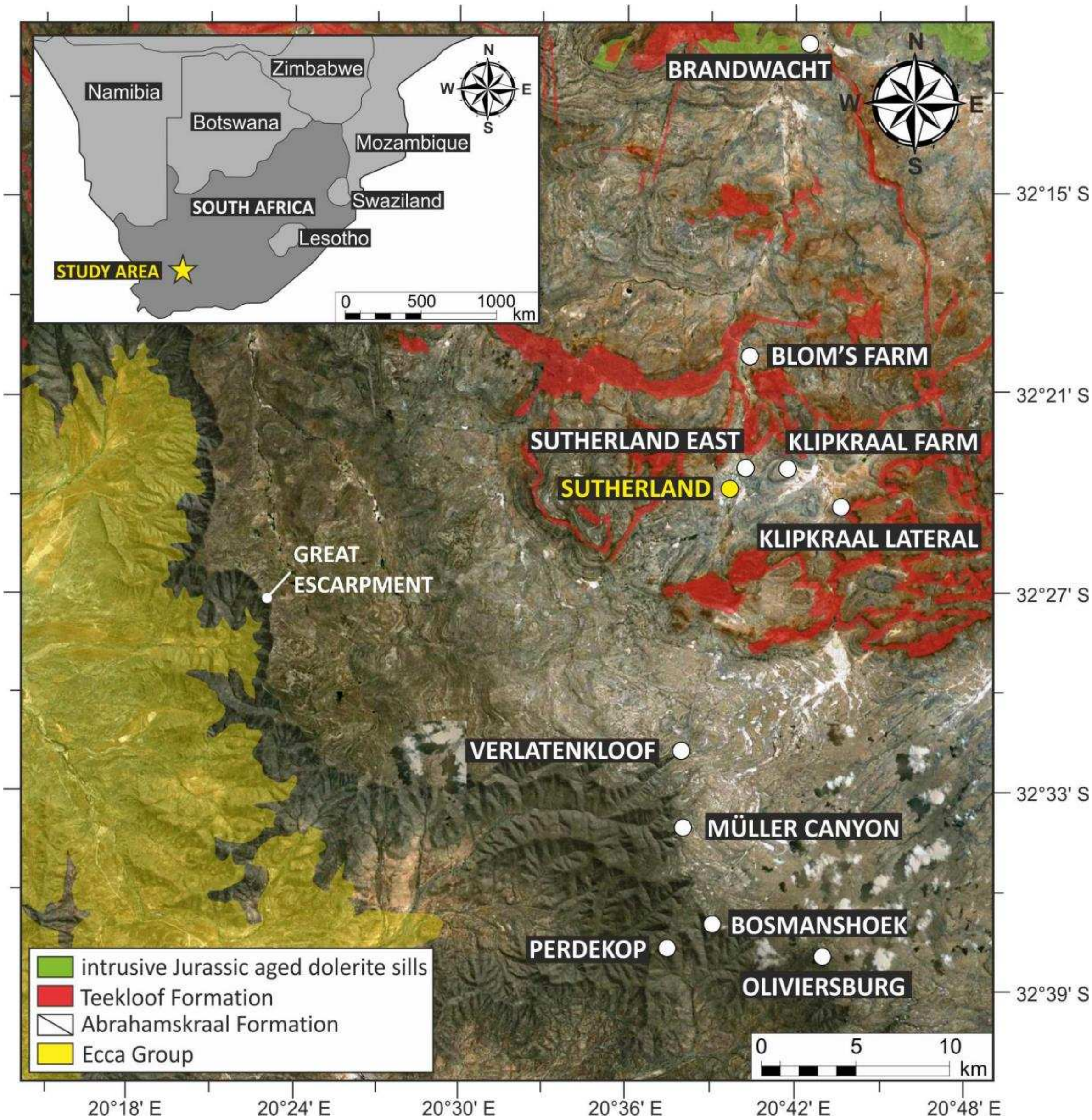

Fig. 1), paleosols are spaced at ~1.5 m intervals (0.5-2 m observed range, n = 12), with no intercalated sand-prone splays. Based on the overbank hierarchical scheme outlined above, these closely stacked paleosols are likely to have developed several kilometers from the channel belt, away from active flooding. In the younger escarpment stratigraphy, multiple crevasse splay elements are present between paleosols > 3 m apart; this architecture indicates greater sediment supply to the floodplain, suggesting a position closer to the parent channel. With reference to Kraus (1987) and Kraus and Aslan (1993), one or more

splays in a section between two paleosols should be time-equivalent to the deposition of a single- or multi-storey channel belt, and by implication, the bounding paleosols also correspond to the distal expression of other channel belts (

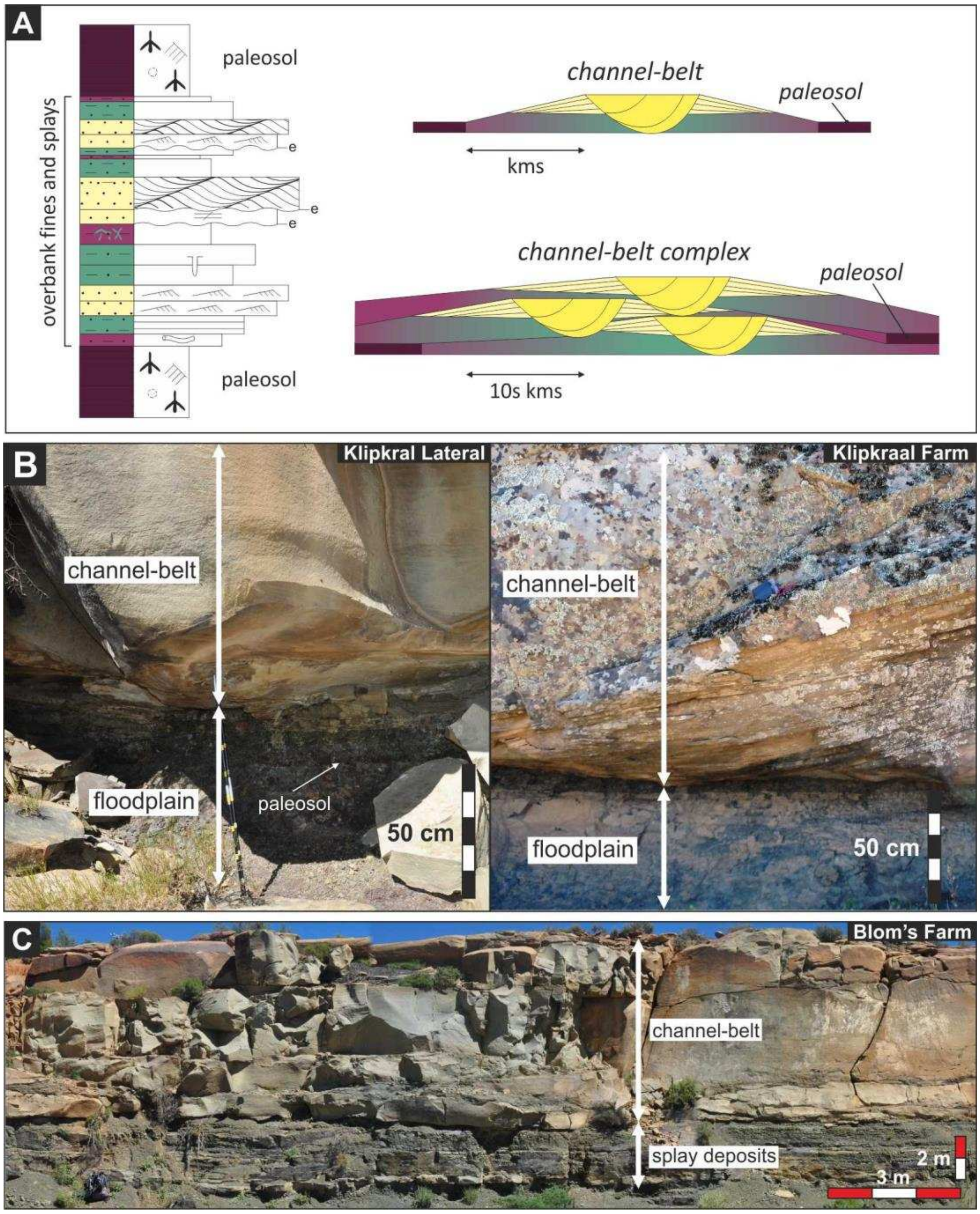

Fig. 13).

6.2 How do crevasse splay sets form?

Figure 14 presents a model for splay evolution from Beaufort Group datasets that may be generally applicable to flashy discharge fluvial systems in non-coal bearing strata. The interpreted ephemeral and flashy nature of the fluvial system with rare plant material, suggests that the banks of the channels were less stable and cohesive than channel belts from organic-rich temperate settings (Smith, 1976) and therefore more prone to crevasse and avulsion processes. Overbank fines typically settle out of suspension following flood events, and siltstone deposits fine down paleoflow (Bridge, 2006), which represents a gradual reduction in flow velocity with increasing distance from the main channel (e.g., Burns et al., 2017). Unconfined crevasse splay elements deposited in distal floodplain settings typically comprise siltstone to very fine-grained sandstone (

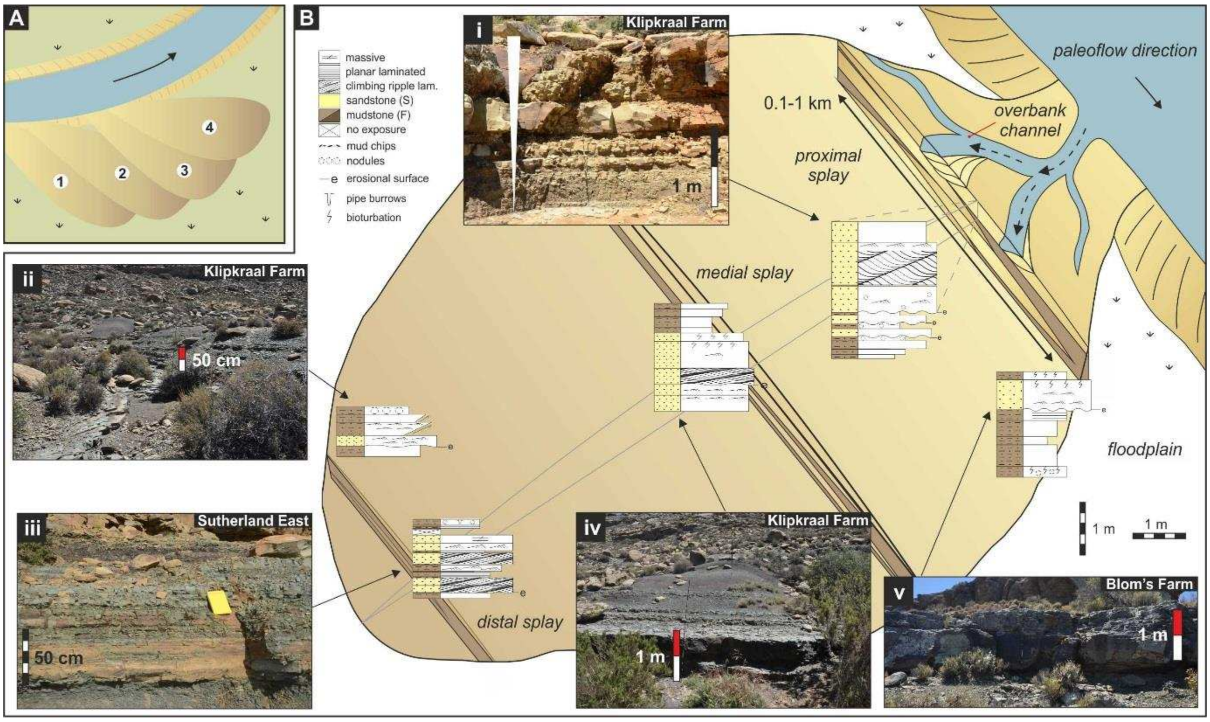

Fig. 14). Each thin splay element appears to thicken slightly at different positions along section, which supports an interpretation of compensational stacking of individual splays in a crevasse splay set (

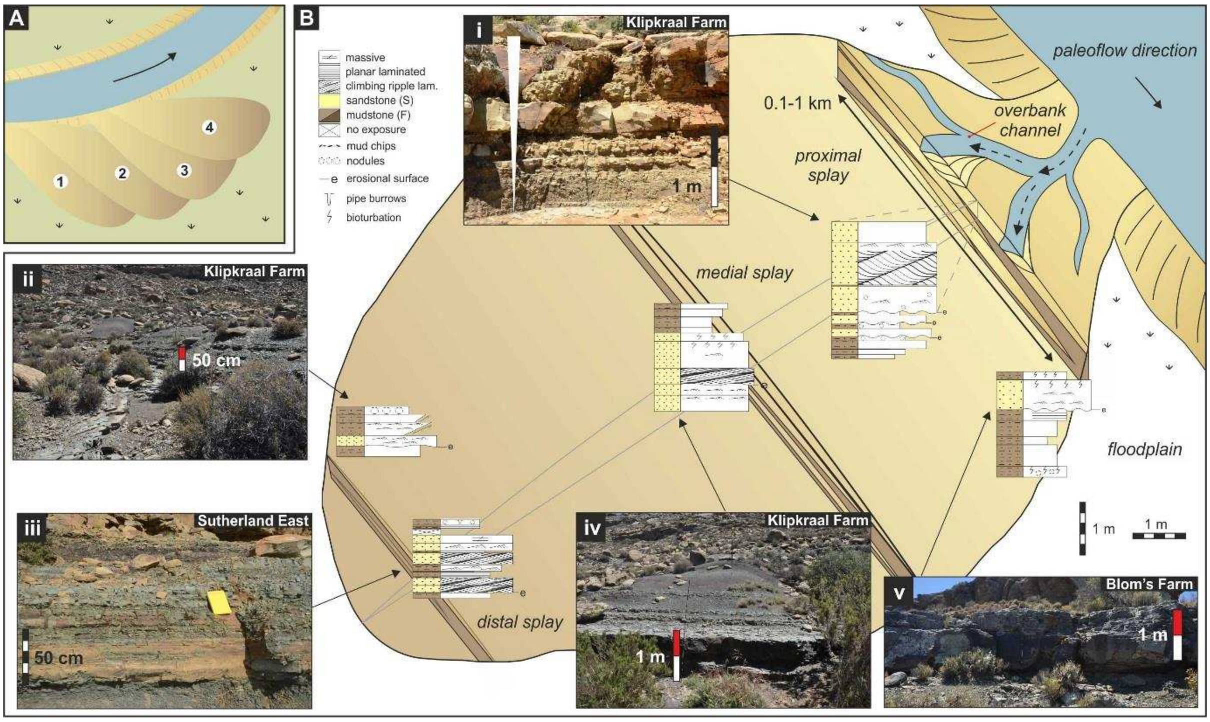

Fig. 14A). Deposits from crevasse splays differ from frontal splays in adjacent strata described by Gulliford et al. (2014) as their proximal deposits are much thinner (< 2 m thick), they are less laterally extensive, and have paleocurrent indicators oblique to the main paleochannel (

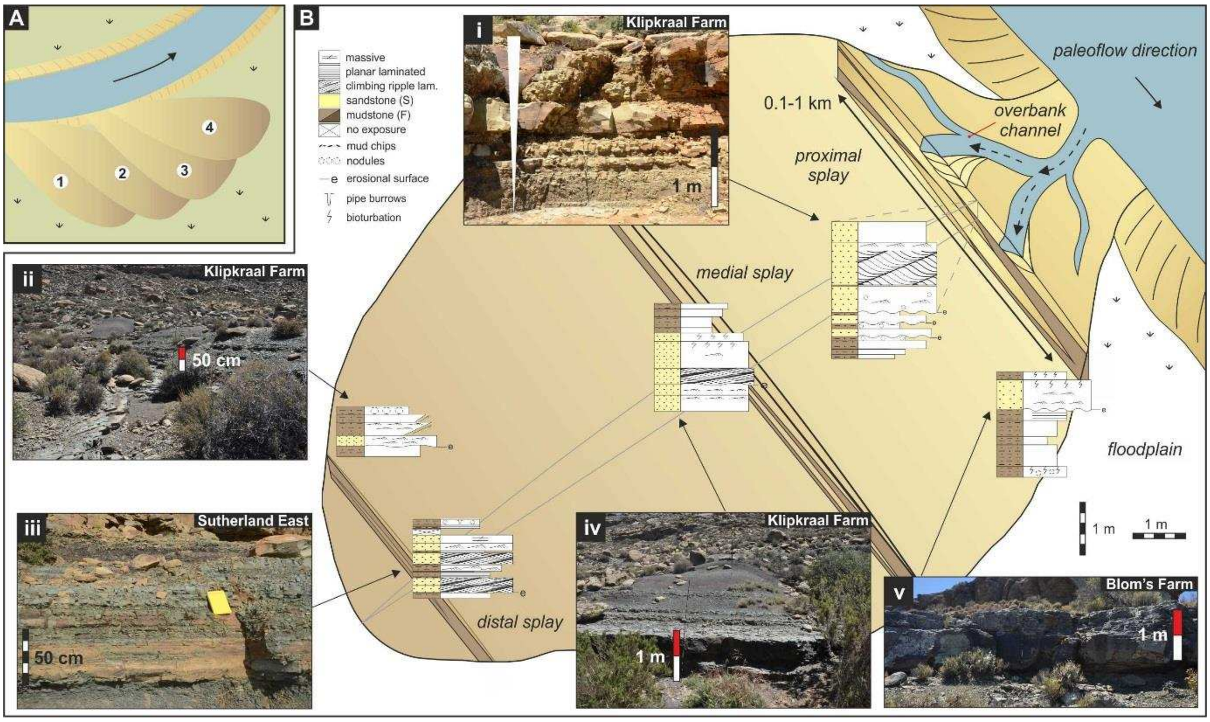

Fig. 14B). Moderate maturity paleosols developed during periods or in areas of reduced overbank flooding (

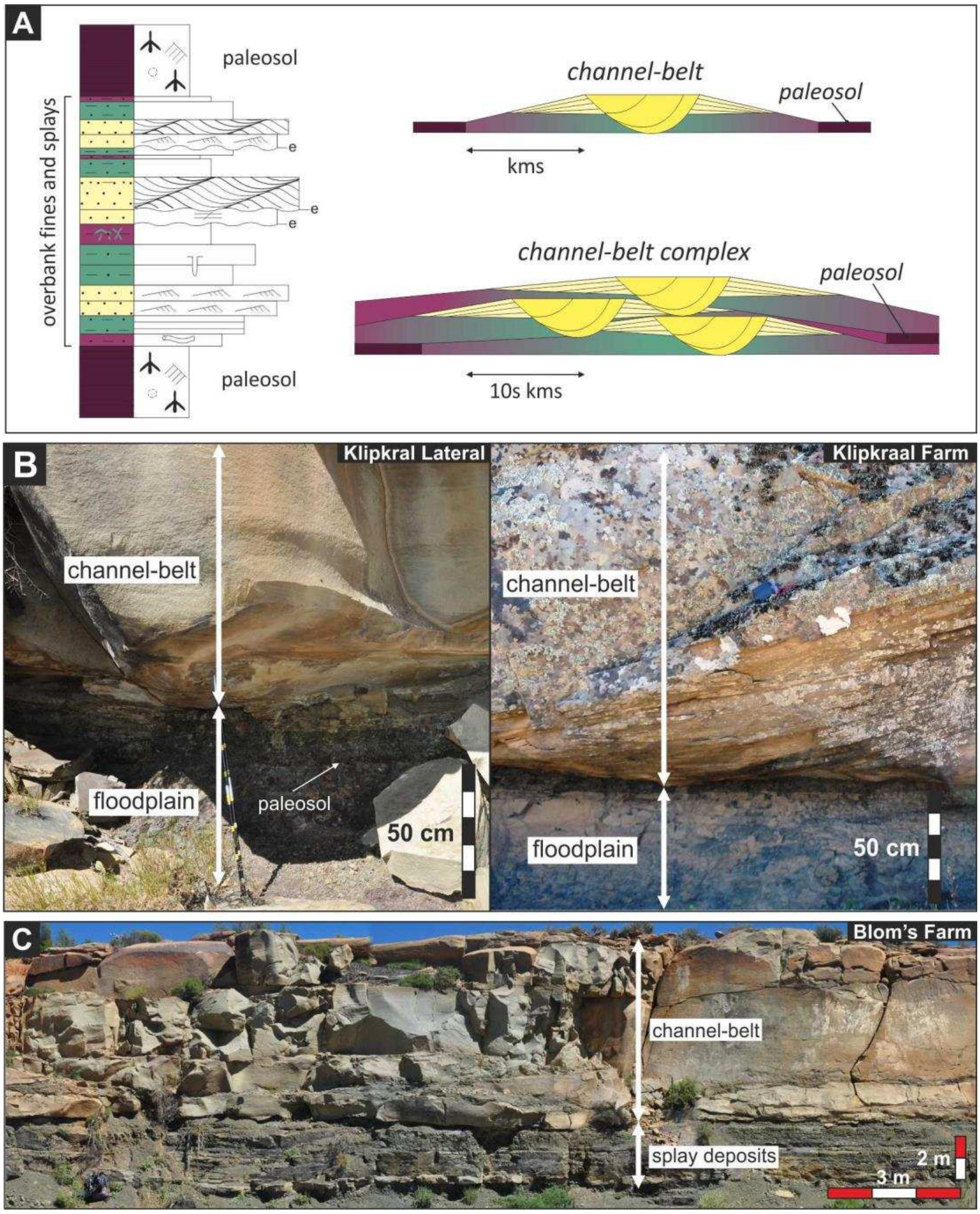

Fig. 13A) as the low sedimentation rate prevented introduction of clastic sediment.

In order for crevasse splay sets to develop, the parent channel belt and the crevasse location must stay relatively fixed during a period of multiple flood events. In crevasse- and avulsion-dominated systems, fluvial channels are highly mobile, meaning that the probability of future re-avulsion into (and out of) the area is high. Sedimentation rate affects the frequency of avulsion, which takes place when the channel belt aggrades to a critical height above the floodplain (Heller and Paola, 1996; Peakall, 1998). Once filled by splay deposits, there is no accommodation for additional material between the floodplain surface and the location of crevasse splay formation. Therefore, we suggest that a splay complex can only form with the combination of low avulsion frequency and high accommodation. In meandering systems, the area of the floodplain most prone to crevasse splay deposits, the outer bank, is also most susceptible to erosion during bend migration.

6.3 Comparison with other splay datasets

The well exposed sections from the Great Escarpment (Supplementary Figs. 1, 2) provide a database of 154 proximal and distal crevasse splay elements (for definition of proximal and distal crevasse splay elements, q.v. Burns et al. [2017]). Individual proximal crevasse splay elements range in thickness between 0.3 and 1.9 m and individual distal crevasse splay elements range between 0.05 and 1.05 m (Supplementary Table 2). Crevasse splay element geometric data from the published literature indicate that most splay elements have an aspect ratio ranging between 20:1 and 4260:1 (Coleman, 1969; Stear, 1983; O'Brien and Wells, 1986; Smith, 1987; Smith et al., 1989; Jordaan, 1990; Bristow et al., 1999; Morozova and Smith, 2000; Farrell, 2001; Stouthamer, 2001; Gulliford et al., 2014; Burns et al., 2017) (Table 3). Therefore, given that preserved mean splay thickness from the Abrahamskraal Formation is 1.1 m (proximal), their lateral extent could range from 22-4686 m. However, previous authors have not taken a hierarchical approach, and some examples are likely crevasse splay sets.

A comparison between published crevasse splay geometry and architecture from modern and ancient rivers is shown in Table 3. Some caution should be exercised when comparing modern (uncompacted) and ancient (lithified) splay thickness, although the silt- and sand-rich nature of these deposits mean that there will not be substantive compaction. Most of these studies relate to splays from temperate climates (e.g., Coleman, 1969; Smith et al., 1989; Bristow et al., 1999), preserving elongate, lobate and progradational profiles that thin and fine distally. Similar geometries have also been observed in splays deposited under ephemeral and flashy discharge conditions, from Clarence River (O'Brien and Wells, 1986) and from this study. Stage I perennial splays defined by Smith et al. (1989) from the Saskatchewan River are described as small (< 1 km^2) and lobate following initial overbank flooding, and comparable in scale and geometry to the ephemeral crevasse splay elements from Klipkraal and Blom’s Farms. There is no significant change between thicknesses of these perennial and ephemeral-flashy deposits, and the formation of Stage I, II and III splays defined by Smith et al. (1989) do not appear to be constrained to specific climatic conditions (Table 3). However, there appears to be greater lateral variability in crevasse splay deposits from ephemeral systems (Figs. 6-11), interpreted to be the result of more extreme fluctuations in discharge regime, which may intensify channel avulsion behavior (Peakall, 1998). The process of crevasse splay formation may differ slightly between perennial and ephemeral environments, with more common overtopping of channels and increased overland flow in ephemeral systems. The density and type of floodplain vegetation may also be an important variable, particularly in the development of crevasse channels, and the amount of floodplain material entrainment during overbanking.

6.4 Splay elements and splay sets as part of the distributive fluvial system model

Almost one third (31%) of channel-belts analyzed in this study (n = 98) are incised directly into floodplain mudstone (

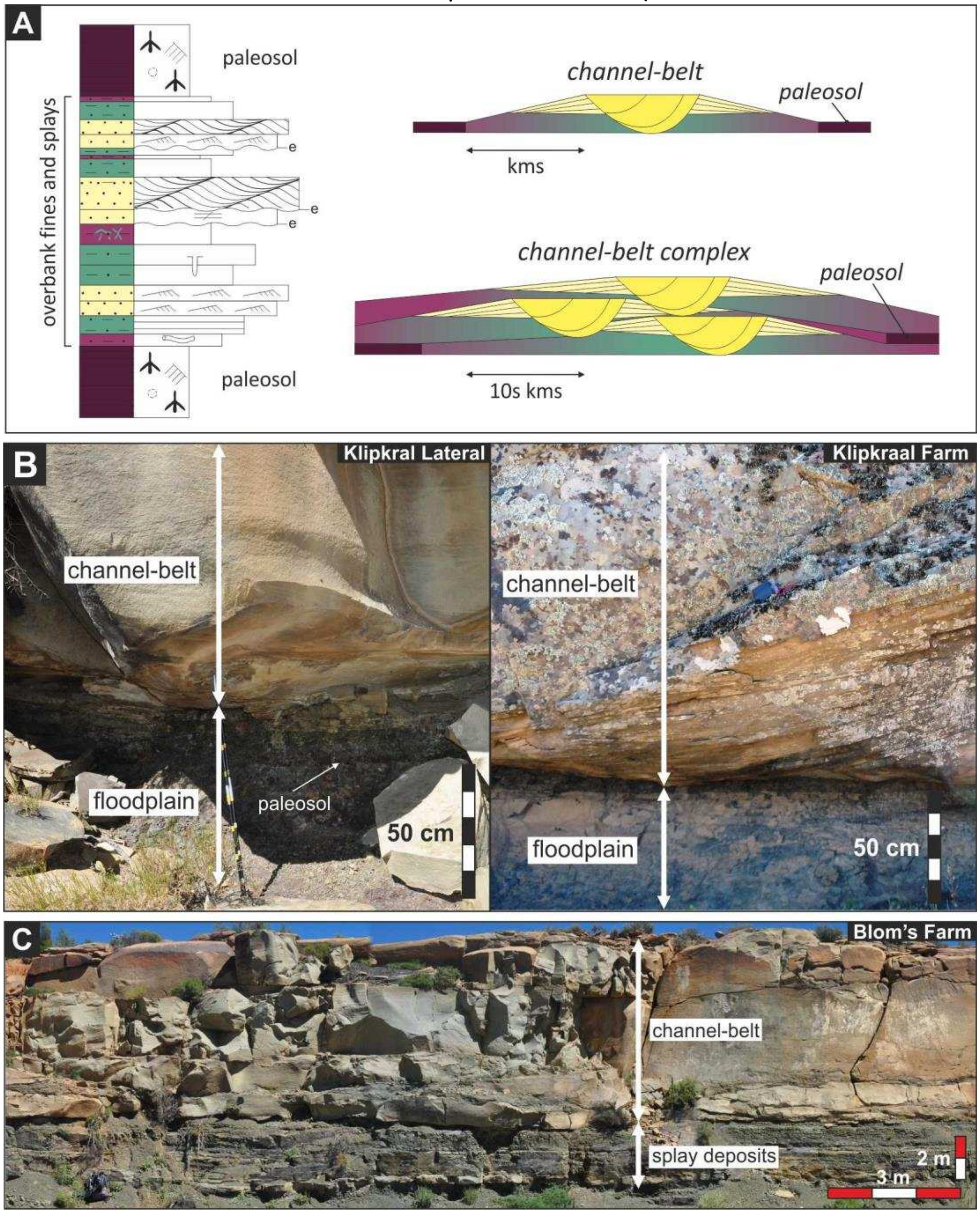

Fig. 13B) rather than into proximal overbank deposits (

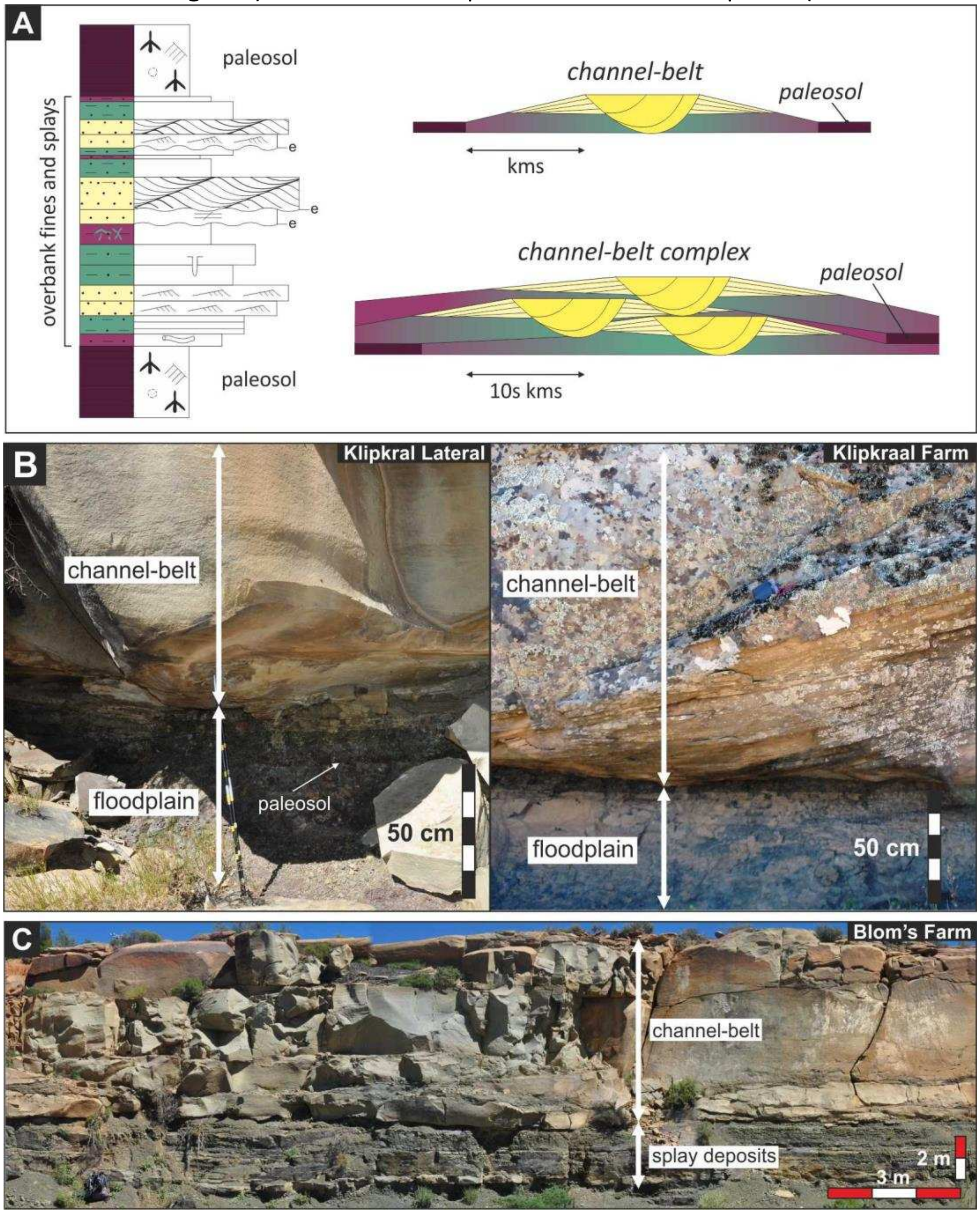

Fig. 13C), consistent with incisional avulsion (Hajek and Edmonds, 2014). However, the majority of Beaufort channel-belts (69%) are underlain by crevasse splay elements and crevasse splay sets. This style of organization has been interpreted to indicate progradational avulsion (Slingerland and Smith, 2004; Jones and Hajek, 2007; Hajek and Edmonds, 2014), in which repeated splay events eventually lead to a full channel avulsion.

The distributive fluvial system (DFS) paradigm refers to deposits from channels and floodplains that radiate from an apex, forming a fan-shaped system (Geddes, 1960; Stanistreet and McCarthy, 1993; Nichols and Fisher, 2007; Weissmann et al., 2010; Weissmann et al., 2011). Not all DFSs flow to the ocean; some terminate on alluvial plains, feed into axial rivers, or drain into lakes (Weissmann et al., 2010). Ancient successions interpreted as DFSs include the Morrison Formation of the Colorado Plateau area (Owen et al., 2017) and the lower Beaufort Group (Wilson et al., 2014; Gulliford et al., 2014).

In proximal DFS settings, Nichols and Fisher (2007) described the main floodplain components as consisting of abandoned channel deposits. In this model, overbank deposits comprising extensive floodplain mudstones and sheet sands (i.e., splays) are only preserved in the medial zones. Distal to terminal settings are also typically delineated by an abundance of thin, isolated sheet sandstones with small, poorly channelized deposits and an increased proportion of floodplain to channel belt facies, associated with a downstream decrease in the size of the channel system as sedimentation rates decrease (Nichols and Fisher 2007). This would imply that overbank deposits will continue to fine away from the active channel belt to a point where they are not inundated by sediment-charged floodwaters, enabling paleosols to develop. This is consistent with findings from the lower Beaufort Group where deposition of splays increases in the medial to distal reaches of the DFS (Gulliford et al., 2014), and crevasse splay elements are more likely to stack into crevasse splay sets (i.e., at Sutherland East). The progradational trend of crevasse splays and splay sets beneath channel belts) may correspond to the progradation of the DFS (Gulliford et al., 2014), which would then predict a greater abundance of crevasse splay elements and crevasse splay sets to be deposited within the distal to medial reaches of the advancing DFS, and a stratigraphic change from predominantly frontal to crevasse splays (Gulliford et al. 2014). This stratigraphic motif may therefore be an additional criterion for recognition of DFSs in the ancient record.

7. Conclusions

Crevasse splay deposits are important components of fluvial-overbank successions, particularly in aggradational mud-rich systems such as the lower Beaufort Group where they form up to 12% of the total 810 m studied section. Locally, individual crevasse splay elements stack to form crevasse splay sets up to 4 m thick. There is evidence for both incisional and progradational styles of avulsion. Incisional avulsion is recognized by channel belt deposits directly overlying floodplain fines. However, the great majority (69%) of crevasse deposits are characterized by a gradual upwards increase in splay deposition below a channel belt sandstone and interpreted to represent progradation(

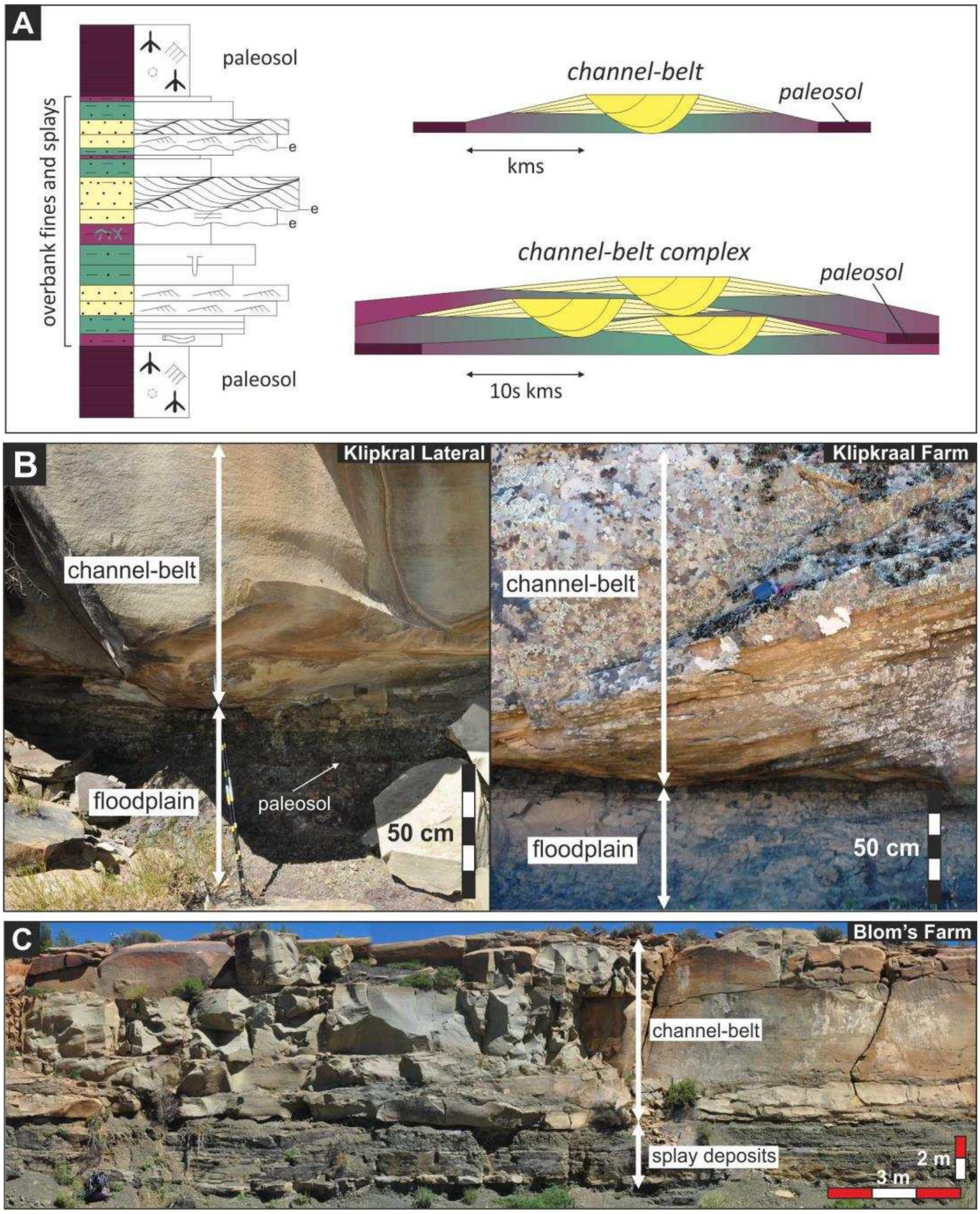

Fig. 13C). The dominance of progradational styles may be characteristic of a distributive fluvial system, rather than a trunk river system.

Overall, the thicknesses of splay deposits are comparable in different climatic settings; however, the major fluctuations in flood hydrograph and increased frequency of splay deposits associated with ephemeral systems such as the Beaufort Group is reflected in the wider range of crevasse splay widths (and aspect ratios) in deposits from small ephemeral streams, compared to those from larger perennial rivers. Crevasse splay deposits have previously been understudied in distributive fluvial systems. Splay abundance, sedimentological characteristics and stacking patterns all play an important role in identifying DFS zones (i.e., proximal, medial, distal, terminal), as well as determining avulsion frequency and floodbasin accommodation.

Acknowledgements

We acknowledge Chevron Australia Pty Ltd for funding the Beaufort Project. Special thanks to Tobias Payenberg, Anne Powell and Brian Willis. John Kavanagh, Laura Fielding, Ashley Clarke, Janet Richardson and Andrew Wilson are thanked for their support in the field. We also acknowledge the many landowners in the Sutherland area for kindly granting land access. In addition, this manuscript has significantly benefited from detailed and constructive feedback from Frank Ethridge, an anonymous reviewer and the editor, Jasper Knight.

References

Abels, H.A., Kraus, M.J., Gingerich, P.D., 2013. Precession-scale cyclicity in the fluvial lower Eocene Willwood Formation of the Bighorn Basin, Wyoming (USA). Sedimentology 60, 1467−1483.

Allen, J.R.L., 1973. A classification of climbing-ripple cross-lamination. Journal of the Geological Society 129, 537−541.

Allen, J.R.L., 1983. Studies in fluviatile sedimentation: Bars, bar-complexes and sandstone sheets (low-sinuosity braided streams) in the Brownstones (L. Devonian), Welsh Borders. Sedimentary Geology 33, 237−293.

Ambrose, W.A., Lakshminarasimhan, S., Holtz, M.H., Nunez-Lopez, V., Hovorka, S.D., Duncan, I., 2008. Geologic factors controlling CO_2 storage capacity and permanence: case studies based on experience with heterogeneity in oil and gas reservoirs applied to CO_2 storage. Environmental Geology 54, 1619−1633.

Ayers Jr, W.B., 2002. Coalbed gas systems, resources, and production and a review of contrasting cases from the San Juan and Powder River basins. AAPG Bulletin 86, 1853−1890.

Blakey, R.C., Gubitosa, R., 1984. Controls of sandstone body geometry and architecture in the Chinle Formation (Upper Triassic), Colorado Plateau. Sedimentary Geology 38, 51−86.

Bridge, J.S., 1984. Large-scale facies sequences in alluvial overbank environments. Journal of Sedimentary Petrology 54, 583−588.

Bridge, J.S., 2003. Rivers and floodplains: Forms, processes, and sedimentary record. Blackwell Science, Oxford 491 pp.

Bridge, J.S., 2006. Fluvial facies models: Recent developments. In: Posamentier, H.W., Walker, R.G. (Eds.), Facies Models Revisited. SEPM Special Publication 84, Tulsa, OK., pp. 85−170.

Bridge, J.S., Tye, R.S., 2000. Interpreting the dimensions of ancient fluvial channel bars, channels, and channel belts from wireline-logs and cores. AAPG Bulletin 84, 1205−1228.

Bristow, C.S., Skelly, R.L., Ethridge, F.G., 1999. Crevasse splays from the rapidly aggrading, sand-bed, braided Niobrara River, Nebraska: effect of base-level rise. Sedimentology 46, 1029−1048.

Burns, C.E., Mountney, N.P., Hodgson, D.M., Colombera, L., 2017. Anatomy and dimensions of fluvial crevasse-splay deposits: Examples from the Cretaceous Castlegate Sandstone and Neslen Formation, Utah, USA. Sedimentary Geology, 351, 21-35.

Coleman, J.M., 1969. Brahmaputra River: channel processes and sedimentation. Sedimentary Geology 3, 129−239.

Colombera, L., Mountney, N.P., McCaffrey, W.D., 2012. A relational database for the digitization of fluvial architecture concepts and example applications. Petroleum Geoscience 18, 129−140.

Colombera, L., Mountney, N.P., McCaffrey, W.D., 2013. A quantitative approach to fluvial facies models: Methods and example results. Sedimentology 60, 1526−1558.

Council for Geoscience, 1983. Geological map 3220 Sutherland Council for Geoscience, Pretoria.

Dubiel, R.F., 1987. Sedimentology of the Upper Triassic Chinle Formation southeastern Utah: Paleoclimatic implications. Journal of the Arizona-Nevada Academy of Science 22, 35−45.

Ethridge, F.G., Jackson, T.J., Youngberg, A.D., 1981. Floodbasin sequence of a fine-grained meander belt subsystem: the coal-bearing Lower Wasatch and Upper Fort Union Formations Southern Powder River Basin, Wyoming. In: Ethridge, F.G., Flores, R.M. (Eds.). Recent and ancient nonmarine depositional environments – Models for exploration: SEPM Special Publication 31, 191−209.

Farrell, K.M., 2001. Geomorphology, facies architecture, and high-resolution, non-marine sequence stratigraphy in avulsion deposits, Cumberland Marshes, Saskatchewan. Sedimentary Geology 139, 93−150.

Fielding, C.R., 2006. Upper flow regime sheets, lenses and scour fills: Extending the range of architectural elements for fluvial sediment bodies. Sedimentary Geology 190, 227−240.

Fielding, C.R., Allen, J.P., Alexander, J., Gibling, M.R., 2009. Facies model for fluvial systems in the seasonal tropics and subtropics. Geology, 37, 623-626.

Fielding, C.R., Ashworth, P.J., Best, J.L., Prokocki, E.W., Sambrook Smith., S.H., 2012. Tributary, distributary and other fluvial patterns: What really represents the norm in the continental rock record?. Sedimentary Geology 261, 15-32.

Fisher, J.A., Krapf, C.B.E., Lang, S.C., Nichols, G.J., Payenberg, T.H.D., 2008. Sedimentology and architecture of the Douglas Creek terminal splay, Lake Eyre, central Australia. Sedimentology 55, 1915−1930.

Flint, S.S., Hodgson, D.M., Sprague, A.R., Brunt, R.L., Van der Merwe, W.C., Figueiredo, J., Prélat, A., Box, D., Di Celma, C., Kavanagh, J.P., 2011. Depositional architecture and sequence stratigraphy of the Karoo basin floor to shelf edge succession, Laingsburg depocentre, South Africa. Marine and Petroleum Geology 28, 658−674.

Flores, R.M., 1983. Basin facies analysis of coal-rich Tertiary fluvial deposits, northern Powder River Basin, Montana and Wyoming. In: Collinson, J.D., Lewin, J. (Eds.), Modern and ancient fluvial systems: International Association of Sedimentologists Special Publication 6, Oxford, pp. 499−515.

Ford, G.L., Pyles, D.R., 2014. A hierarchical approach for evaluating fluvial systems: Architectural analysis and sequential evolution of the high net-sand content middle Wasatch Formation, Uinta Basin, Utah. AAPG Bulletin 98, 1273−1304.

Friend, P.F., 1983. Towards the field classification of alluvial architecture or sequence. Modern and ancient fluvial systems. International Association of Sedimentologists Special Publication Oxford 345 pp.

Geddes, A., 1960. The alluvial morphology of the Indo-Gangetic Plain: Its mapping and geographical significance. Transactions and Papers (Institute of British Geographers) 28, 253-276.

Gouw, M.J.P., Berendsen, H.J.A., 2007. Variability of channel belt dimensions and the consequences for alluvial architecture: observations from the Holocene Rhine-Meuse delta (The Netherlands) and Lower Mississippi Valley (USA). Journal of Sedimentary Research 77, 124−138.

Gulliford, A.R., 2014. Controls on river and overbank processes in an aggradation-dominated system: Permo-Triassic Beaufort Group, South Africa. PhD Thesis, University of Manchester, UK, 361 pp.

Gulliford, A.R., Flint, S.S., Hodgson, D.M., 2014. Testing applicability of models of distributive fluvial systems or trunk rivers in ephemeral systems: Reconstructing 3-D fluvial architecture in the Beaufort Group, South Africa. Journal of Sedimentary Research 84, 1147−1169.

Hajek, E.A., Edmonds, D.A., 2014. Is river avulsion style controlled by floodplain morphodynamics? Geology 42, 199−202.

Hartley, A.J., Weissmann, G.S., Nichols, G.J., Scuderi, L.A., 2010a. Fluvial form in modern continental sedimentary basins: Distributive fluvial systems: REPLY. Geology 38, 231-231.

Hartley, A.J., Weissmann, G.S., Nichols, G.J., Warwick, G.L., 2010b. Large distributive fluvial systems: characteristics, distribution, and controls on development. Journal of Sedimentary Research 80, 167-183.

Hasiotis, S.T., Van Wagoner, J.C., Demko, T.M., Wellner, R.W., Jones, C.R., Hill, R.E., McCrimmon, G.G., Feldman, H.R., Drzewiecki, P.A., Patterson, P. and Donovan, A.D. (2002). Continental ichnology: using terrestrial and freshwater trace fossils for environmental and climatic interpretations. SEPM Short Course, 51.

Heller, P.L., Paola, C., 1996. Downstream changes in alluvial architecture: an exploration of controls on channel-stacking patterns. Journal of Sedimentary Research 66, 297-306.

Horne, J.C., Ferm, J.C., Caruccio, F.T., Baganz, B.P., 1978. Depositional models in coal exploration and mine planning in Appalachian region. AAPG Bulletin 62, 2379−2411.

Iwere, F.O., Moreno, J.E., Apaydin, O.G., 2006. Numerical Simulation of Thick Tight Fluvial Sands. SPE Reservoir Evaluation and Engineering 9, 374−381.

Jenson, M.A., Pedersen, G.K., 2010. Architecture of vertically stacked fluvial deposits, Atane Formation, Cretaceous, Nuussuaq, central West Greenland. Sedimentology 57, 1280−1314.

Jerrett, R.M., Hodgson, D.M., Flint, S.S., Davies, R.C., 2011. Control of Relative Sea Level and Climate on Coal Character in the Westphalian C (Atokan) Four Corners Formation, Central Appalachian Basin, USA. Journal of Sedimentary Research 81, 420−445.

Johnson, M.R., Van Vuuren, C.J., Visser, J.N.J., Cole, D.I., Wickens, H.D.V., Christie, A.D.M., Roberts, D.L., 1997. The foreland Karoo Basin, South Africa. In: Selley, R.C. (Ed.), Sedimentary Basins of the World. African Basins. Elsevier Science, Amsterdam, pp. 269−317.

Jones, H.L., Hajek, E.A., 2007. Characterizing avulsion stratigraphy in ancient alluvial deposits. Sedimentary Geology 202, 124−137.

Jopling, A.V., Walker, R.G., 1968. Morphology and origin of ripple-drift cross-lamination, with examples from the Pleistocene of Massachusetts. Journal of Sedimentary Research 38, 971−984.

Jordaan, M.J., 1990. Basin analysis of the Beaufort Group in the western part of the Karoo Basin. PhD Thesis, University of the Orange Free State, South Africa, 283 pp.

Jørgensen, P.J., Fielding, C.R., 1996. Facies architecture of alluvial floodbasin deposits: three-dimensional data from the Upper Triassic Callide Coal Measures of east-central Queensland, Australia. Sedimentology 43, 479−495.

Kraus, M.J., 1987. Integration of channel and floodplain suites, II. Vertical relations of alluvial paleosols. Journal of Sedimentary Research 57, 602−612.

Kraus, M.J., Aslan, A., 1993. Eocene hydromorphic paleosols: significance for interpreting ancient floodplain processes. Journal of Sedimentary Research 63, 453-463.

Kraus, M.J., Wells, T.M., 1999. Recognizing avulsion deposits in the ancient stratigraphical record. In: Smith, N.D., Rogers, J. (Eds.), Fluvial Sedimentology VI, Special Publication International Association of Sedimentologists 28, 251−268.

Kraus, M.J., Hasiotis, S.T., 2006. Significance of different modes of rhizolith preservation to interpreting paleoenvironmental and paleohydrologic settings: examples from

Paleogene paleosols, Bighorn Basin, Wyoming, USA. Journal of Sedimentary Research 76, 633−646.

Leeder, M.R., 1975. Pedogenic carbonates and flood sediment accretion rates: a quantitative model for alluvial arid-zone lithofacies. Geological Magazine 112, 257−270.

Miall, A.D., 1985. Architectural-element analysis − a new method of facies analysis applied to fluvial deposits. Earth-Science Reviews 22, 261−308.

Miall, A.D., 1988. Architectural elements and bounding surfaces in fluvial deposits: anatomy of the Kayenta Formation (Lower Jurassic), south-west Colorado. Sedimentary Geology 55, 233−262.

Miall, A.D., 1996. The geology of fluvial deposits. Springer-Verlag, New York, 582 pp.

Mjøs, R., Walderhaug, O., Prestholm, E., 1993. Crevasse splay sandstone geometries in the Middle Jurassic Ravenscar Group of Yorkshire, UK. In: Marzo, M., Puigdefábregas, C. (Eds.), Alluvial Sedimentation, International Association of Sedimentologists, Special Publication 17. John Wiley and Sons, Oxford, 184 pp.

Mohrig, D., Heller, P.L., Paola, C., Lyons, W.J., 2000. Interpreting avulsion process from ancient alluvial sequences: Guadalope-Matarranya system (northern Spain) and Wasatch Formation (western Colorado). Geological Society of America Bulletin 112, 1787-1803.

Morozova, G.S., Smith, N.D., 2000. Holocene avulsion styles and sedimentation patterns of the Saskatchewan River, Cumberland Marshes, Canada. Sedimentary Geology 130, 81−105.

Nanson, G.C., Croke, J.C., 1992. A genetic classification of floodplains. Geomorphology 4, 459−486.

Nichols, G.J., 2009. Sedimentology and stratigraphy. John Wiley and Sons, Oxford, 432 pp.
Nichols, G.J., Fisher, J.A., 2007. Processes, facies and architecture of fluvial distributary system deposits. Sedimentary Geology 195, 75−90.
Owen, A., Nichols, G.J., Hartley, A.J., Weissmann, G.S., 2017. Vertical trends within the prograding Salt Wash distributive fluvial system, SW United States. Basin Research 29, 64-80.
O'Brien, P.E., Wells, A.T., 1986. A small, alluvial crevasse splay. Journal of Sedimentary Research 56, 876−879.
Pashin, J.C., 1998. Stratigraphy and structure of coalbed methane reservoirs in the United States: an overview. International Journal of Coal Geology 35, 209−240.
Payenberg, T.H.D., Reilly, M.R.W., Lang, S.C., Kassan, J., 2004. Sedimentary processes in an ephemeral river and terminal splay complex, Lake Eyre, Central Australia - observation from the February 2003 flooding event. AAPG Search and Discovery Article #90034.
Payenberg, T.H.D., Willis, B.J., Bracken, B., Posamentier, H.W., Pyrcz, M.J., Pusca, V., Sullivan, M.D., 2011. Revisiting the subsurface classification of fluvial sandbodies. AAPG Search and Discovery Article #90124.
Peakall, J., 1998. Axial river evolution in response to half-graben faulting: Carson River, Nevada, USA. Journal of Sedimentary Research 68, 788-799.
Pranter, M.J., Cole, R.D., Panjaitan, H., Sommer, N.K., 2009. Sandstone-body dimensions in a lower coastal-plain depositional setting: Lower Williams Fork Formation, Coal Canyon, Piceance Basin, Colorado. AAPG Bulletin 93, 1379−1401.
Pysklywec, R.N., Mitrovica, J.X., 1999. The role of subduction-induced subsidence in the evolution of the Karoo Basin. The Journal of Geology 107, 155−164.

Sambrook Smith, G.H., Best, J.L., Ashworth, P.J., Fielding, C.R., Goodbred, S.L., Prokocki, E.W., 2010. Fluvial form in modern continental sedimentary basins: Distributive fluvial systems: Comment. Geology 38, 230-230.

Shanley, K.W., Cluff, R.M., Robinson, J.W., 2004. Factors controlling prolific gas production from low-permeability sandstone reservoirs: Implications for resource assessment, prospect development, and risk analysis. AAPG Bulletin 88, 1083−1121.

Singh, H., Parkash, B., Gohain, K., 1993. Facies analysis of the Kosi megafan deposits. Sedimentary Geology 85, 87−113.

Slingerland, R., Smith, N.D., 2004. River avulsions and their deposits. Annual Review of Earth and Planetary Sciences 32, 257−285.

Smith, D.G., 1976. Effect of vegetation on lateral migration of anastomosed channels of a glacier meltwater river. Geological Society of America Bulletin 87, 857−860.

Smith, N.D., Cross, T.A., Dufficy, J.P., Clough, S.R., 1989. Anatomy of an avulsion. Sedimentology 36, 1−23.

Smith, R.M.H., 1987. Morphology and depositional history of exhumed Permian point bars in the southwestern Karoo, South Africa. Journal of Sedimentary Petrology 57, 19−29.

Smith, R.M.H., 1990a. Alluvial Paleosols and Pedofacies Sequences in the Permian Lower Beaufort of the Southwestern Karoo Basin, South-Africa. Journal of Sedimentary Petrology 60, 258−276.

Smith, R.M.H., 1990b. A review of stratigraphy and sedimentary environments of the Karoo Basin of South Africa. Journal of African Earth Sciences 10, 117−137.

Smith, R.M.H., 1993a. Sedimentology and Ichnology of Floodplain Paleosurfaces in the Beaufort Group (Late Permian), Karoo Sequence, South Africa. Palaios 8, 339−357.

Smith, R.M.H., 1993b. Vertebrate taphonomy of Late Permian floodplain deposits in the southwestern Karoo Basin of South Africa. Palaios 8, 45−67.

Stear, W.M., 1978. Sedimentary structures related to fluctuating hydrodynamic conditions in flood plain deposits of the Beaufort Group near Beaufort West, Cape. Transactions of the Geological Society of South Africa 81, 393−399.

Stear, W.M., 1980. The sedimentary environment of the Beaufort Group Uranium Province in the vacinity of Beaufort West, South Africa. PhD Thesis, University of Port Elizabeth, South Africa, 257 pp.

Stear, W.M., 1983. Morphological characteristics of ephemeral stream channel and overbank splay sandstone bodies in the Permian lower Beaufort Group, Karoo Basin, South Africa. In: Collinson, J.D., Lewin, J. (Eds.), Modern and ancient fluvial systems: International Association of Sedimentologists Special Publication 6, Oxford, pp. 405−420.

Stouthamer, E., 2001. Sedimentary products of avulsions in the Holocene Rhine–Meuse delta, The Netherlands. Sedimentary Geology 145, 73−92.

Stuart, J.Y., Mountney, N.P., McCaffrey, W.D., Lang, S., Collinson, J.D., 2014. Prediction of channel connectivity and fluvial style in the flood basin successions of the Upper Permian Rangal Coal Measures (Queensland). AAPG Bulletin 98, 191−212.

Tankard, A., Welsink, H., Aukes, P., Newton, R., Stettler, E., 2009. Tectonic evolution of the Cape and Karoo basins of South Africa. Marine and Petroleum Geology 26, 1379−1412.

Taylor, A.M., Goldring, R., 1993. Description and analysis of bioturbation and ichnofabric. Journal of the Geological Society 150, 141−148.

Turner, B.R., 1981. Possible origin of low angle cross-strata and horizontal lamination in Beaufort Group sandstones of the southern Karoo Basin. Transactions of the Geological Society of South Africa 84, 193−197.

Tyler, N., Ethridge, F.G. (Eds.), 1983. Fluvial architecture of Jurassic uranium-bearing sandstones, Colorado Plateau, western United States. Modern and ancient fluvial systems. International Association of Sedimentologists Special Publication Oxford, 575 pp.

van Toorenenburg, K.A., Donselaar, M.E., Noordijk, N.A., Weltje, G.J., 2016. On the origin of crevasse-splay amalgamation in the Huesca fluvial fan (Ebro Basin, Spain): Implications for connectivity in low net-to-gross fluvial deposits. Sedimentary Geology 343, 156-164.

Walling, D.E., He, Q., 1998. The spatial variability of overbank sedimentation on river floodplains. Geomorphology 24, 209−223.

Weissmann, G.S., Hartley, A.J., Nichols, G.J., Scuderi, L.A., Olson, M., Buehler, H., Banteah, R., 2010. Fluvial form in modern continental sedimentary basins: Distributive fluvial systems. Geology 38, 39-42.

Weissmann, G.S., Hartley, A.J., Nichols, G.J., Scuderi, L.A., Olson, M.E., Buehler, H.A., Massengill, L.C., 2011. Alluvial facies distributions in continental sedimentary basins—distributive fluvial systems. In: Davidson, S.K., Leleu, S., North, C.P. (Eds.), From River to Rock Record: The Preservation of Fluvial Sediments and their Subsequent Interpretation. SEPM Special Publication 97, Tulsa, OK., pp. 327-355.

Wickens, H., 1994. Basin floor fan building turbidites of the Southwestern Karoo Basin, Permian Ecca Group, South Africa. PhD Thesis, University of Port Elizabeth, South Africa, 233 pp.

Willis, B.J., Behrensmeyer, A.K., 1994. Architecture of Miocene overbank deposits in northern Pakistan. Journal of Sedimentary Research 64, 60−67.

Wilson, A., Flint, S.S., Payenberg, T.H.D., Tohver, E., Lanci, L., 2014. Architectural styles and sedimentology of the fluvial lower Beaufort Group, Karoo Basin, South Africa. Journal of Sedimentary Research 84, 326−348.

Wright, V.P., Marriott, S.B., 1993. The sequence stratigraphy of fluvial depositional systems: the role of floodplain sediment storage. Sedimentary Geology 86, 203−210.

Wright, V.P., Taylor, K.G., Beck, V.H., 2000. The paleohydrology of Lower Cretaceous seasonal wetlands, Isle of Wight, Southern England. Journal of Sedimentary Research 70, 619−632.

Figure Captions

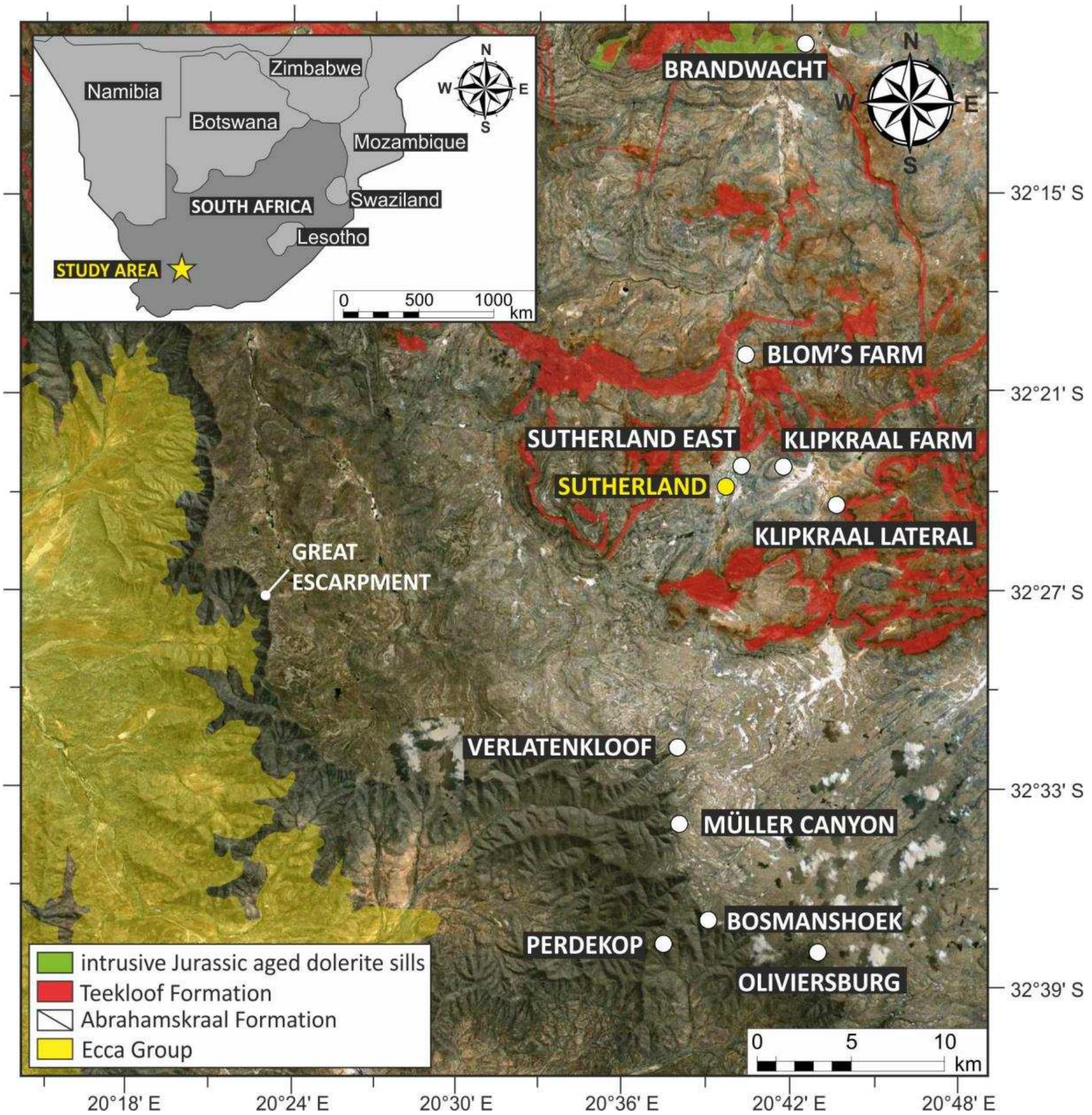

Fig. 1. GoogleEarth™ Landsat image of the main localities, marked by the white dots, the Great Escarpment and the town of Sutherland. The satellite image is overlain by a simplified geological map of the area (Council for Geoscience, 1983). Localities (all listed using UTM WGS84) include: Blom's Farm [468920.64 m E, 6422756.7 m N, 34H]; Boschmanshoek [467594.89 m E, 6391162.5 m S, 34H]; Brandwacht [470425.59 m E, 6439131.2 m N, 34H]; Klipkraal Farm [471280.65 m E, 6417284.1 m N, 34H]; Klipkraal Lateral [474445.12 m E, 6414923.2 m N, 34H]; Müller Canyon [465094.72 m E, 6396063.1 m N, 34H]; Oliviersburg West [473316.4 m E, 6389355.8 m N, 34H]; Perdekop [464577.65 m E, 6390132.1 m N, 34H]; Sutherland East [468682.08 m E, 6416176 m N, 34H]; Verlatenkloof [465716.15 m E, 6401131 m N, 34H]. Inset: map of southern Africa, highlighting the study area, within the SW Karoo Basin, Northern Cape Province.

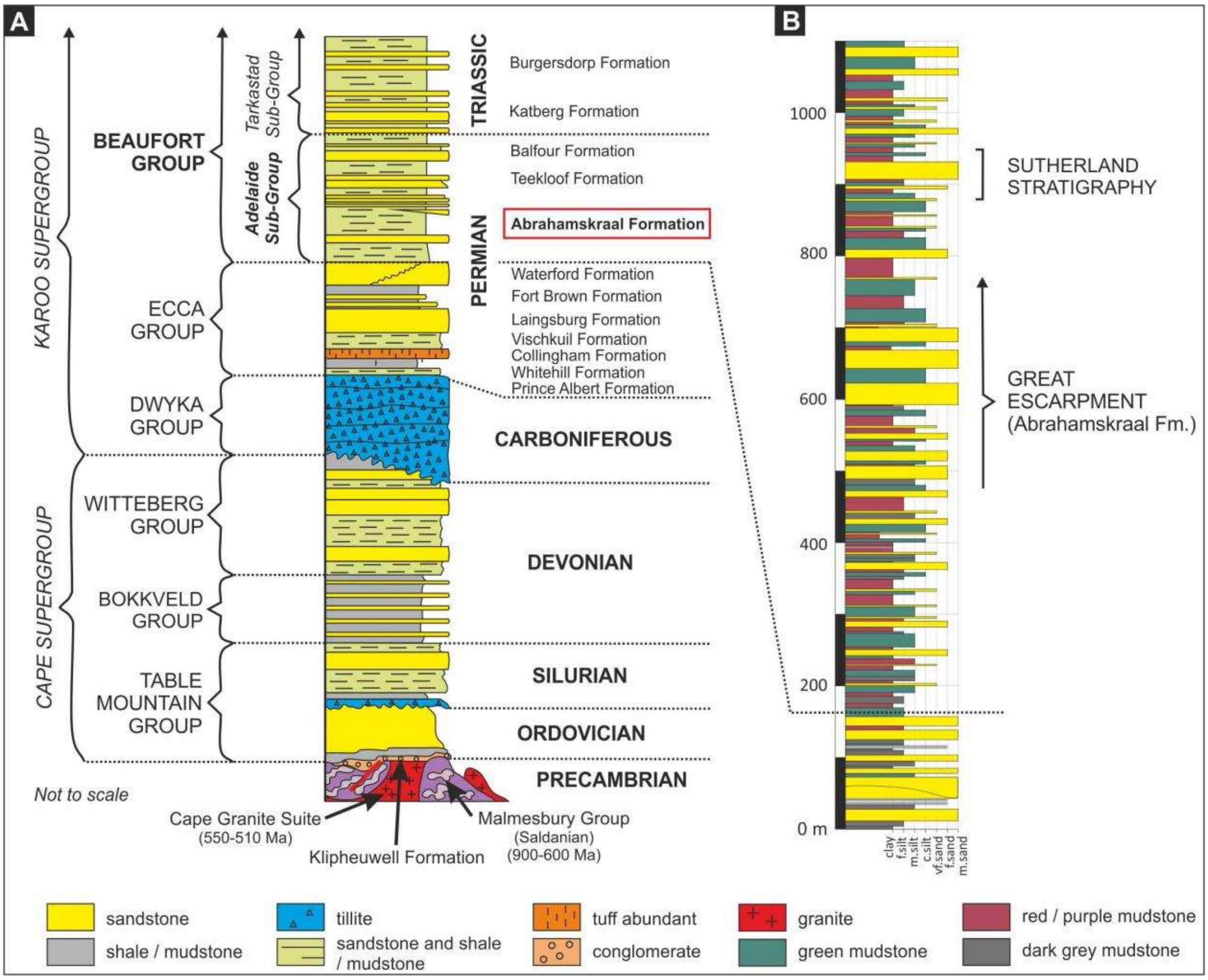

Fig. 2. Lithostratigraphy of the SW Karoo Basin. (A) Cape and Karoo Supergroups highlighting the Abrahamskraal Formation, lower Beaufort Group, redrawn after Wickens (1994) and Flint et al. (2011). (B) Schematic illustration of the Abrahamskraal Formation exposed on the Great Escarpment (Verlatenkloof and Müller Canyon – refer to Figure 1 for GPS coordinates) and in the Sutherland area (Klipkraal, Sutherland East, and Blom's Farm).

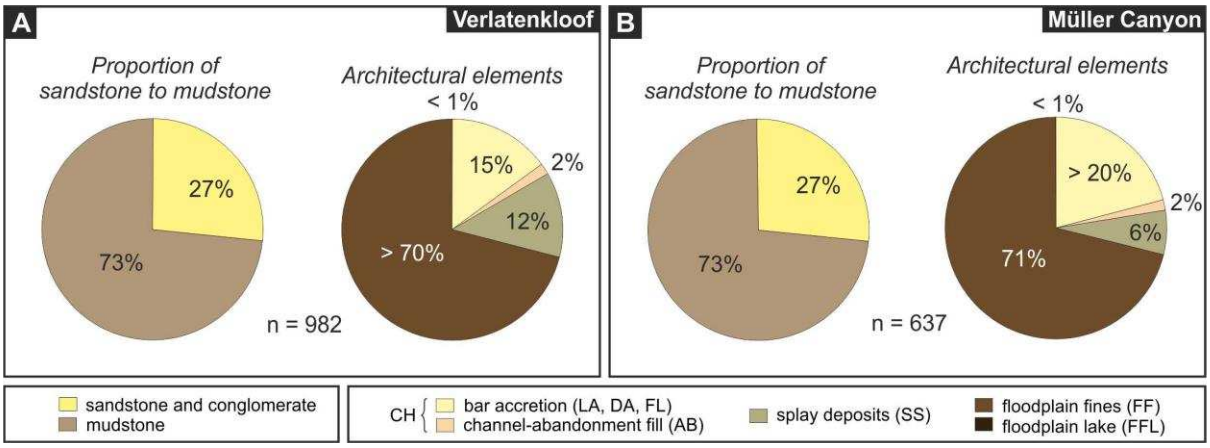

Fig. 3. Sandstone to mudstone proportions and architectural elements in sedimentary logs from (A) Verlatenkloof, (B) Müller Canyon. See Figure 1 for locations and Supplementary Spreadsheet 1 for supporting dataset.

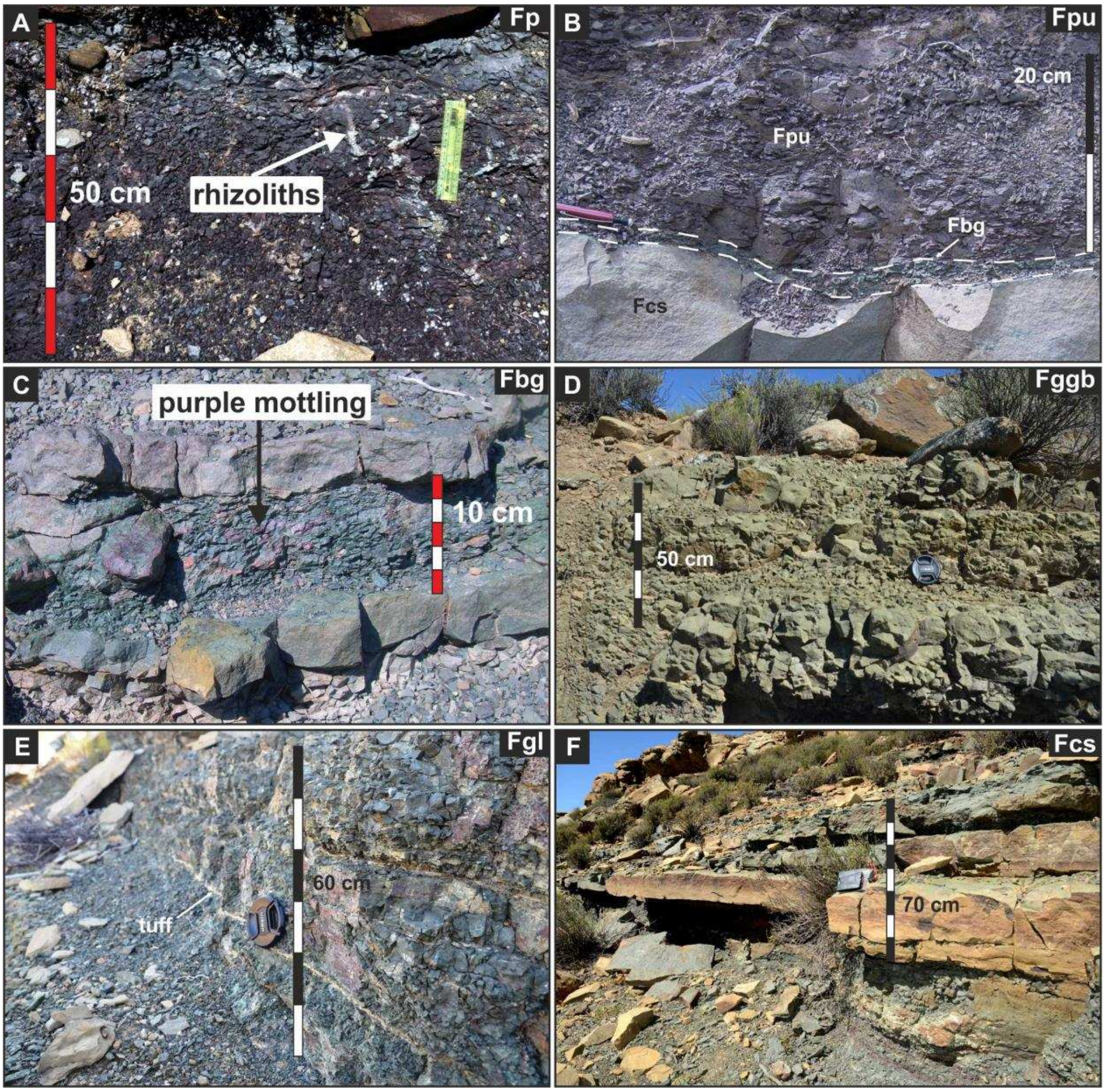

Fig. 4. Mudstone facies from the Abrahamskraal Formation. (A) Downward-branching fossil root structures (rhizoliths) preserved as alteration-reduction halos (Hasiotis et al., 2002) in a paleosol (Fp), (B) Poorly sorted purple siltstone (Fpu), overlying Fbg, above Fcs. Dashed white lines show a sharp lower bounding surface, (C) Bright green massive mudstone (Fbg), mottled purple. Facies is flanked by sharp-topped, erosive based coarse-grained siltstone to very fine-grained sandstone. Fbg is typically lenticular, (D) Poorly sorted, green-gray-blue, coarse-grained siltstone (Fggb) forming laterally extensive sheets. (E) Laminated organic-rich dark gray mudstone (Fgl). Fgl facies is thinly-bedded (< 5 cm thick) flanking a possible tuff deposit (~1 cm thick). (F) Thinly-bedded coarse-grained siltstone to very fine-grained sandstone (Fcs), with sharp upper and lower bounding surfaces from Sutherland East. Fcs facies is gray colored, weathering orange.

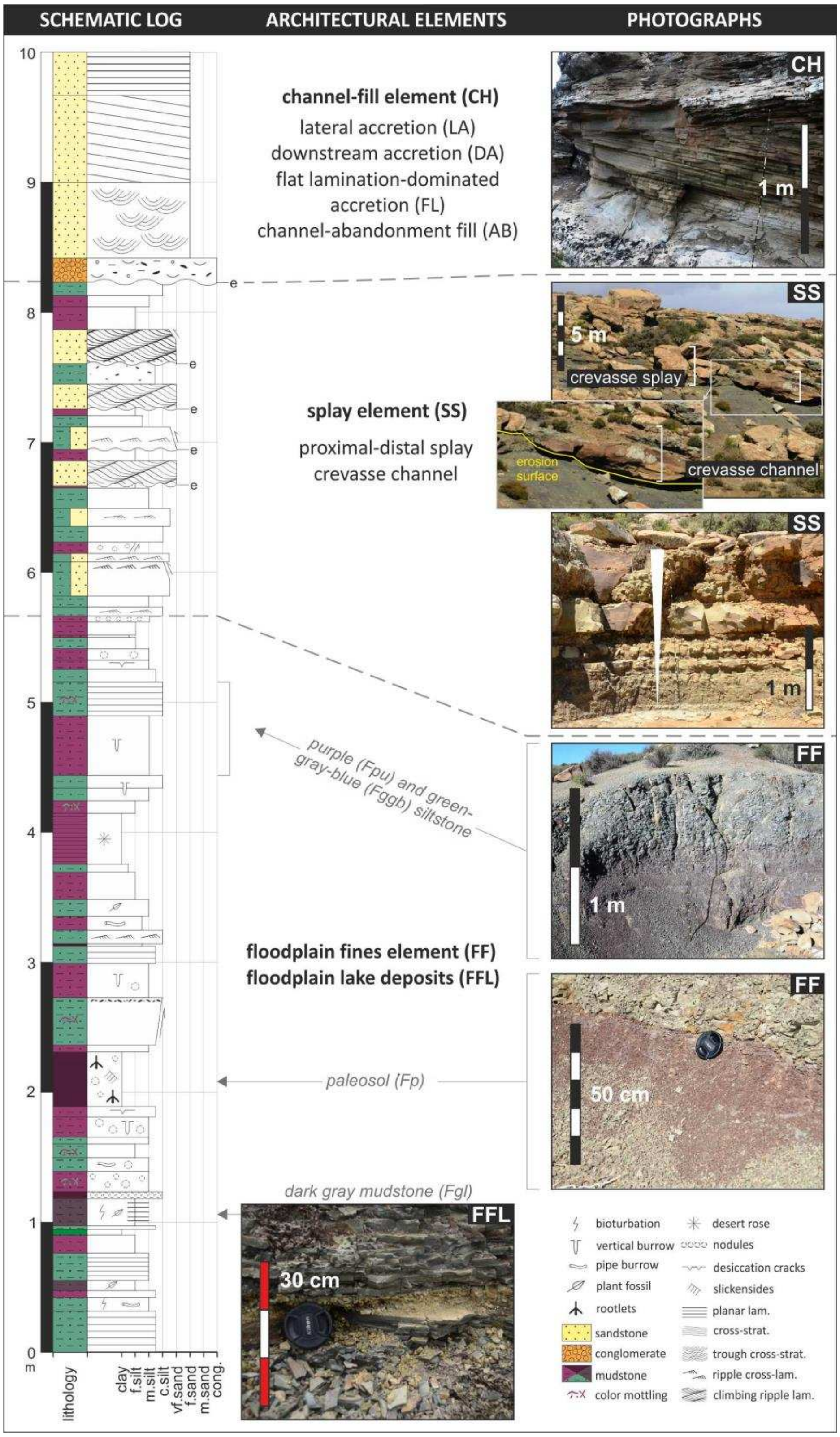

Fig. 5. Idealized sedimentary log showing relative proportions of overbank deposits observed throughout the study area, focusing on floodplain lake deposits (FFL), floodplain fines element (FF) and splay element (SS) comprising proximal to distal splay and crevasse channel deposits.

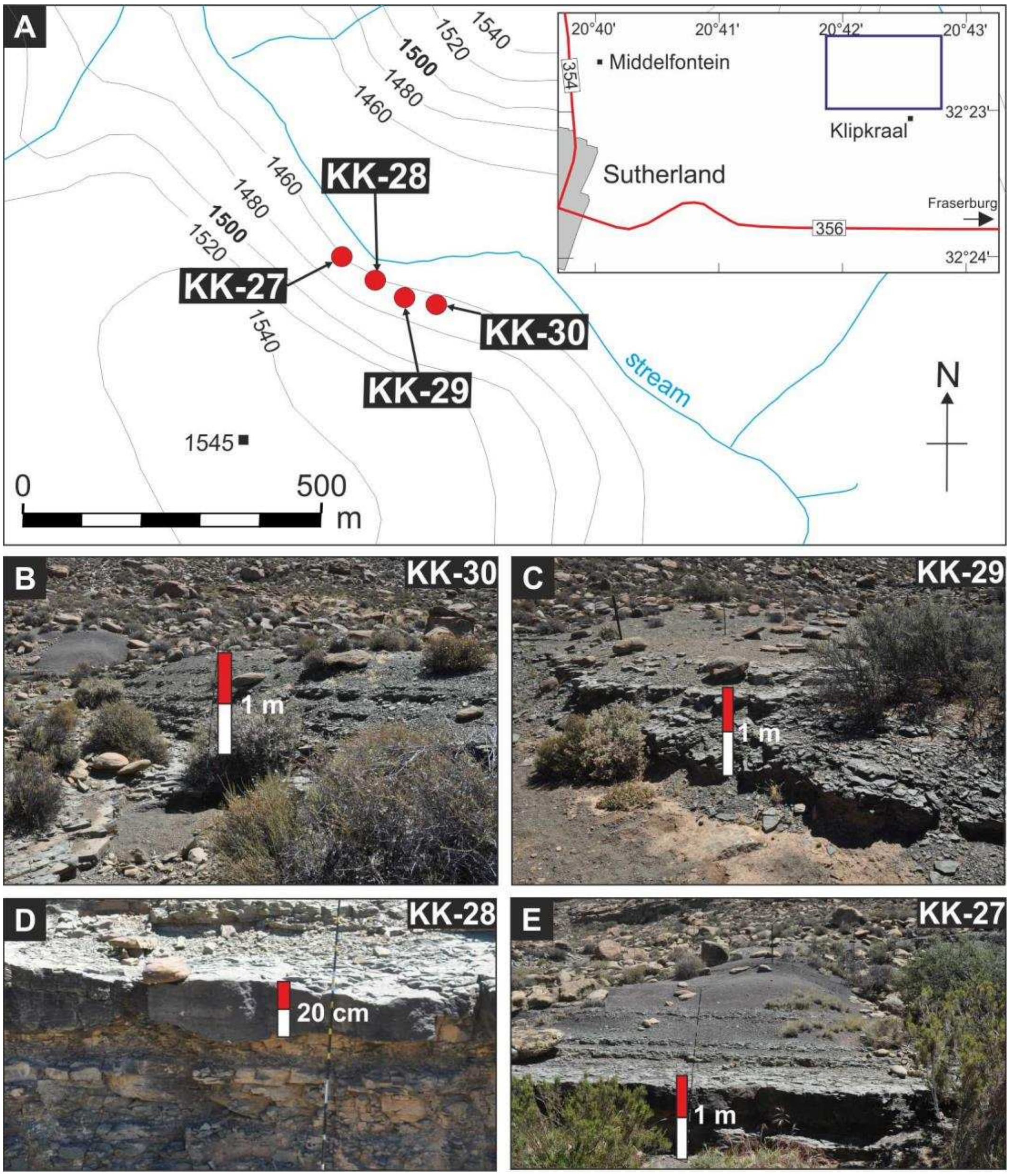
A
1540
1520
1500
1480
1460
20°40'
20°41'
20°42'
20°43'
354
Middelfontein
32°23'
Klipkraal
Sutherland
Fraserburg
356
32°24'
KK-28
KK-27
KK-30
KK-29
stream
N
1545
0
500
m
B
KK-30
1 m
C
KK-29
1 m
D
KK-28
20 cm
E
KK-27
1 m

Fig. 6. Overview map and representative photographs of an interpreted crevasse splay element. (A) Overview map of Klipkraal Farm, near Sutherland (

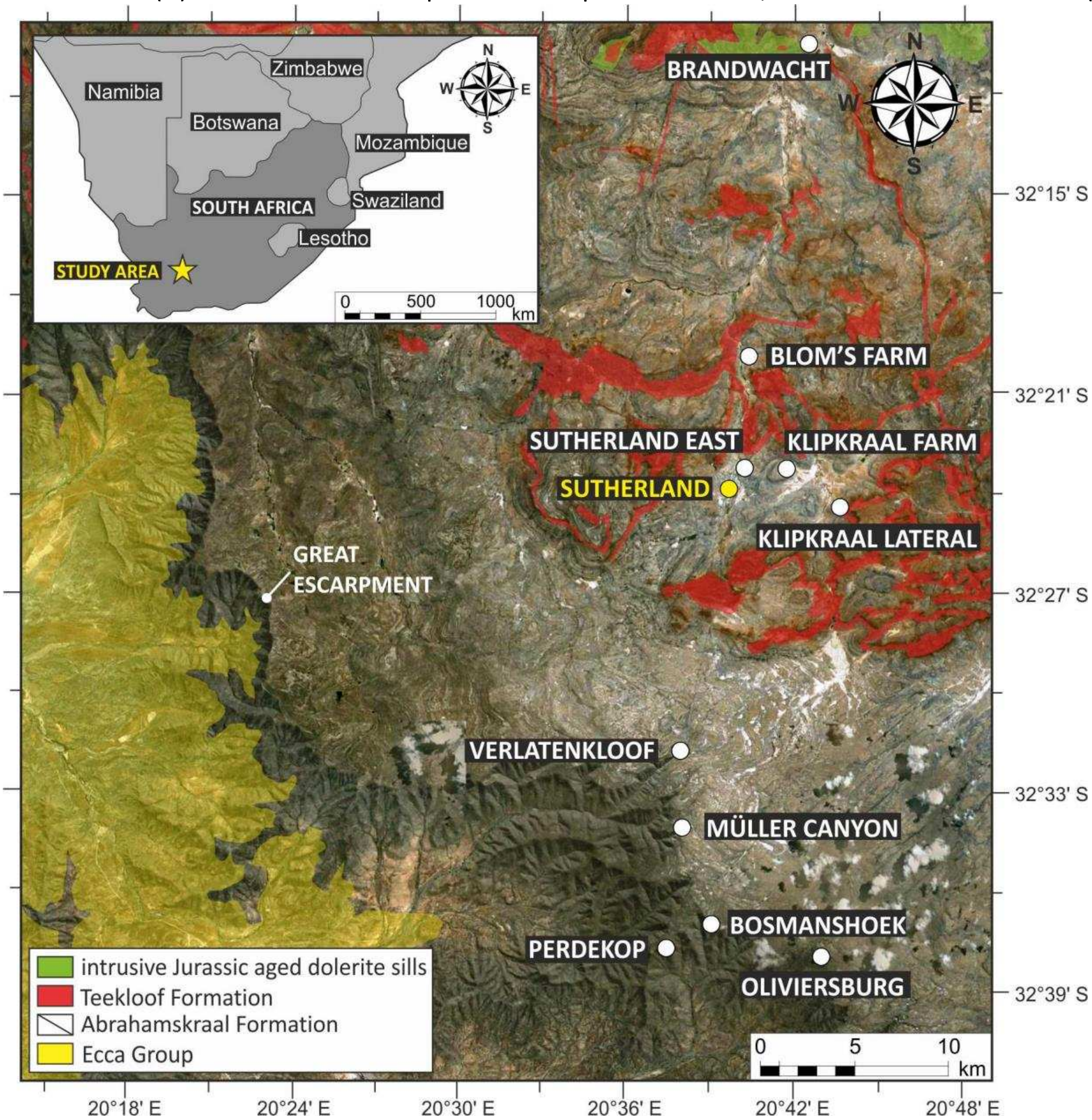

Fig. 1). The location of this map is given by the blue rectangle in the inset map. Red dots denote sedimentary log localities. (B) Photograph of log locality KK-30. Refer to Figure 7 for each sedimentary log. (C) Photograph of log locality KK-29. (D) Photograph of log locality KK-28. (E) Photograph of log locality KK-27.

824

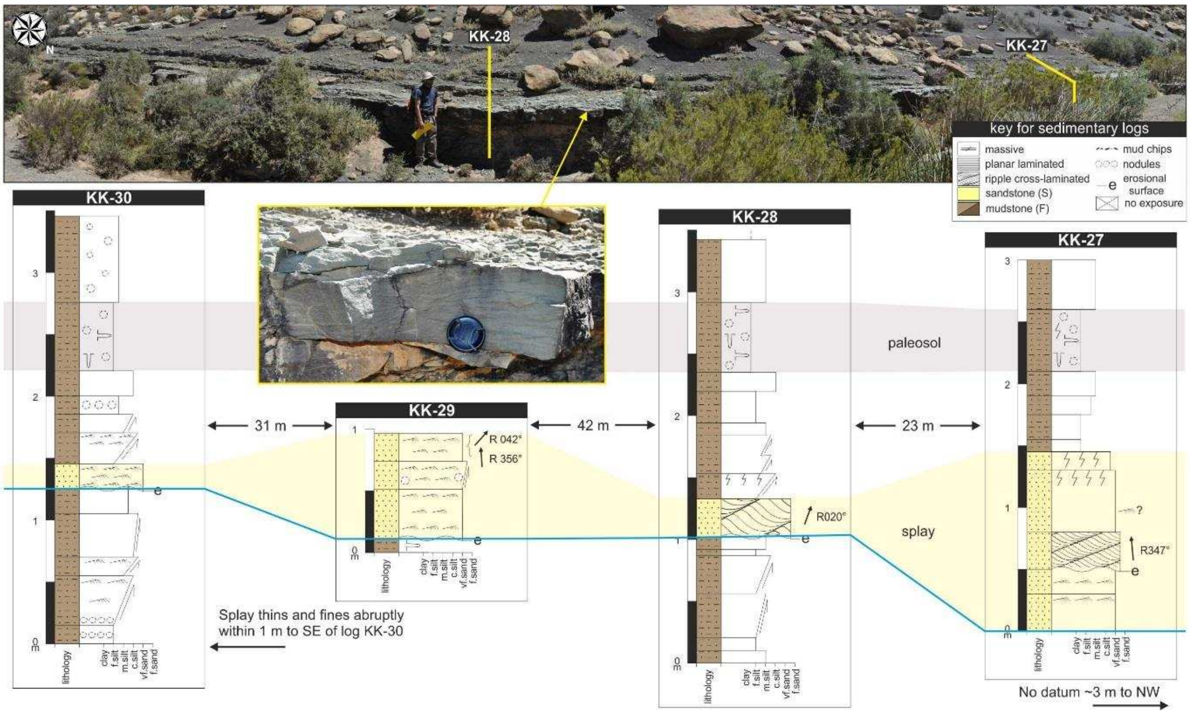

KK-28
KK-27
N
key for sedimentary logs
massive
planar laminated
ripple cross-laminated
sandstone (S)
mudstone (F)
mud chips
nodules
erosional surface
no exposure
KK-30
KK-29
KK-28
KK-27
paleosol
splay
31 m
42 m
23 m
R 042°
R 356°
R020°
R347°
lithology
clay
f.silt
m.silt
c.silt
vf.sand
f.sand
Splay thins and fines abruptly within 1 m to SE of log KK-30
No datum ~3 m to NW

Fig. 7. Sedimentary logs through an interpreted crevasse splay element 1.5 m thick at Klipkraal Farm, near Sutherland (

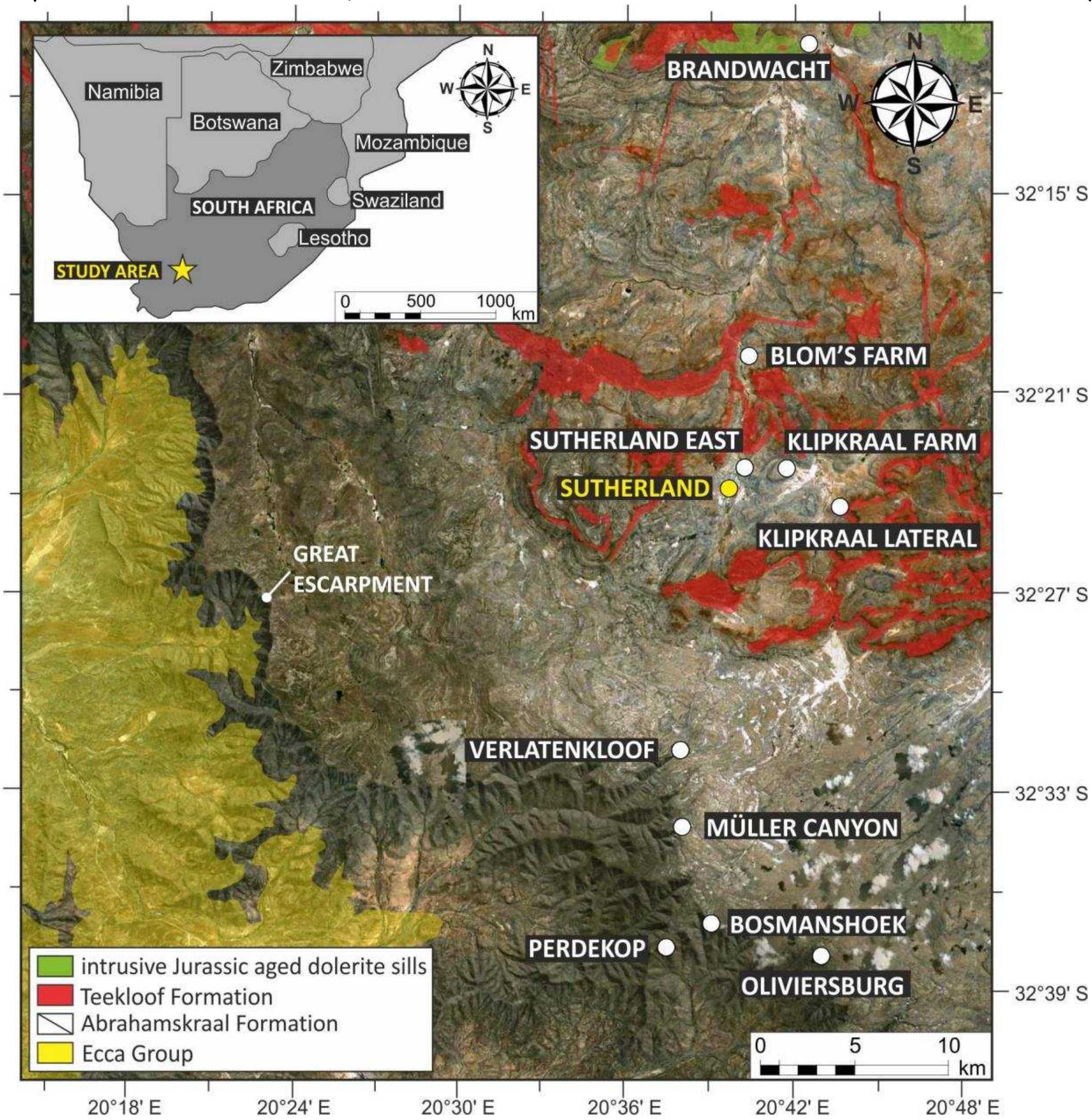

Fig. 1). Paleocurrents from ripple and climbing-ripple cross-lamination are to the north. A laterally extensive paleosol is present < 1 m above the top of the crevasse splay sandstone. Erosional base of splay is highlighted in blue. Inset: Photograph of climbing-ripple cross-lamination. Refer to Figure 6 for locality map.

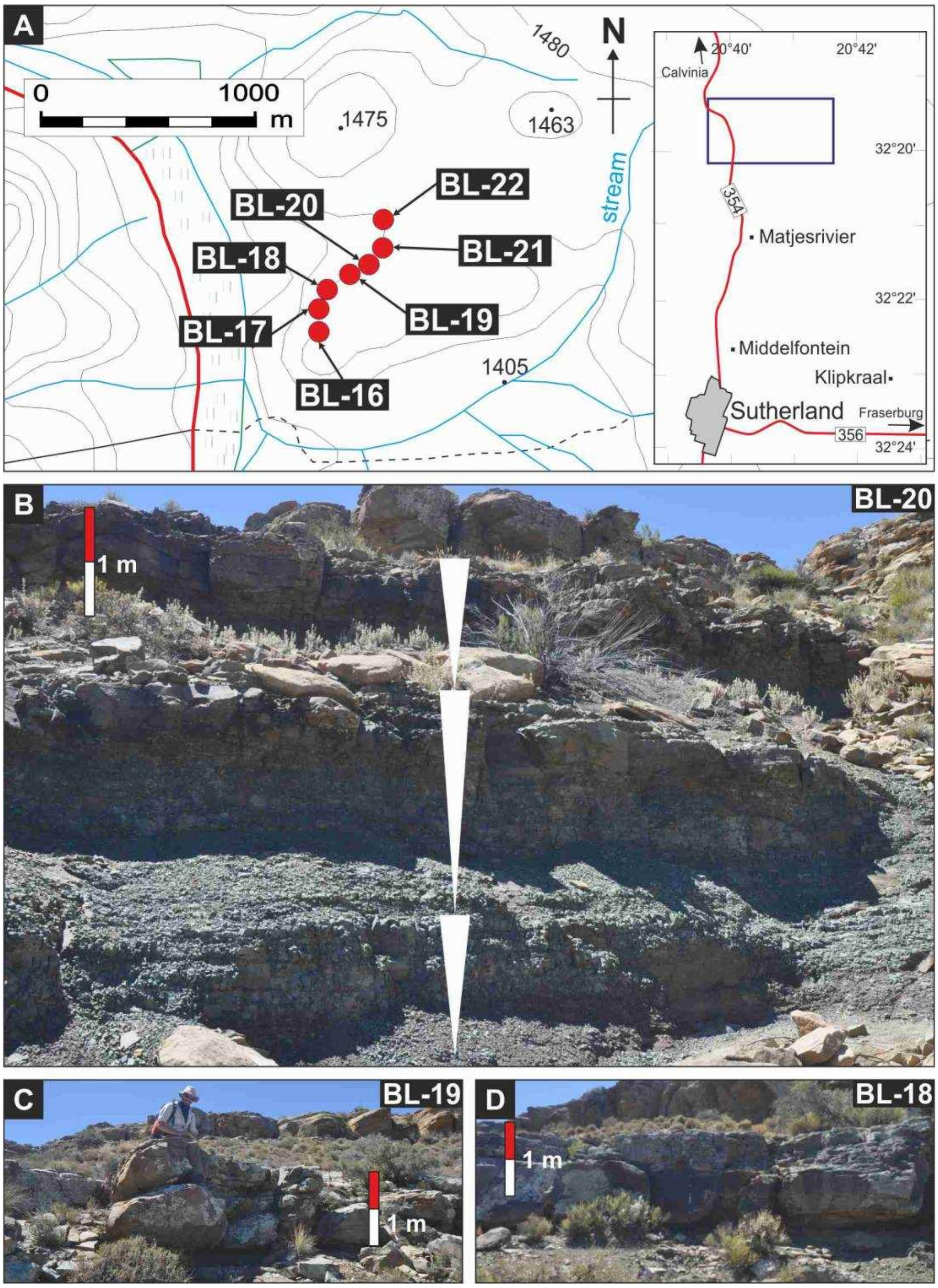
A
0
1000
m
1480
1475
1463
N
stream
BL-22
BL-20
BL-21
BL-18
BL-19
BL-17
BL-16
1405
Calvinia
20°40'
20°42'
32°20'
354
Matjesrivier
32°22'
Middelfontein
Klipkraal
Sutherland
Fraserburg
356
32°24'
B
BL-20
1 m
C
BL-19
1 m
D
BL-18
1 m

832

Fig. 8. Overview map and representative photographs of an interpreted crevasse splay element. (A) Overview map of Blom's Farm, near Sutherland (

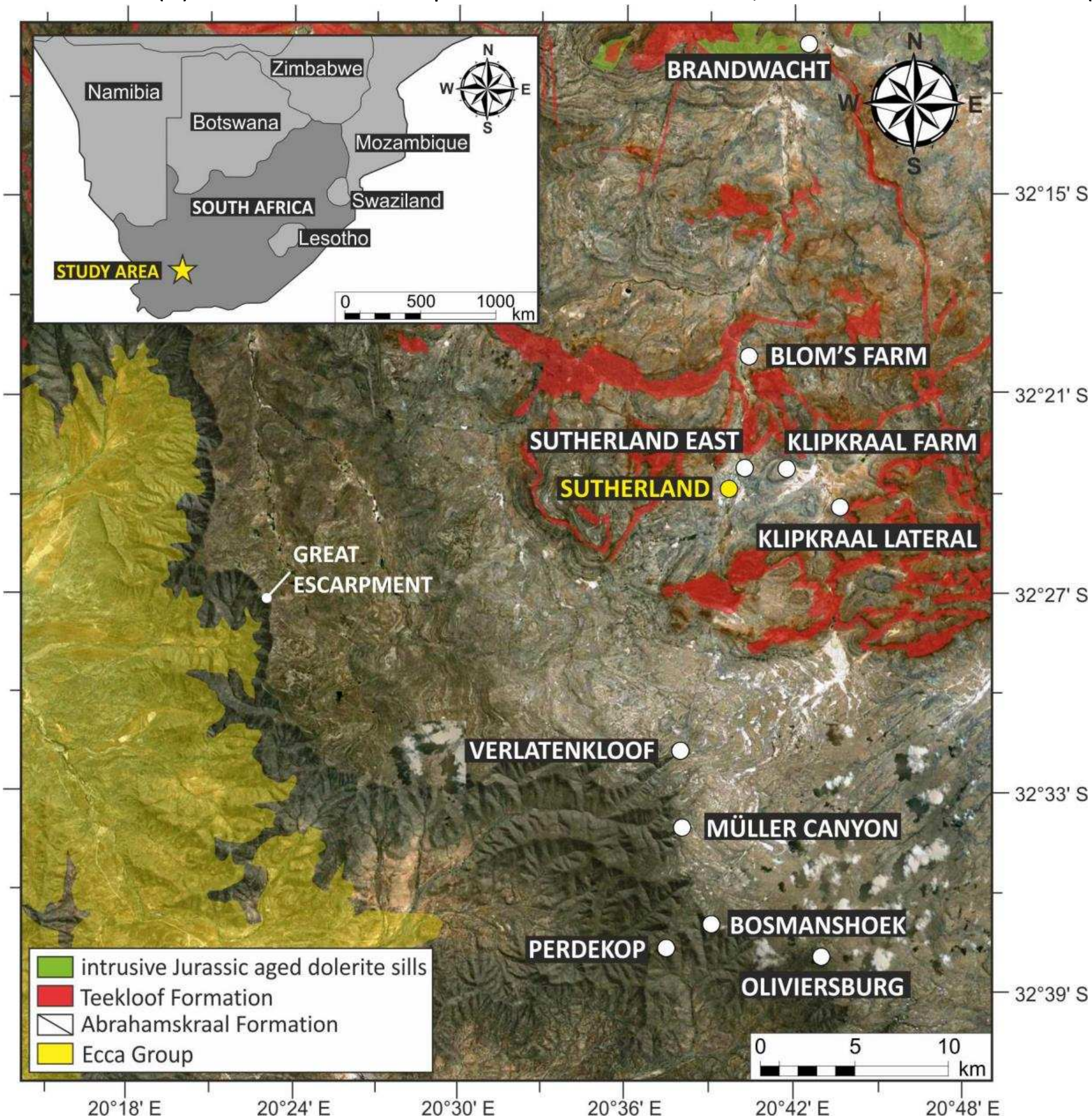

Fig. 1). The location of this map is given by the blue rectangle in the inset map. Red dots denote sedimentary log localities. (B) Photograph of log locality BL-20, comprising three coarsening-upward packages. Refer to Figure 9 for each sedimentary log. (C) Photograph of log locality BL-19. (D) Photograph of log locality BL-18.

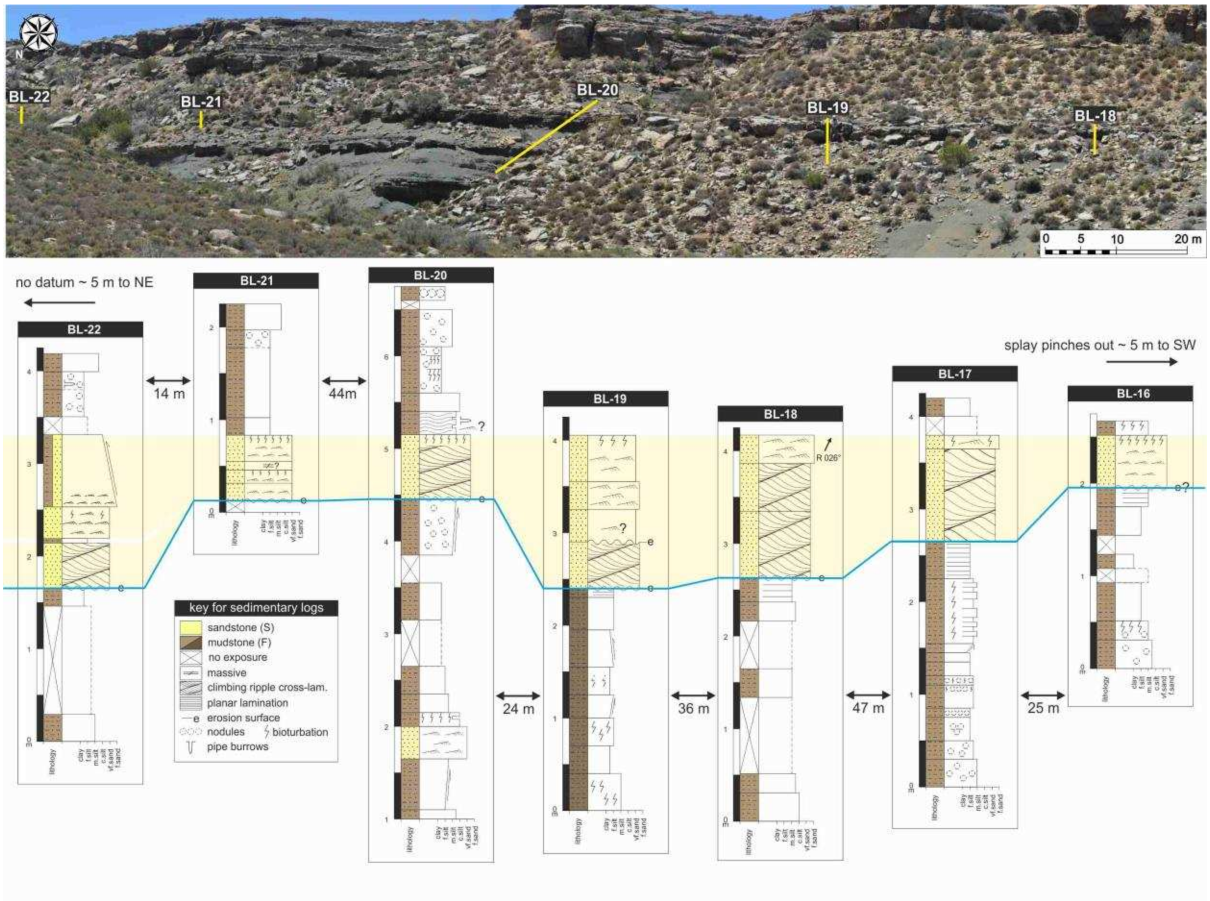

BL-22
BL-21
BL-20
BL-19
BL-18
0 5 10 20 m
no datum ~ 5 m to NE
splay pinches out ~ 5 m to SW
14 m
44m
24 m
36 m
47 m
25 m
BL-17
BL-16
key for sedimentary logs
sandstone (S)
mudstone (F)
no exposure
massive
climbing ripple cross-lam.
planar lamination
erosion surface
nodules
bioturbation
pipe burrows
R 026°

840

Fig. 9. Sedimentary logs through a a < 1.5 m thick very fine-grained sandstone crevasse splay element at Blom's Farm (

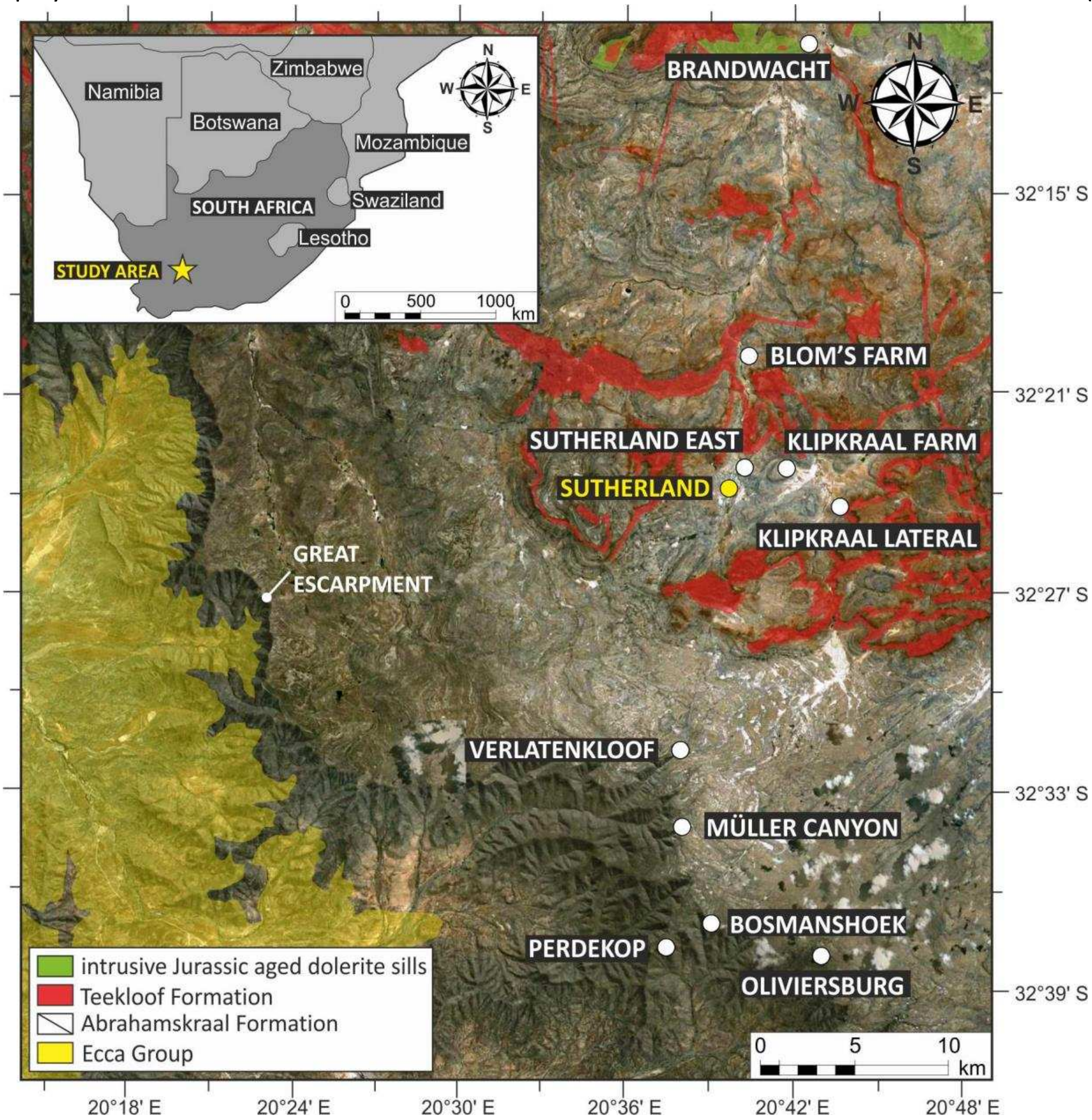

Fig. 1). Climbing ripple cross-lamination is overlain by ripple cross-lamination, with paleoflow north-northeastward. Erosional base of splay is highlighted in blue. Refer to Figure 8 for locality map.

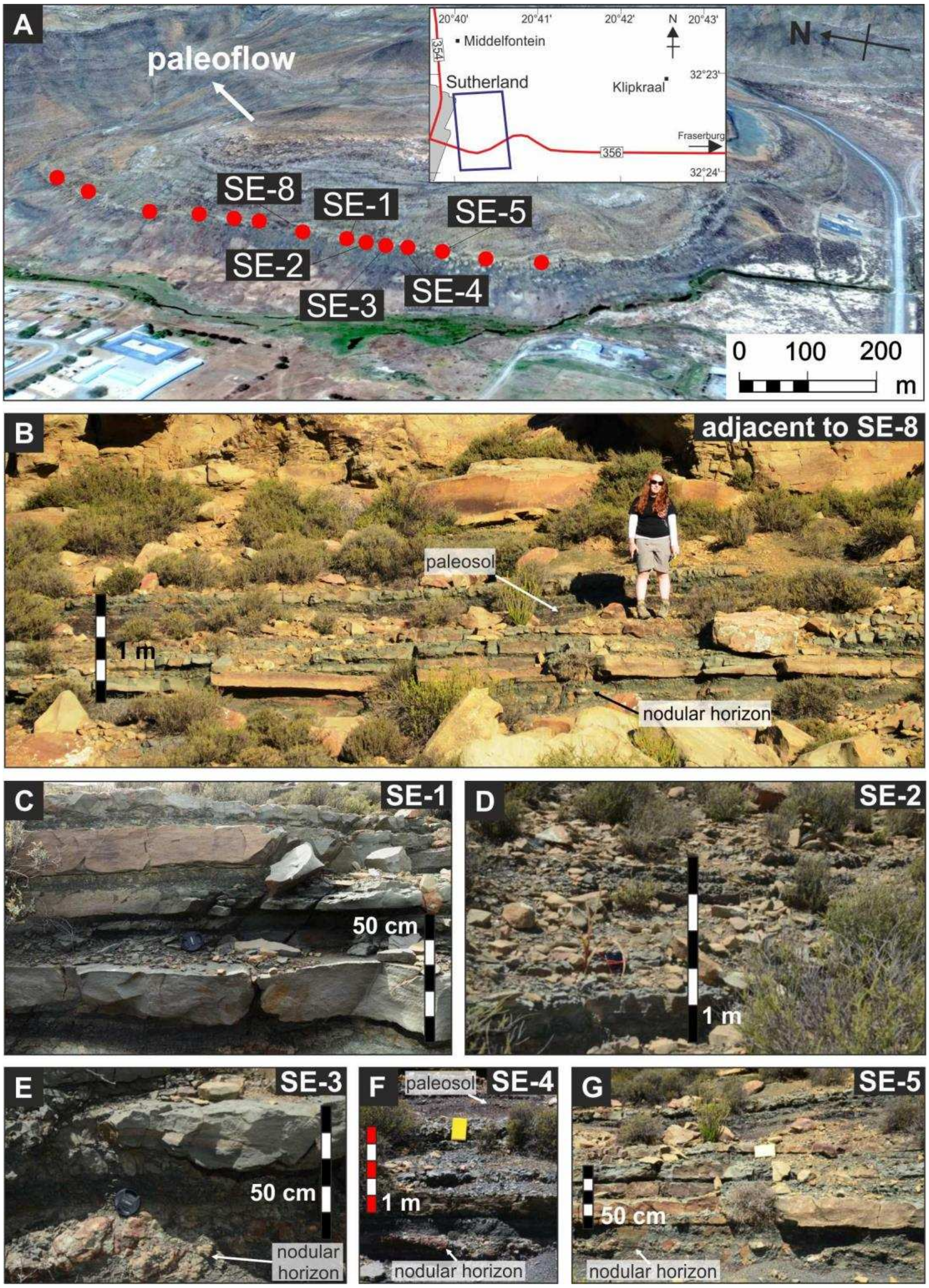
A
paleoflow
20°40'
20°41'
20°42'
20°43'
N
Middelfontein
354
Sutherland
Klipkraal
32°23'
Fraserburg
356
32°24'
N
SE-8
SE-1
SE-5
SE-2
SE-4
SE-3
0 100 200
m
B
adjacent to SE-8
paleosol
1 m
nodular horizon
C
SE-1
50 cm
D
SE-2
1 m
E
SE-3
50 cm
nodular horizon
F
paleosol
SE-4
1 m
nodular horizon
G
SE-5
50 cm
nodular horizon

847

Fig. 10. Overview map and representative photographs of an interpreted crevasse splay set. (A) Overview map of Sutherland East (

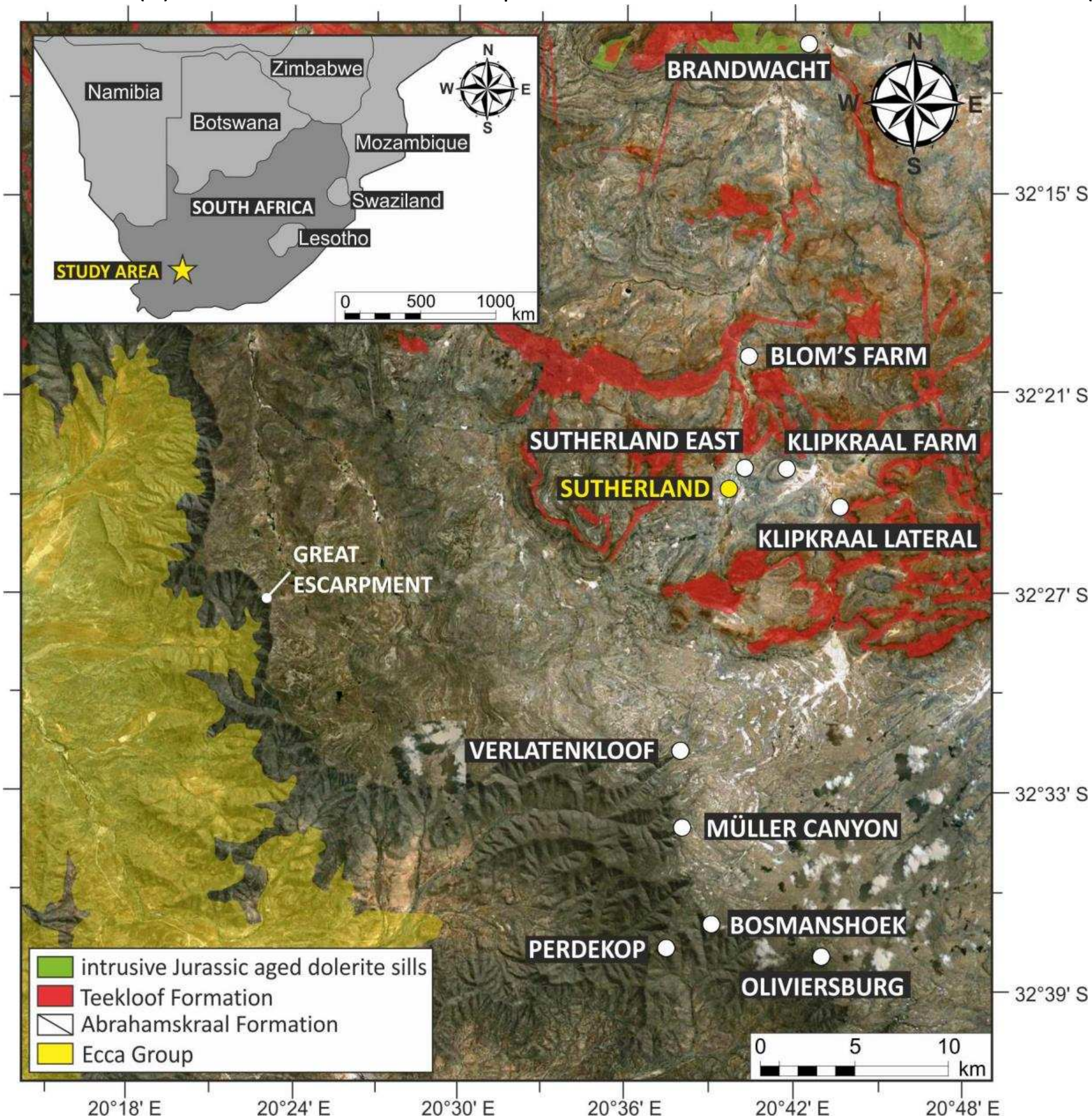

Fig. 1), near Sutherland (3 x vertical exaggeration applied with perspective view). The location of this map is given by the blue rectangle in the inset map. Red dots denote sedimentary log localities. (B) Crevasse splay elements adjacent to log locality SE-8. Refer to Figure 11 for each sedimentary log. (C) Photograph of log locality SE-1, showing ripple to climbing ripple cross-laminated very fine- to fine-grained sandstone sheets separated vertically by thin siltstone deposits. (D) Photograph of log locality SE-2 displaying laterally extensive crevasse splay elements. (E) Photograph of log locality SE-3. A laterally extensive nodular horizon can be observed beneath a tabular very fine-grained sandstone. (F) Photograph of log locality SE-4, depicting an interpreted crevasse splay set bound above by a paleosol and below by a nodular horizon. (G) Photograph of log locality SE-5, showing stacked crevasse splay elements above a nodular horizon.

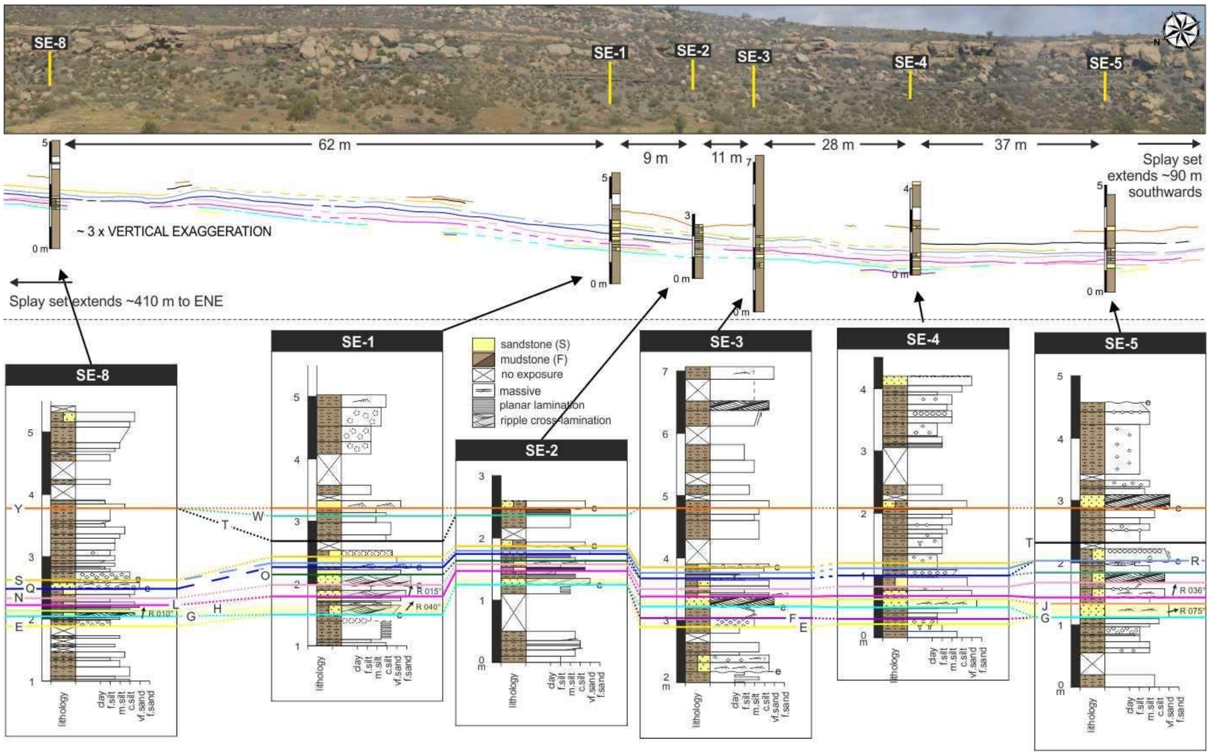

SE-8
SE-1
SE-2
SE-3
SE-4
SE-5
62 m
9 m
11 m
28 m
37 m
Splay set extends ~90 m southwards
~ 3 x VERTICAL EXAGGERATION
Splay set extends ~410 m to ENE
sandstone (S)
mudstone (F)
no exposure
massive
planar lamination
ripple cross-lamination
lithology
clay
f.silt
m.silt
c.silt
vf.sand
f.sand

Fig. 11. Detailed photo panel interpretation of crevasse splay elements from Sutherland East (

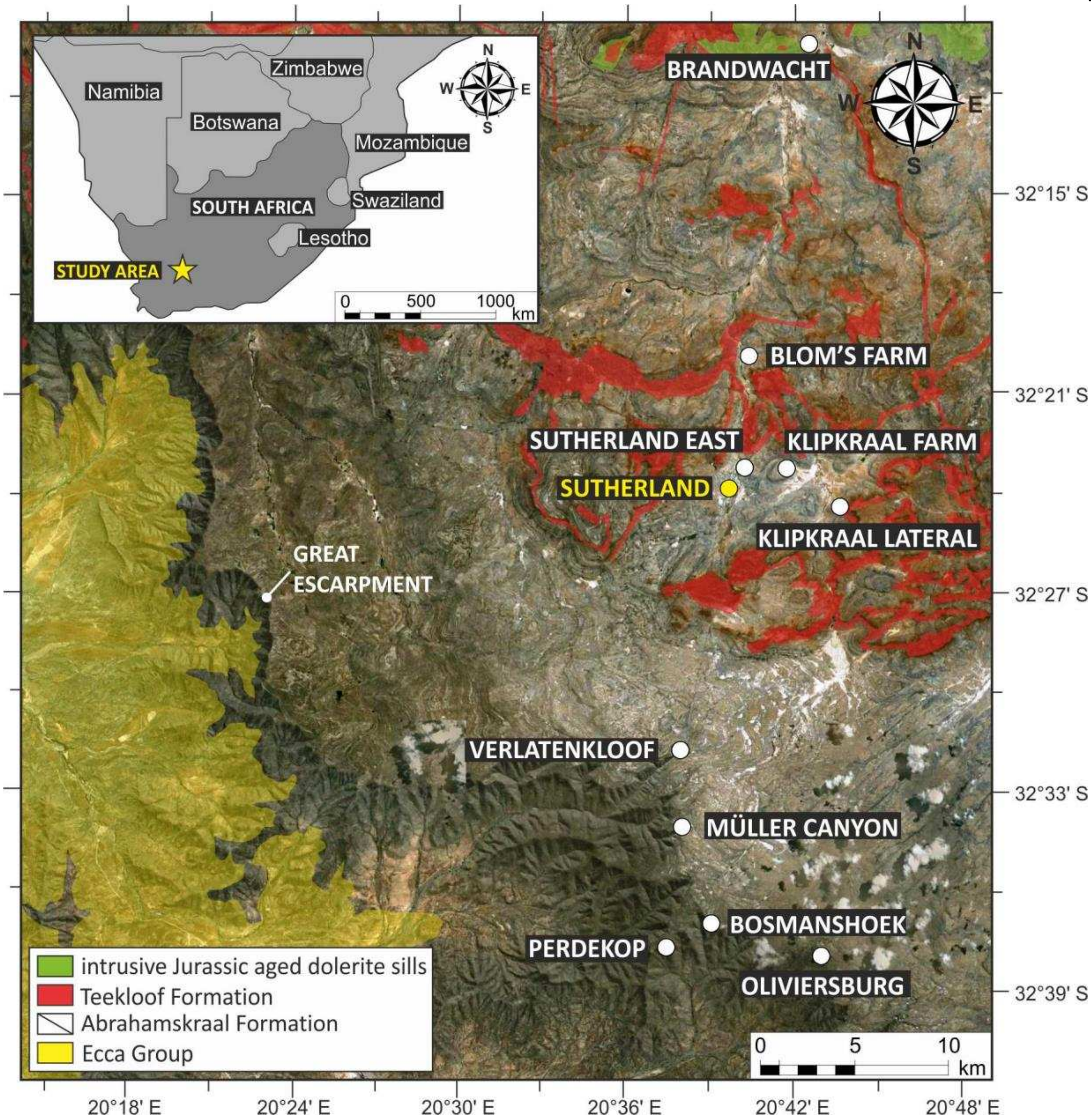

Fig. 1), with sedimentary log positions and correlated surfaces (E to Y) overlain. Paleoflow from ripple cross-laminated very fine-grained sandstone ranges between 010° and 079° (n = 9). The sedimentary facies distributions are shown on the accompanying logs. Refer to Figure 10 for locality map.

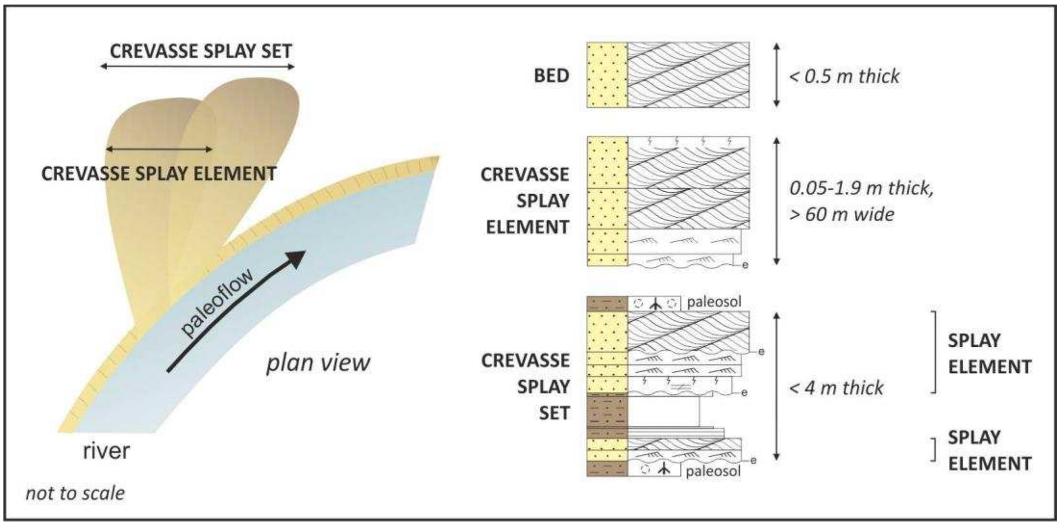

Fig. 12. Crevasse splay hierarchical scheme. Individual crevasse splay elements stack to form crevasse splay sets. Each crevasse splay set is separated by a laterally extensive paleosol.

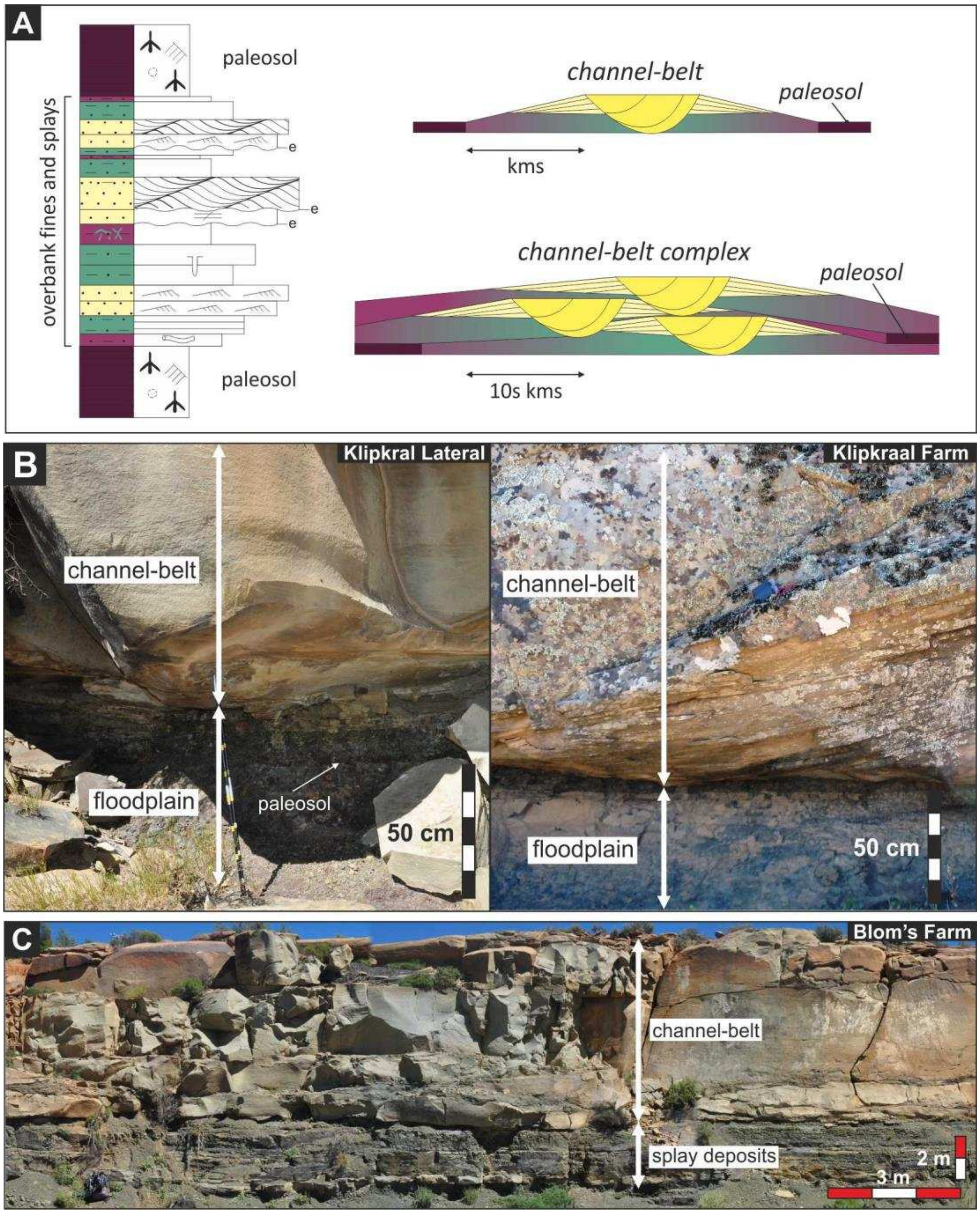

Fig. 13. Crevasse products in the Abrahamskraal Formation. (A) Schematic diagram depicting the formation of paleosols through time. Paleosols may represent the distal expression of channel belts, developing during the equivalent time that it takes for them to form. Alternatively, the paleosol may represent a major avulsion, and may be the hierarchical expression of a channel belt complex, implying that the overbank fines between each paleosol are potentially the hierarchical equivalent to a channel belt complex. (B) Examples of channel belts that incise into distal floodplain mudstones, indicating incisional avulsion. (C) Example of channel belt deposits overlying laterally extensive splay deposits, , indicative of the dominant progradational avulsion style.

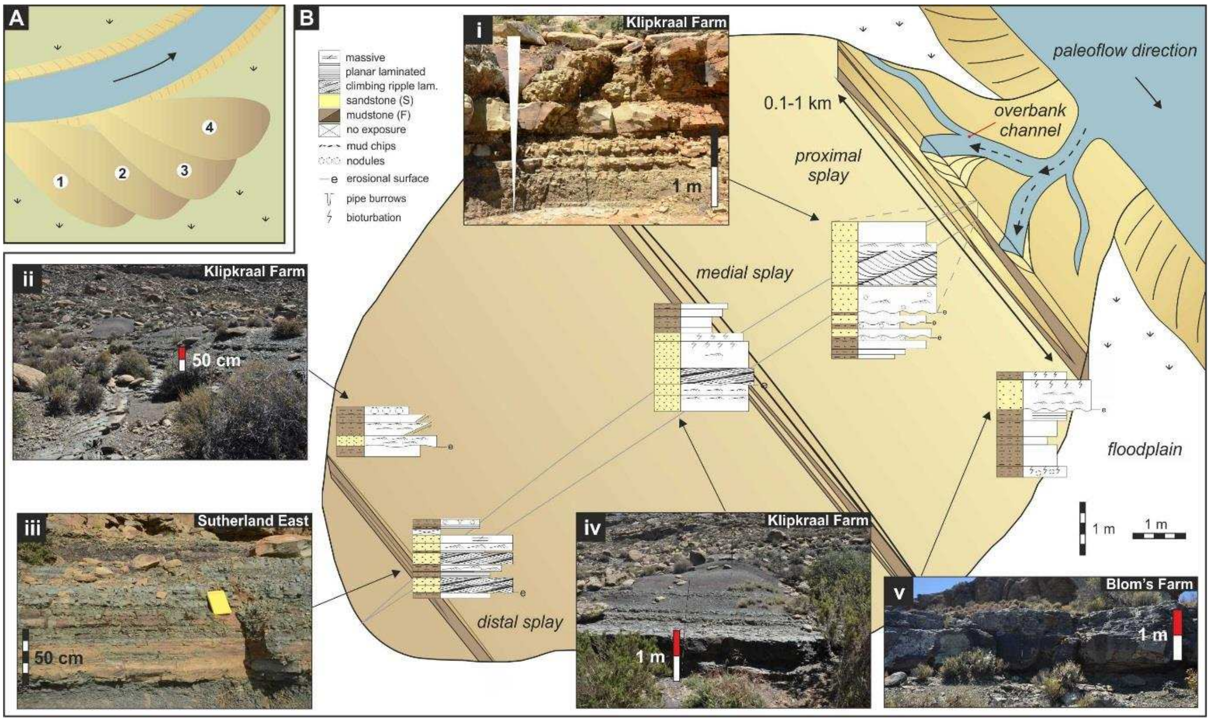

Fig. 14. Idealized crevasse splay model. (A) Compensationally stacked splay deposits infilling topographic lows. Numbers relate to order of deposition. (B) Crevasse splay 3-D model based on observations made in this study, modified after Bridge (2003); (i) Klipraal Farm [472104 m E, 6417930 m N, 34H]; (ii) Klipkraal Farm, log KK-30 [472263 m E, 6417545 m N, 34H]; (iii) Sutherland East [468634 m E, 6415960 m N, 34H]; (iv) Klipkraal Farm, log KK-27 [472188 m E, 6417598 m N, 34H]; (v) Blom's Farm, log BL-18 [469120 m E, 6423019 m N, 34H].

Table Captions

Overbank facies (%)		Overbank architectural elements (%)		Grain size of elements
Fp	3.66, n = 48	FF (floodplain fines)	79.78	claystone, siltstone (very fine- to medium-grained)
Fpu	31.92, n = 375			
Fbg	0.17, n = 8			
Fggb	44.03, n = 518			
Fgl	0.21, n = 7	FFL (floodplain lake deposits)	0.21	claystone, siltstone (very fine- to medium-grained)
Fcs	9.22, n =107	SS (proximal to distal splay deposits and crevasse channel)	20.01	siltstone (medium to coarse-grained), sandstone (very fine- to fine-grained)
Sr	4.20, n = 45			
Sm	5.68, n = 55			
Sh	0.32, n = 3			
Sl	0.43, n = 4			
St	0.12, n = 1			

Fp, fissile purple mudstone; Fpu, poorly-sorted purple siltstone; Fbg, bright green massive mudstone; Fggb, poorly-sorted green-gray-blue siltstone; Fgl, laminated organic-rich dark gray mudstone; Fcs, sharp-based thinly bedded coarse siltstone or very fine sandstone; Sr, ripple cross-laminated sandstone; Sm, massive / structureless sandstone; Sh, planar-laminated sandstone; Sl, low angle cross-stratified sandstone; St, trough cross-stratified sandstone.

Table 1. Approximate overbank proportions of facies and architectural elements within the Abrahamskraal Formation, averaged from sedimentary logs measured at Verlatenkloof and Müller Canyon. Facies and elements are adapted from schemes by Allen (1983), Friend (1983), Miall (1985, 1988, 1996) and Colombera et al. (2012, 2013). Data from channelized deposits are excluded, as are ambiguous data where the exposure is too poor to accurately quantify facies. Refer to Figure 4 for mudstone facies photographs.

Locality	Architecture	Sedimentary facies	Apparent W (m)	W* (m)	T (m)	Aspect ratio*	Paleocurrent direction	L (m)
Klipkraal Farm	Crevasse splay	Very fine-grained sandstone. Structureless to normally graded or ripple and climbing ripple cross-lamination.	100	78	< 1.5	52	Observed range 347° to 042° (n = 11)	-
Blom's Farm	Crevasse splay	Very fine-grained sandstone. Abundant climbing ripple cross-lamination overlain by ripple cross-lamination.	190	62	< 2	31	Observed range 356° to 066° (n = 14)	190
Sutherland East	Splay set	Ripple and climbing-ripple cross-laminated very fine-grained sandstone.	> 700m	-	4	-	Observed range 010° to 079° (n = 12)	-

W, width; T, maximum thickness recorded from splay (or splay set) axis; L, minimum length of crevasse splay as recorded from total outcrop exposure. *Width corrected for paleocurrent relative to the strike of the outcrop using trigonometry (i.e., true width).

Table 2. Geometric data for crevasse splay deposits from the Abrahamskraal Formation.

Stratigraphic section	Age	Climate	Characteristics	Width	Thickness	Aspect ratio	Reference
Brahmaputra River, Bangladesh	Modern	Humid tropical monsoon	Single and multichannel crevasse splays encompassing silt and fine-grained sand. Distal margins are sharp.	-	1 - 3 m	-	Coleman (1969)
Sandy Creek, Clarence River, New South Wales, Australia	Modern	Humid subtropical to temperate	Ephemeral stream deposits. Lobe-shaped in plan view. Progradational in cross-section, thinning marginally. Sand-dominated, comprising cross-lamination, ripple-cross lamination and parallel lamination. Interpreted by Smith et al. (1989) to represent Stage I splays.	< 20 m (by ~40 m)	0.4 m	50	O'Brien and Wells (1986)
Niobrara River, U.S.A - east splay	Modern	Temperate (with swamps)	Coarsening-up sequences, individual beds fine up. Single channel, sand-dominated crevasse splays.	200 m (by 1000 m)	2.5 m	80	Bristow et al. (1999)
Niobrara River, U.S.A - west splay				150 m (by 250 m)	1.2 m	125	
Cumberland Marshes, Saskatchewan, Canada	Holocene to Modern	Subhumid, boreal (wetlands)	Smaller stage I crevasse splays are lobate in plan view and wedge-shaped in the direction of progradation. Stage II and III splays form elliptical to elongate sets, comprising silt to very fine-grained sand.	200 – 500 m (area < 1 km² to < 20 km²)	< 2 m	~100 – 250	Smith et al. (1989), Morozova and Smith (2000), Farrell (2001)
Rhine-Meuse Delta, The Netherlands	Holocene	Temperate	Sandstone-siltstone-claystone sheets with a sharp to gradational basal contact. Stage II and III splays of Smith et al. (1989).	100s of m	0.5 - 2 m	~50 – 600	Stouthamer (2001)
Castlegate Sandstone & Neslen Formation, Utah, U.S.A. – proximal splay	Cretaceous	Humid subtropical, green house	Fine-grained siltstone to upper fine-grained sandstone. Structureless sandstone and ripple cross-laminated sandstones dominate in proximal settings, with structureless and soft sediment deformed chaotic sandstone and siltstone in distal settings.	75 – 676 m; mean 278 m (by 55 – 189 m; mean 129 m)	1.0 – 3.7 m (mean 2.1 m)	~20 – 676	Burns et al. (2017)
Castlegate Sandstone & Neslen Formation, Utah, U.S.A. – distal splay				113 – 852 m; mean 399 m (by 118 – 286 m; mean 229 m)	0.2 – 1.6 m (mean 0.8 m)	~71 – 4260	
Lower Beaufort Group, Karoo Basin, South Africa	Permo-Triassic	Semi-arid (seasonal)	Ephemeral deposits. Fine-grained sandstone sheets with a sharp or erosional basal contact. Stage II and III splay sets of Smith et al. (1989) recognized in proximal sequences.	> 600 m to several km along strike	0.5 – 2 m	< 1200	Stear (1983); Smith (1987); Jordaan (1990); Smith (1993); Gulliford et al. (2014)

Table 3. Comparison of Beaufort Group crevasse splay architecture and geometry with examples from modern and ancient fluvial systems.

Supplementary Information

Additional supplementary data may be found in the online version of this article:

Supplementary Figure 1. Overview maps and complete sedimentary log sections from Verlatenkloof Pass (R354), near Sutherland (refer to Figure 1 and Supplementary Table 1 for GPS coordinates).

Supplementary Figure 2. Overview maps and complete sedimentary log sections from Müller Canyon, Gunsfontein, near Sutherland (refer to Figure 1 and Supplementary Table 1 for GPS coordinates).

Supplementary Table 1. Main locality names, abbreviations and coordinates relating to the location of sedimentary logs within this study, listed alphabetically.

Supplementary Table 2. Database of proximal and distal splay thicknesses measured from sedimentary logs at Verlatenkloof and Müller Canyon. Average thicknesses across these 154 proximal and distal splays is 110 cm and 45 cm, respectively.

Supplementary Spreadsheet 1: Excel spreadsheet comprising thickness, lithology, facies and architectural element for beds measured at Verlatenkloof and Müller Canyon. Refer to Figure 2 and Supplementary Table 1 for GPS coordinates, and Supplementary Figures 1 and 2 for Verlatenkloof and Müller Canyon sedimentary logs. This spreadsheet corresponds to the sandstone to mudstone proportions and architectural elements pie charts presented in Figure 3.